Technical Division
SRF Department

Pressure Vessel Engineering Note For the 1.3-GHz Helium Vessel, Dressed Cavity AES-031 (Cavity TB9AES031, Vessel HE005), EN01819

Prepared by:
Joshua Kaluzny
Andrea Palagi

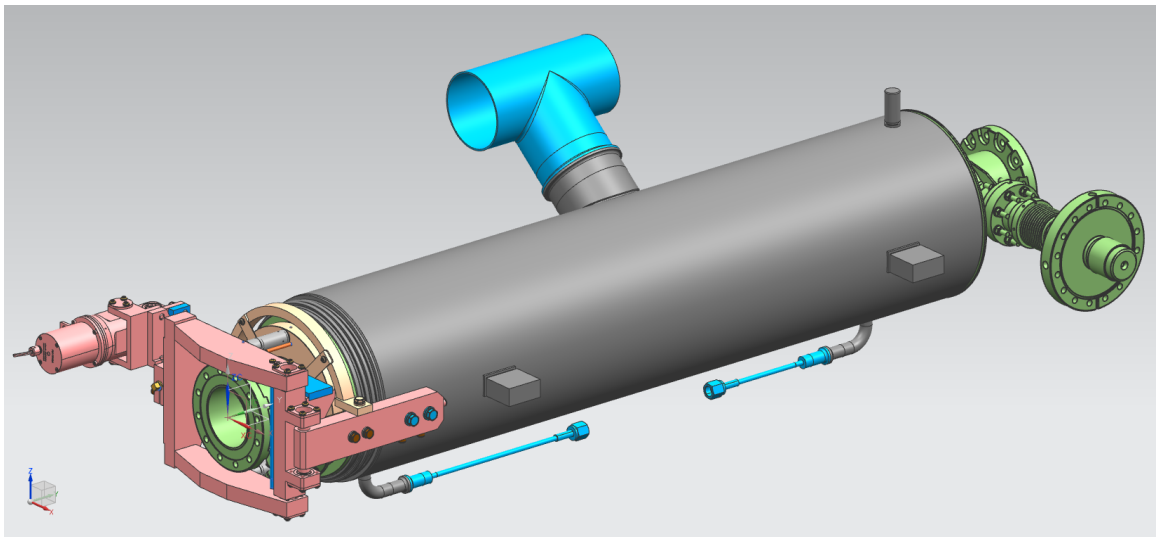

Reviewed by:
Kurt J Krempetz
PPD Mechanical Engineering Dept.
Fermilab

FESHM 5031.6 DRESSED SRF CAVITY ENGINEERING NOTE FORM

Prepared by: Joshua Kaluzny, Andrea Palagi Preparation Date: 5/11/2015

SRF Cavity Title: Pressure Vessel Engineering Note For the 1.3-GHz Helium Vessel, Dressed Cavity AES-031 (Cavity TB9AES031, Vessel HE005)

Lab Location / Cryomodule ID:

- As single dressed cavity: tested at Meson Detector Building (FIMS #408)
- Installed in cryomodule: tested at New Muon Lab (FIMS #700)

Purpose of system / System description: Liquid helium containment for nine-cell 1.3-GHz Superconducting Radio Frequency (SRF) cavity

Pressure Vessel ID Number: EN01819

Design Pressure 1: 2.05 bar Design Temperature 1: 80 – 300 K
Design Pressure 2: 4.1 bar Design Temperature 2: 1.8 – 80 K
Beam Vacuum: 3.0-bar (45-psia)

Materials: Niobium, titanium, niobium-titanium, stainless steel

Drawing Numbers (PID's, weldments, etc.): F10017493, 4904.101-MD-440004, F10010529

Designer/Manufacturer: FNAL / Incodema / AES

Test Pressure: 34.5-psig Test Date: _____

Statements of Compliance

SRF Cavity conforms to FESHM 5031.6 and ***is <u>not</u> exceptional***: Yes / No

Reviewer's Signature: Kurt Krempetz Date: _____
Print name: _____

D/S Head's Signature: David Harding Date: _____
Print name: _____

Additional approvals if vessel is exceptional

ES&H Director's Signature: Martha Michels Date: _____
Print name: _____

Director's Signature: Nigel Lockyer Date: _____
Print name: _____

Contents

A Extended Engineering Note **4**

A.1 Introduction . . . 4

A.2 Exceptional Vessel Discussion . . . 4

A.2.1 Reasons for Exception . . . 4

A.2.2 Analysis and use of the ASME Code . . . 5

A.2.3 Analytic Tools . . . 5

A.2.4 Fabrication . . . 5

A.2.5 Hazard Analysis . . . 6

A.2.6 Pressure Test . . . 6

A.3 Description and Identification . . . 7

A.3.1 Drawing Tree . . . 9

A.3.2 Serial Number of Cells . . . 11

A.3.3 Processing History . . . 11

A.3.4 Fermi Lever Tuner . . . 12

A.4 Design Verification . . . 12

A.4.1 Introduction and Summary . . . 12

A.4.2 Non-Code Elements . . . 13

A.4.3 Geometry . . . 14

A.4.4 Material Properties . . . 16

A.4.5 Loadings . . . 23

A.4.6 Stress Analysis Approach . . . 24

A.4.7 Division 1 Calculations by Rule . . . 27

A.4.8 Finite Element Model . . . 32

A.4.9 Stress Analysis Results . . . 33

A.5 System Venting Verification . . . 47

A.5.1 Summary . . . 47

A.5.2 Detailed Calculation for System Venting . . . 48

A.6 Welding Information . . . 49

A.7 Fabrication Information . . . 55

B Verification of ANSYS Results **55**

B.1 Hoop Stress in Ti Cylinder 55

B.2 Buckling of Spherical Shell - Approximation to Cell Buckling 56

B.3 Bucking of Ti Cylinder 57

C Fatigue Analysis of the Titanium Bellows **60**

D Pressure Test Results **66**

E HTS Adapting Hardware **71**

F Stainless Steel to Titanium Transitions **72**

F.1 Samples 72

F.2 Tensile Test 73

F.3 Charpy Impact Test 75

F.4 Transition Test 75

F.5 Finite Element Analysis 77

G Bellows Brace and Analysis **83**

G.1 Brace Analysis 83

G.2 Full Analysis 90

Appendix

A Extended Engineering Note

A.1 Introduction

The 1.3-GHz "dressed cavity" is a niobium superconducting radio frequency (SRF) cavity surrounded by a titanium vessel. The vessel contains liquid helium which surrounds the SRF cavity. During operation of the Dressed SRF Cavity, the liquid helium is at a temperature around 2K.

The current design of the LCLS-II Helium Vessel RF Cavity Assembly is a modified version of the Generation 3 (G3) design. The G3 Helium Vessel RF Cavity Assembly was a TESLA TTF design modified for more efficient fabrication. The G3 design was the result of collaboration between FNAL and INFN.

The Dressed SRF Cavity is planned to be sent to JLab for horizontal test and installation into an LCLS II prototype cryomodule. For the purposes of this note, the vessel will be analyzed as if it may be tested in the Horizontal Test Stand (HTS) at the Meson Detector Building as an individual entity and at the NML building as part of a cryomodule.

This pressure vessel engineering note describes the design and fabrication of the AES-031 1.3-GHz Dressed SRF Cavity. This document also summarizes how HE005, as a helium vessel, follows the requirements of the FESHM Chapter 5031.6 for Dressed SRF Cavities[1]. The note contains venting verification for the Dressed SRF Cavity when it is installed in HTS and also includes the system venting verification for NML. This document and supporting documents for the HE005 helium vessel may be found within the Teamcenter database.

A.2 Exceptional Vessel Discussion

A.2.1 Reasons for Exception

Dressed SRF Cavities, as defined in FESHM Chapter 5031.6, are designed and fabricated following "Guidelines for the Design, Fabrication, Testing and installation of SRF Nb Cavities"[1]. These guidelines are to ensure an equivalent level of safety to the ASME Boiler and Pressure Vessel Code (the Code)[2]. The 1.3-GHz Dressed SRF Cavity as a helium pressure vessel has materials and complex geometry that are not conducive to complete design and fabrication following the Code. Since the vessel design and fabrication methods cannot exactly follow the "Guidelines for the Design, Fabrication, Testing and installation of SRF Nb Cavities," the vessel requires a Director's Exception. Table 1 lists the specific areas of exception to the "Guidelines for the Design, Fabrication, Testing and installation of SRF Nb Cavities," where in the note this is addressed, and how the vessel is shown to be safe. Table 2 goes into details of why the design or the fabrication method cannot follow the "Guidelines for the Design, Fabrication, Testing and installation of SRF Nb Cavities"

Item or Procedure	Reference	Explanation for Exception	How the Vessel is Safe
No liquid penetrant testing was performed on the titanium sub-assembly.	Pages 13, 15	All joints in titanium vessels must be examined by the liquid penetrant method (see the Code, Div. 1, UNF-58(b)).	The evaluation of all welds is based on a de-rating of the allowable stress by a factor given in Div. 1, Table UW-12 for welds not radiographed. For the corner joints, the joint efficiency has to be less than 1.00.
Fabrication procedure for the niobium cavity assembly does not include WPS, PQR, or WPQ	Pages 49, 54	The fabrication procedure for the niobium cavity is proprietary. Detailed information on the procedure is not available.	The RF performance of the niobium cavity is acceptable, showing indirectly that all welds in the cavity are full penetration
No liquid penetrant testing was performed on the welds of the bellows sub-assembly.	Pages 30, 54	All welds in the bellows expansion joint shall be examined by liquid penetrant testing (see the Code, para. 26-11)	The evaluation of the longitudinal weld is based on a de-rating of the allowable stress by a factor given in Div. 1, Table UW-12 for welds not radiographed. The circumferential attachment welds between the bellows and the weld ends are radiographed.

Table 1: Areas of Exception to the "Guidelines for the Design, Fabrication, Testing and installation of SRF Nb Cavities" - Safety

A.2.2 Analysis and use of the ASME Code

The extended engineering note presents the results of the analysis that was performed on the entire vessel.

A.2.3 Analytic Tools

Analysis was done using ANSYS Workbench 14.5 and Mathcad version 14.

A.2.4 Fabrication

All fabrication documents are located in Teamcenter:

Item or Procedure	Reason
No liquid penetrant testing was performed on the titanium sub-assembly.	Any acceptable pores within the weld will hold the liquid penetrant. Temperature changes in the weld, and thus the liquid penetrant, may result in degradation in the weld integrity.
Fabrication procedure for the niobium cavity assembly does not include WPS, PQR, or WPQ	The fabrication procedure is proprietary information.
No liquid penetrant testing was performed on the bellows sub-assembly.	Any acceptable pores within the weld will hold the liquid penetrant. Temperature changes in the weld, and thus the liquid penetrant, may result in degradation in the weld integrity.

Table 2: Areas of Exception to the "Guidelines for the Design, Fabrication, Testing and installation of SRF Nb Cavities" - Design and Manufacturing Issues

- X-ray results of the welds for any given dressed cavity helium vessel
- Fabrication documents, such as the material certifications and weld documents: Weld Procedure Specifications (WPS), Procedure Qualification Record (PQR), and Welder Performance Qualification (WPQ)

A.2.5 Hazard Analysis

Whether tested in the HTS or a part of a cryomodule at NML, the 1.3-GHz helium vessel is completely contained within a multilayered structure that protects personnel. The 80K thermal shield completely surrounds the helium vessel, and the outer vacuum vessel encases the 80K thermal shield. From a personnel safety standpoint, the helium vessel is well contained within both the test cryostat and the cryomodule. Vacuum safety reliefs vent any helium spill.

A.2.6 Pressure Test

The helium vessel MAWP is 2.05-bar. This means that during testing at HTS and when installed in the cryomodule, the helium vessel maximum allowable pressure differential is 0.205 MPa across the vessel outer wall to insulating vacuum and across the cavity wall to beam vacuum. The helium vessel pressure test takes place at a surrounding environment of atmospheric pressure. So the required test pressure is at least 110% of 29.7 psig. The pressure test goes up to 34.5-psig, which is 116% of the MAWP.

A.3 Description and Identification

The Dressed SRF Cavity is called an LCLS II Helium Vessel RF Cavity Assembly. The dressed cavity consists of the niobium nine-cell 1.3-GHz cavity, with a unique serial number, and the titanium helium vessel, also with unique serial number. The top assembly drawing of the assembly, drawing F10017493, is shown in Figure 1. The LCLS II Cavity Assembly consists essentially of two sub-assemblies: the niobium SRF (bare) cavity and the titanium helium vessel weldment.

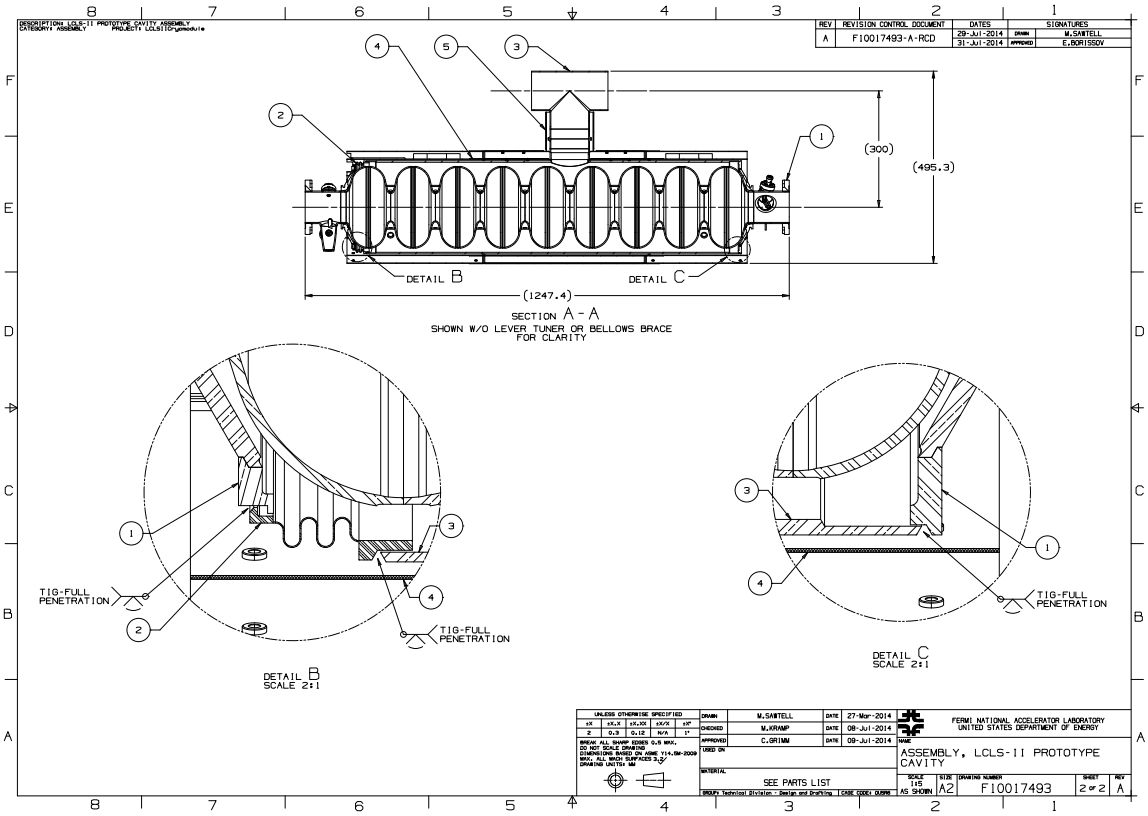

Figure 1: LCLS-II Cavity Assembly

The niobium SRF cavity is an elliptical nine-cell assembly. A drawing of the nine-cell cavity is shown in Figure 2 (drawing 4904.010-MD-440004). A single cell, or a dumbbell, consists of two half-cells that are welded together at the equator of the cell. Rings between the cells stiffen the assembly to a point. Some flexibility in the length of the nine-cell cavity is required to tune the cavity and optimize its resonance frequency. The end units each consist of a half cell, an end disk flange, and a transition flange. The transition flange is made of a titanium-niobium alloy. The iris' minimum inner diameter is 35-mm (1.4-in), and the maximum diameter of a dumbbell is 211.1-mm (8.3-in) (see drawing 4904.010-MD-439173). The length of the cavity, flange-to-flange, is 1247.4-mm (49.1-in.) (see drawing 4904.010-MD-440004). Refer to A.3.1 for the location of the drawings not shown in this note.

The titanium helium vessel encases the niobium SRF bare cavity. Figure 3 shows the drawing of the titanium vessel assembly (drawing F10015802). The vessel has two helium fill ports at the

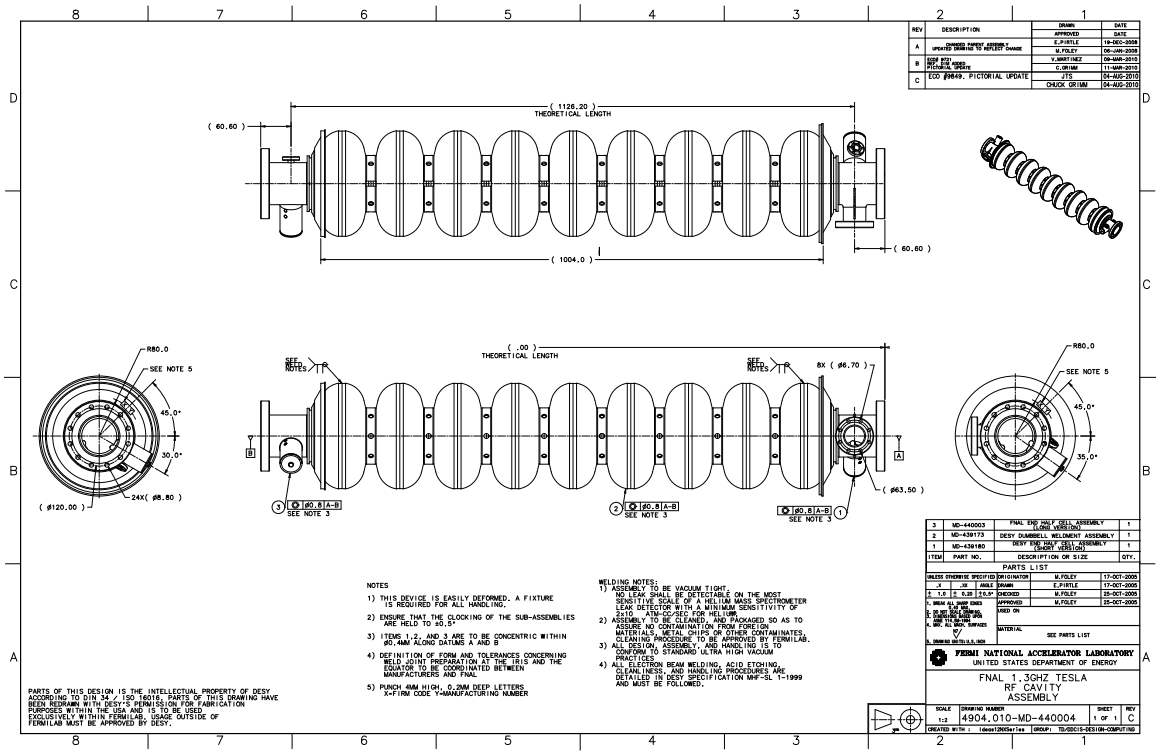

Figure 2: 1.3 GHz Nine Call RF Cavity Assembly

bottom and in the center of the vessel there is the two-phase helium return line. At the sides of the vessel are tabs which support the vessel within the HTS cryostat or cryomodule. The vessel is flexible in length due to a bellows at the field probe end. This flexibility in the vessel allows for accommodating the change in the nine-cell cavity length due to thermal contraction at cryogenic temperature and for tuning the niobium cavity during operation. A lever tuner supports the vessel at the bellows. Two control systems act on the lever tuner to change the length of the vessel, and thus change the length of the cavity. A slow-control tuner system that consists of a stepper motor that changes the vessel length. The stepper motor extends the length of the cavity by less than 2.0-mm (0.079-in.) to bring it to the desired resonance frequency to counteract the combined effects of thermal contraction and pressurization during cool down. A fast-control tuner system consisting of two piezoelectric actuators prevents detuning of the cavity during operation due to Lorentz Forces and noise sources (microphonics) [3]. The piezos provide an increase in bellows length (bellows expansion) of 13 micrometers during operation. The vessel is expected to have a lifetime of 10-years. The minimum inner diameter of the cylindrical part of the vessel (both the tubes and bellows) is 230-mm (9.1-in.). Refer to the tube drawings F10008818 and bellows drawing F10010529.

The design of the niobium nine-cell cavity is the same as the cavities used in the TESLA facility at DESY (Hamburg, Germany), which has been in operation for the past 10 years. The design of the helium vessel is a modification of the TESLA design. The location of the titanium bellows, along with the lever tuner and control systems, is a modification of the TESLA design.

The Dressed SRF Cavity may be performance tested in HTS. The results will determine whether

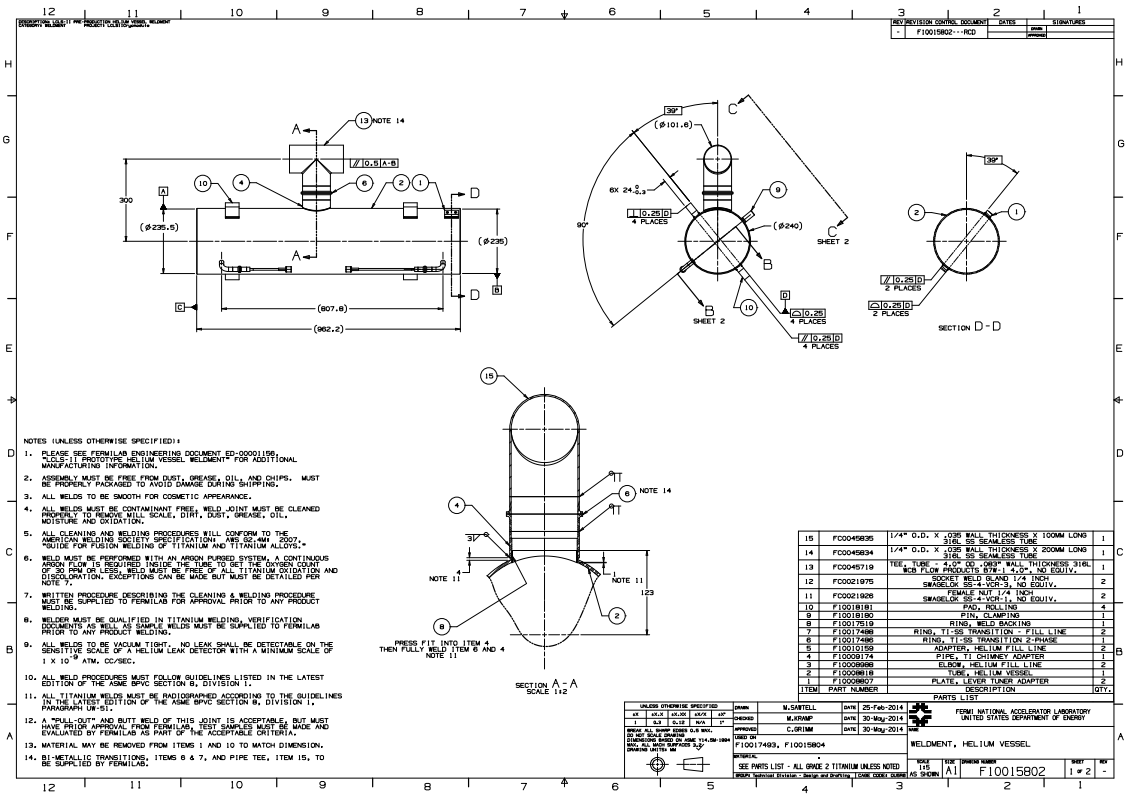

Figure 3: LCLS-II Helium Vessel weldment

or not it will be used in a future cryomodule. The results of the testing will also be feedback in optimizing the design and fabrication process for future LCLS II dressed cavities which will be used in a cryomodule.

The Dressed SRF Cavity has two internal maximum allowable working pressures (MAWP). At a design temperature range of 80K - 300K, the (warm) internal MAWP is 2.0-bar. The vessel will be pressure tested in room temperature. The internal MAWP for cold temperatures (1.8K - 80K) is 4.0-bar. The external MAWP is 1.0-bar.

The beam vacuum has an internal MAWP of 3-bar (45-psia). At NML, where the string of dressed cavities within the cryomodule is tested, the niobium cavity would operate under vacuum as part of the beam vacuum. The beam pipe venting line has a rupture disk with a set pressure as high as 25-psig (0.18 MPa). In the failure mode where liquid helium leaks into the cavity, and then the cavity is warmed up, the helium would expand and pressurize the cavity.

A.3.1 Drawing Tree

A drawing tree for the LCLS II Helium Vessel RF Cavity Assembly is shown in Table 3. All drawings are located in Teamcenter.

Drawing No.	Rev .	Title
F10017493	–	LCLS II He Vessel RF Cavity Assembly
F10015802	–	LCLS II Helium Vessel Weldment
F10008807	–	Plate, HV tuner adapter
F10008818	–	Tube Helium Vessel
F10008988	–	Elbow, .62” OD, .083” Wall
F10009174	–	Pipe, 1.3 Ti Chimney
F10010159	–	Adapter, 5/8” tube 1/3” tube 316L SS
F10017486	–	Ring, Ti-SS transition 3.76” ID
F10017488	–	Ring, Ti-SS transition .460” ID
F10017519	–	Ring, Weld backing
F10018080	–	Pin, Clamping
F10018081	–	Pad, Rolling
F10019625	–	Tube, Extension SS316 200 mm
F10019626	–	Tube Extension SS316, 200 mm
F10029256	–	Tee, Pipe 3 1/2” xSCH 5, 304 SS
813175	A	Support Plate Adapter
440004	A	RF Cavity Assembly
449180	D	Short End Half Cell Assembly
439178	B	End Disk Weldment - Short Version
439164	A	End Tube Spool Piece
439152	B	End Cap Flange
439168	–	End Cap Disk (Short Version)
439163	–	RF Half Cell (Short Version)
439177	A	End Tube Weldment - Short Version
439175	–	Short Version HOM Assembly
439166	–	Short Version HOM Formteil Housing
439150	–	HOM Spool Piece
439162	–	Short Version Formteil
439161	B	Short Version End Tube
439171	–	Coupler Spool Piece
439169	–	Coupler Rib
439159	–	NW78 Beam Flange
439158	–	NW40 Coupler Flange
439157	–	NW12 HOM Flange
813185	A	Cavity Transition Ring MC End
439173	–	DESY Dumbbell Weldment
439172	–	Dumbbell
439156	–	Mid Half Cell
439151	A	Half Support Ring
440003	-	FNAL End Half Cell Assembly
439178	B	End Disk Weldment (Long Version)
439164	A	End Tube Spool Piece
439152	B	End Cap Flange
439167	–	End Cap Disk (Long Version)
439155	–	RF Half Cell (Long Version)
440002	B	FNAL End Tube Weldment (Long Version
439174	–	DESY Long Version HOM Assembly
439165	–	HOM Long Version Formteil Housing
439150	–	HOM Spool Piece
439154	–	Long Version Formteil
440001	–	FNAL Long Version End Tube
439170	A	DESY Antenna Spool Piece
439159	–	DESY NW78 Beam Flange
439160	–	DESY NW8 Antenna Flange
439157	–	DESY NW12 HOM Flange
813195	A	Cavity Transition Ring Field Probe End
F10010529	–	He Vessel Bellows

Table 3: Drawing Tree for LCLS-II Helium Vessel RF Cavity Assembly

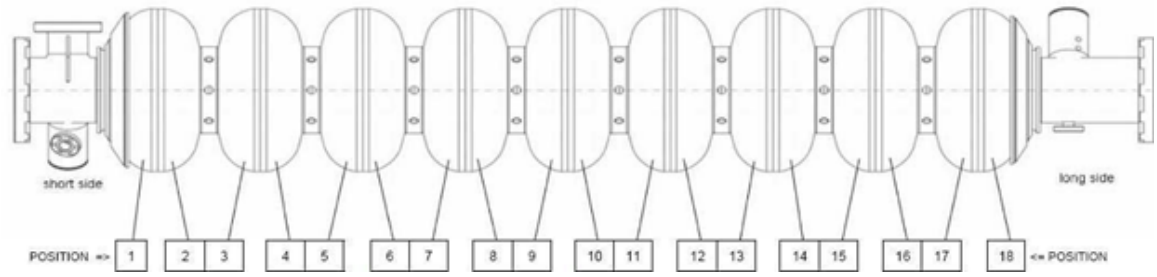

Figure 4: Map of Half Cells

Position	Sheet Number
1	AES-B4-210
2	AES-B4-308
3	AES-B4-218
4	AES-B4-297
5	AES-B4-286
6	AES-B4-294
7	AES-B4-243
8	AES-B4-365
9	AES-B4-236
10	AES-B4-382
11	AES-B4-346
12	AES-B4-291
13	AES-B4-224
14	AES-B4-318
15	AES-B4-223
16	AES-B4-358
17	AES-B4-277
18	AES-B4-199

Table 4: Half Cell Identification

A.3.2 Serial Number of Cells

As previously discussed, the niobium SRF bare cavity is comprised of nine cells, or 18 half cells. The sheet numbers of these half cells are shown in Table 4 in this sample from the incoming inspection traveler.

A.3.3 Processing History

The processing history of RF cavities includes any or all the following: bulk- and light-electropolishing, centrifugal barrel polishing, an 800°C high temperature bake for 3 hours, a 120°C bake for 48 hours, and nitrogen doping. The cavity is tested, and then welded to the helium vessel. The history for FNAL's dressed SRF cavities can be found in the following database under series

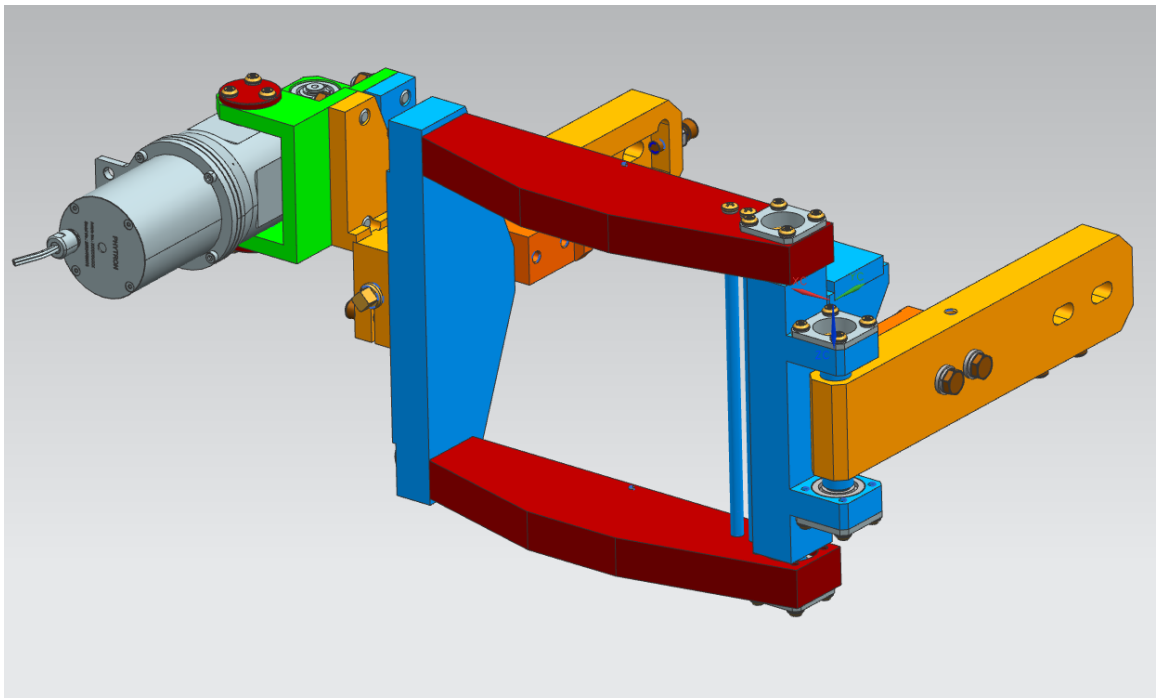

Figure 5: Fermi Lever Tuner Model

Maximum Displacement	1.3	[mm]
Maximum Force	4.5	[kN]

Table 5: Fermi Lever Tuner Specifications

"RFCA": https://vector-onsite.fnal.gov/SelectTravelerReadOnlyFilter.asp

A.3.4 Fermi Lever Tuner

Even though the tuner is not part of the pressure vessel, the forces and displacements act on the vessel during operation. The tuner restrains the cavity where pressure differentials around the bellows cause forces on the cavity. A model of the tuner design is shown in Figure 5, and key specifications [4] are listed in Table 5. Analysis has shown that with the current tuner design some pressure loading scenarios may overload the tuner. Therefore, administrative controls will be in place when the vessel is operated with the tuner.

A.4 Design Verification

A.4.1 Introduction and Summary

This analysis is intended to demonstrate that the LCLS II 1.3 GHz SRF cavity conforms to the ASME Boiler and Pressure Vessel Code (the Code), Section VIII, Div. 1, to the greatest extent

possible.

Where Div. 1 formulas or procedures are prescribed, they are applied to this analysis. For those cases where no rules are available, the provisions of Div. 1, U-2(g) are invoked. This paragraph of the Code allows alternative analyses to be used in the absence of Code guidance.

This cavity contains several features which are not supported by the Code. These are related primarily to materials, weld types, and non-destructive examination, and are addressed in detail in the next section of this report, titled "Non-Code Elements." These are accepted as unavoidable in the context of SRF cavities, and every effort is made to demonstrate thorough consideration of their implications in the analysis.

Advantage is taken of the increase in yield and ultimate strength which occurs in Nb and Ti components at the temperature of 1.88 K.

The design pressures specified for this analysis are 30 psi (2.0-bar) at 293 K and 60 psi (4.0-bar) at 1.88 K. This analysis confirms that the MAWPs of the vessel can be safely set at these pressures. Negligible margin for increase is available at 293 K, but the cold MAWP could be increased substantially above 60 psi (4.0-bar).

In addition to these fundamental operating limits, the cavity was also shown to be stable at external pressures on the Ti shell of 15 psid (1.0-bar), and internal pressures on the Nb cavity of 15 psid (1.0-bar); these loadings could occur under fault conditions, when the beam and insulating vacuums have been compromised, and the helium volume has been evacuated.

A.4.2 Non-Code Elements

With regards to the Design Verification, the LCLS II 1.3 GHz cavity does not comply with Div. 1 of the Code in the following ways:

- Category B joints in titanium must be either Type 1 butt welds (welded from both sides) or Type 2 butt welds (welded from one side with backing strip) only (see Div. 1, UNF- 19(a)). Some category B (circumferential) joints are Type 3 butt welds (welded from one side with no backing strip). Reclassified, see [5].
- All joints in titanium vessels must be examined by the liquid penetrant method. (see Div. 1, UNF-58(b)). No liquid penetrant testing was performed on the vessel.
- All electron beam welds in any material are required to be ultrasonically examined along their entire length. (see UW-11(e)). No ultrasonic examination was performed on the vessel.

The evaluation of the Type 3 butt welds in the titanium is based on a de-rating of the allowable stress by a factor of 0.6, the factor given in Div. 1, Table UW-12 for such welds when not radiographed.

The exceptions listed above do not address Code requirements for material control, weld procedure certification, welder certification, etc. These requirements, and the extent to which the cavity production is in compliance with them, are addressed in section A.6.

A.4.3 Geometry

General This analysis is based on geometry obtained from drawing F10017493 and associated details. Figure 6 shows the Dressed SRF Cavity, complete with magnetic shielding, piping and lever tuner.

For the analysis, only the Nb cavity, conical Ti-45Nb heads, and titanium shells and bellows are modeled, as well as the flanges to which the Helium Vessel is constrained. These components are shown in Figure 7.

The geometric limits of the analysis are further clarified in Figure 8.

The individual cavity component names used in this report are shown in Figure 9 and Figure 10.

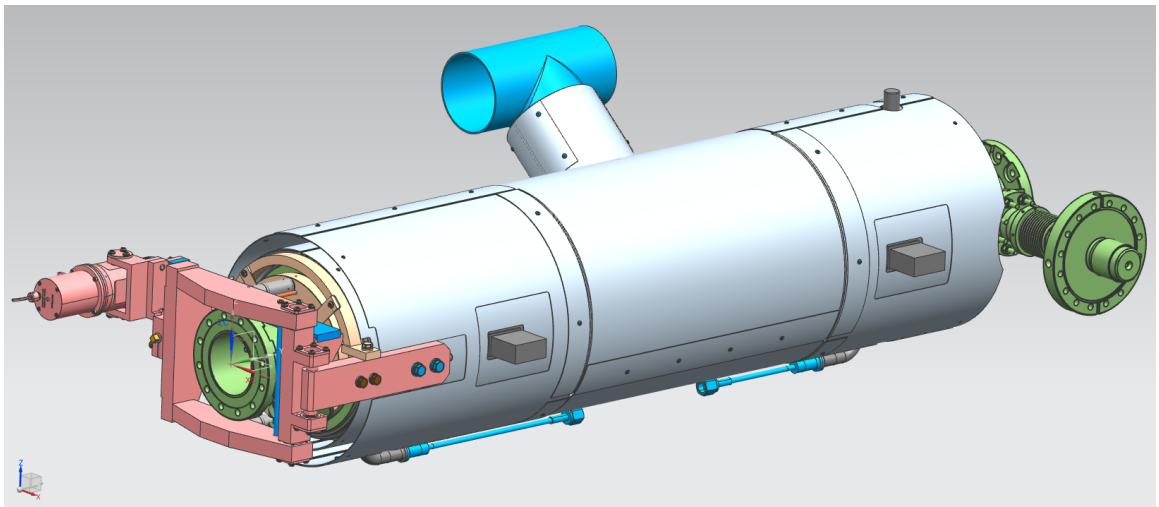

Figure 6: Dressed SRF Cavity, complete with magnetic shielding, piping and lever tuner.

Welds

This section describes the welds as a precursor to the weld stress evaluation. Details regarding the weld fabrication process are shown in section A.6.

Welds are produced by the EBW process (in the Nb, and Nb-to-Ti transitions), and the TIG (GTAW) process (Ti-Ti welds).

All welds on the Dressed SRF Cavity are designed as full penetration butt welds. All welds are performed from one side, with the exception of the Ti-45Nb to Ti transition welds. Those welds are performed from two sides. No backing strips are used for any welds.

Table 6 summarizes the weld characteristics, including the Code classification of both joint category and weld type, and the corresponding efficiency.

The locations of the welds as numbered in Table 6 are shown in Figure 11. Detailed weld configurations are illustrated in Figure 12 and Figure 13. Details of the assumed zones of fusion of the welds are shown in Figures 14, 15, 16, and 17.

Weld	Weld Description	Drawing	Materials Joined	Weld Process	Joint Category	Code Weld Type	Joint Efficiency
1	End Tube Spool Piece to End Cap Flange	MD-439178	Nb-Nb	EBW	B	3	0.6
2	End Tube Spool Piece to RF Half Cell	MD-439178	Nb-Nb	EBW	B	1	0.7
3	End Cap Flange to RF Half Cell	MD-439178	Nb-Nb	EBW	-	3	0.6
4	End Cap Flange to End Cap Disk	MD-439178	Nb-Ti45Nb	EBW	B	3	0.6
5	End Cap Disk to Transition Ring	MD-439180 MD-440003	Ti45Nb-Ti	EBW	B	1	0.7
6	1.3GHz 9 Cell RF Cavity (Transition Ring) to Bellow Assembly	F10017493	Ti-Ti	TIG	C	7	0.6
7 (FP End)	Bellow Assembly to LCLS II Helium Vessel Assembly	F10010493	Ti-Ti	TIG	B	3	0.7
8	Bellow Convolutions to Weld Cuffs	F10010529	Ti-Ti	EBW	B	3	0.6
9	Support Ring to Half Cell	MC-439172	Nb-Nb	EBW	-	3	0.6
10	Dumbbell to Dumbbell	MD-439173	Nb-Nb	EBW	B	3	0.6
11	Half Cell to Half Cell	MC-439172	Nb-Nb	EBW	B	3	0.6
12 (MC End)	Transition Ring to LCLS II Helium Vessel Assembly	F10017493	Ti-Ti	TIG	C	7	0.6

Table 6: Summary of Weld Characteristics

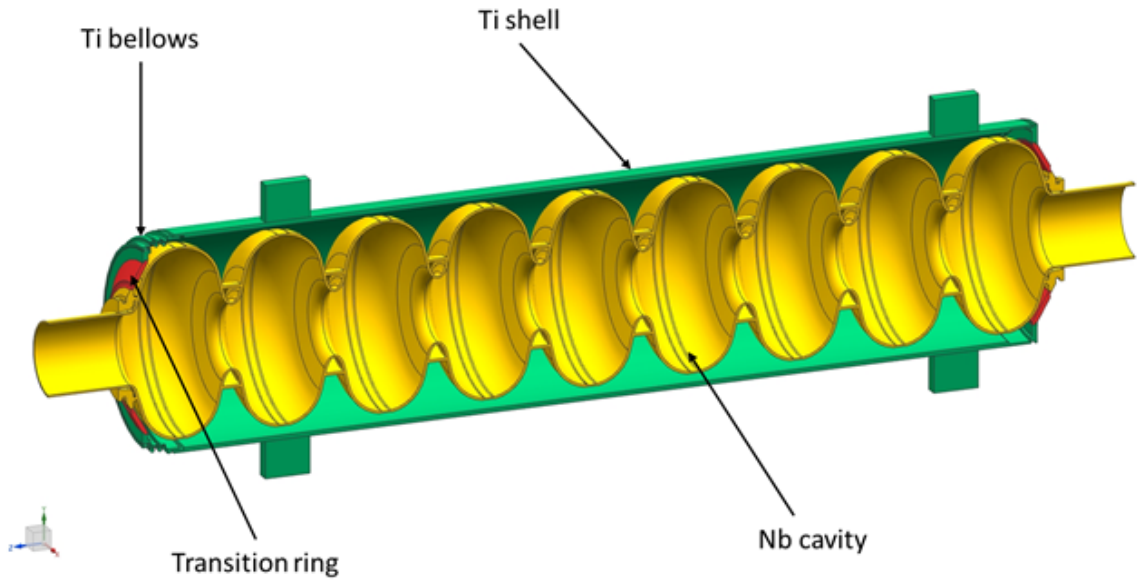

Figure 7: Components included in the analysis

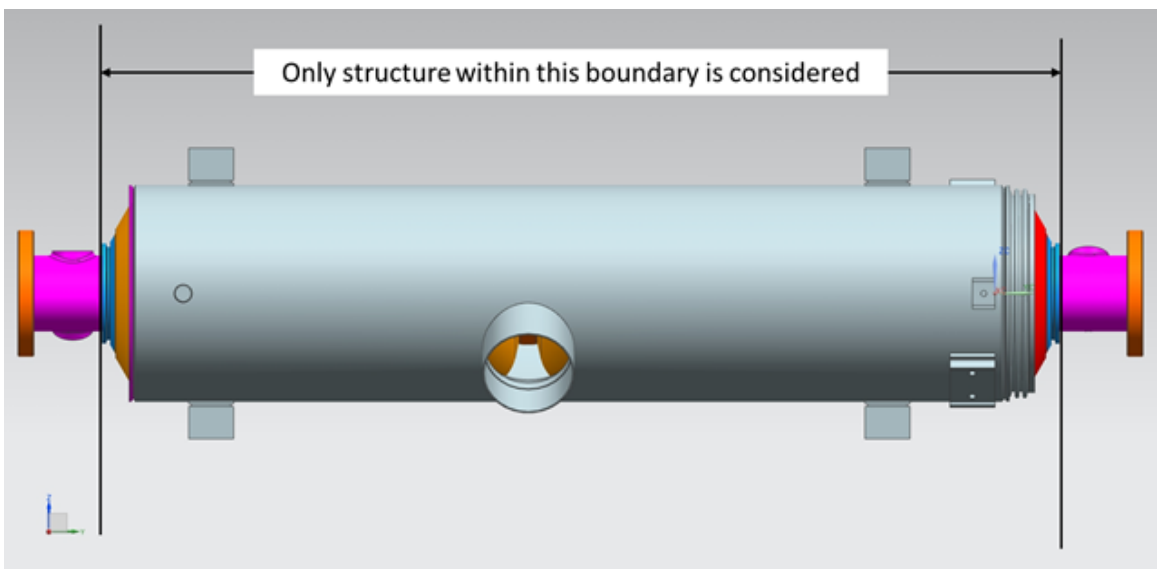

Figure 8: Geometric limits of the analysis

A.4.4 Material Properties

General The Dressed SRF Cavity is constructed of three materials: Pure niobium, Ti-45Nb alloy, and Grade 2 titanium. Of these materials, only Grade 2 Ti is approved by Div. 1 of the Code, and hence has properties and allowable stresses available from Section II, Part D.

The room temperature material properties and allowable stresses for this analysis (are the ones

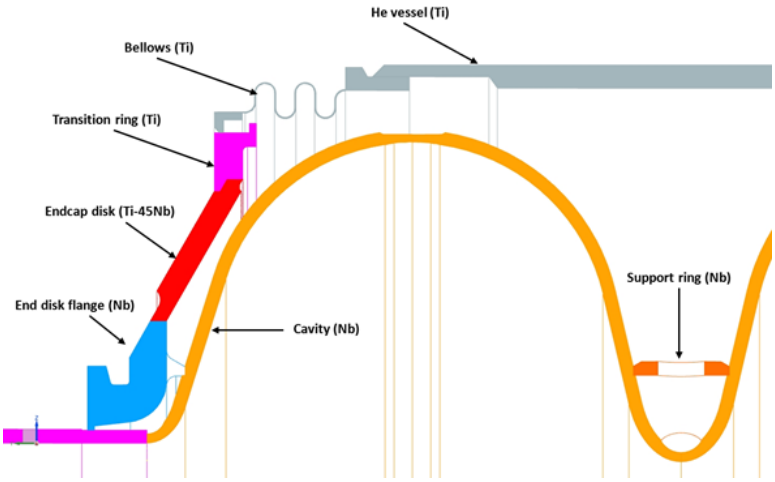

Figure 9: Parts and Materials in the Field Probe End

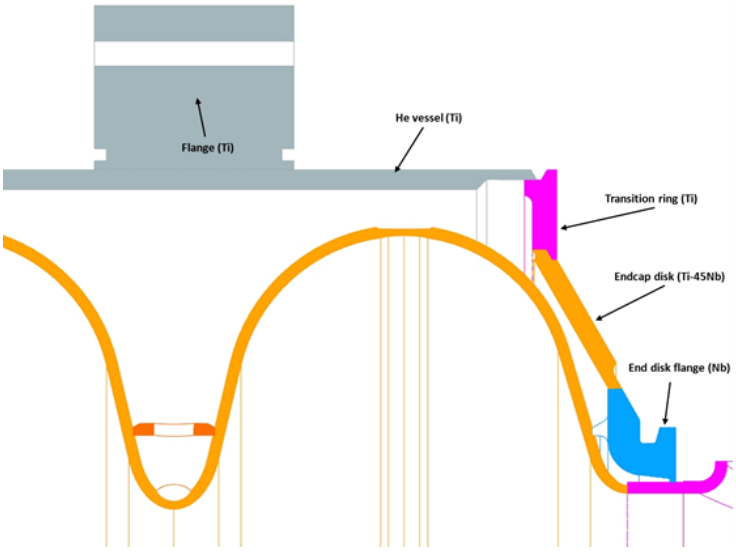

Figure 10: Parts and Materials in the Main Coupler End

from the Technical Division Technical Note TD-09-005) are identical to those established in the analysis of the 3.9 GHz elliptical cavity [6]. The determination of the allowable stresses was based on Code procedures, and employed a multiplier of 0.8 for additional conservatism.

For the cryogenic temperature load cases, advantage was taken of the increase in yield and ultimate stress for the Nb and Ti. As with the room temperature properties, the properties for these materials at cryogenic temperature were also established by previous work related to the 3.9 GHz cavity [7].

Room temperature properties were used for the Ti-45Nb alloy for all temperatures, as no low temperature data on that alloy were available. However, it is highly likely that, like the elemental Nb and Ti, substantial increases in strength occur.

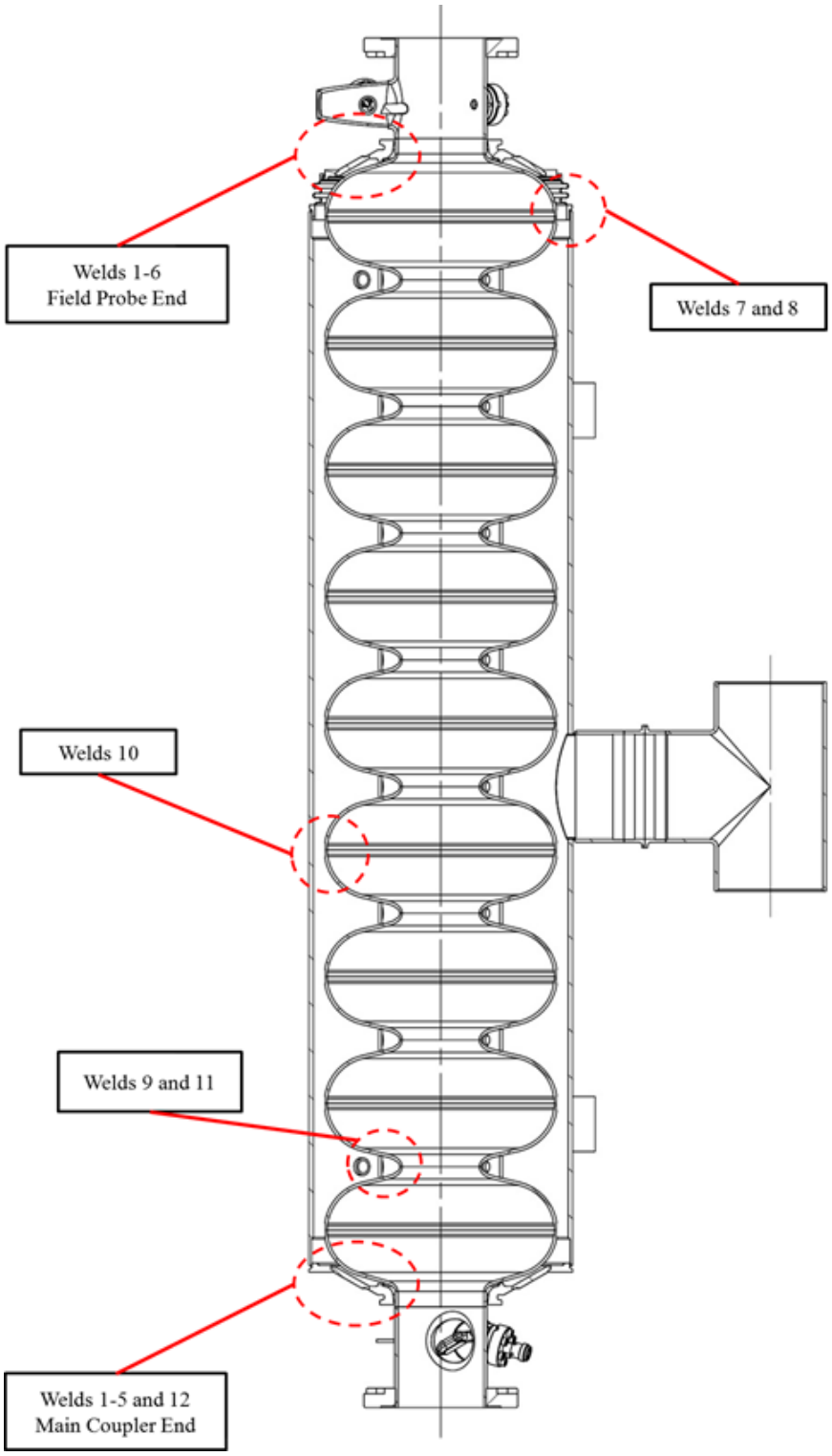

Figure 11: Welds numbered as in Table 6

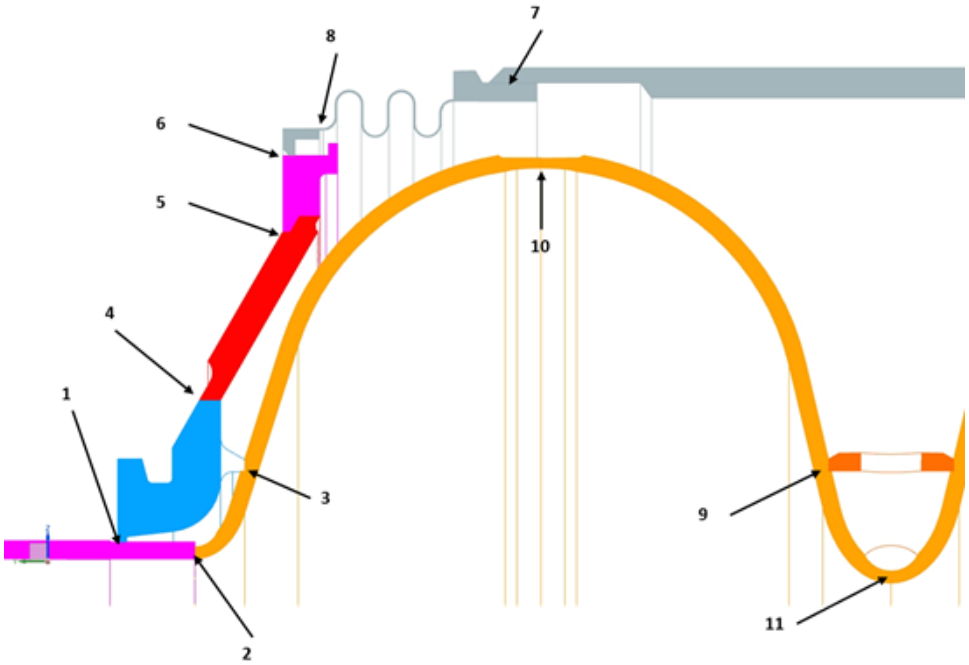

Figure 12: Weld Numbering at Field Probe End

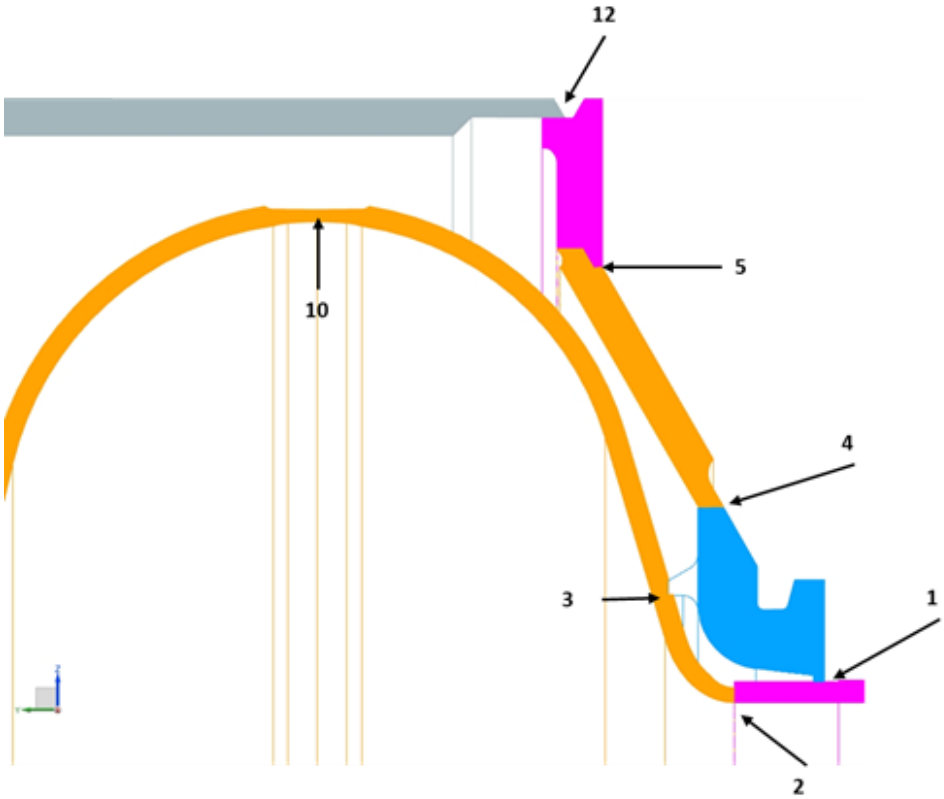

Figure 13: Weld Numbering at Main Coupler End

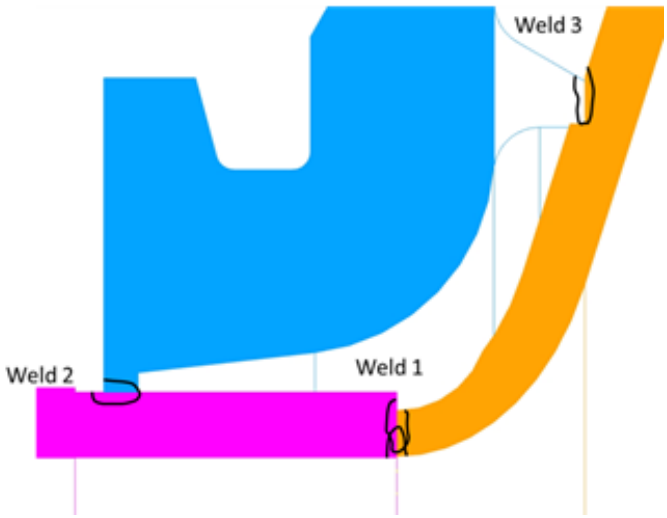

Figure 14: Assumed fusion zones - welds 1-3

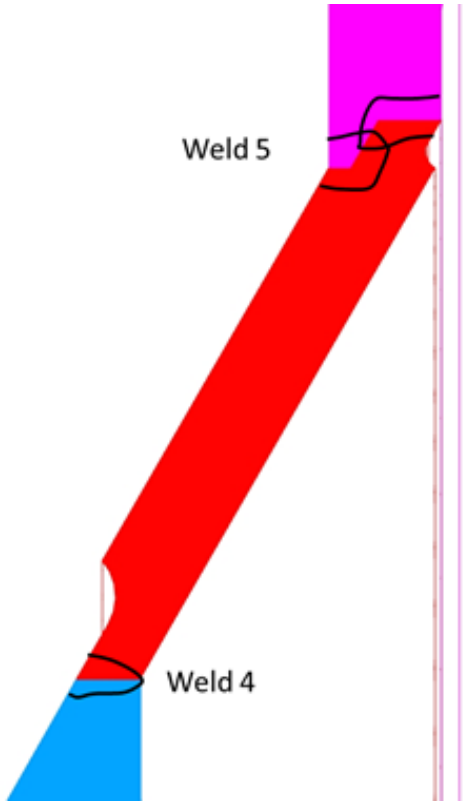

Figure 15: Assumed fusion zones - welds 4-5

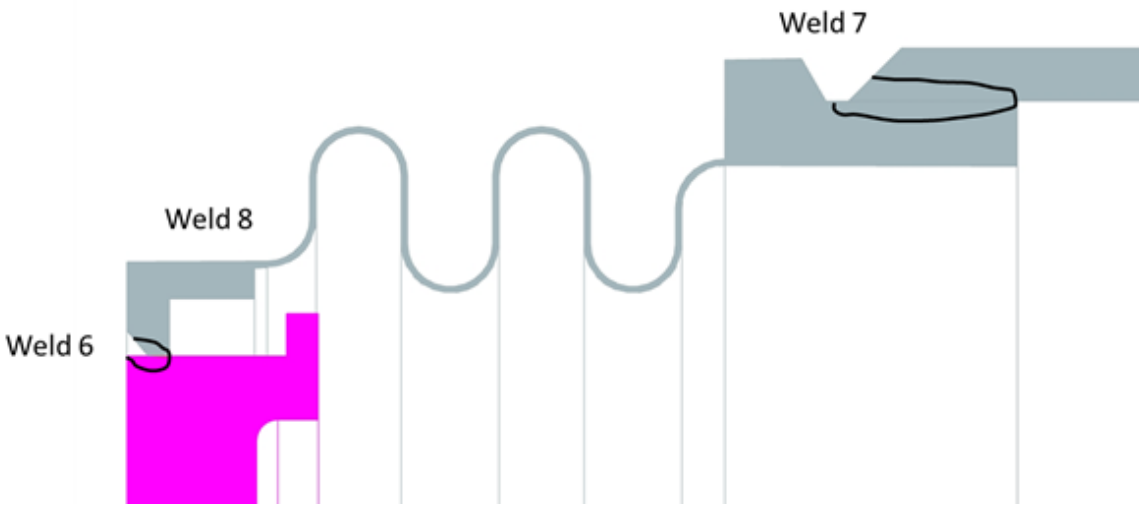

Figure 16: Assumed fusion zones - welds 6-8

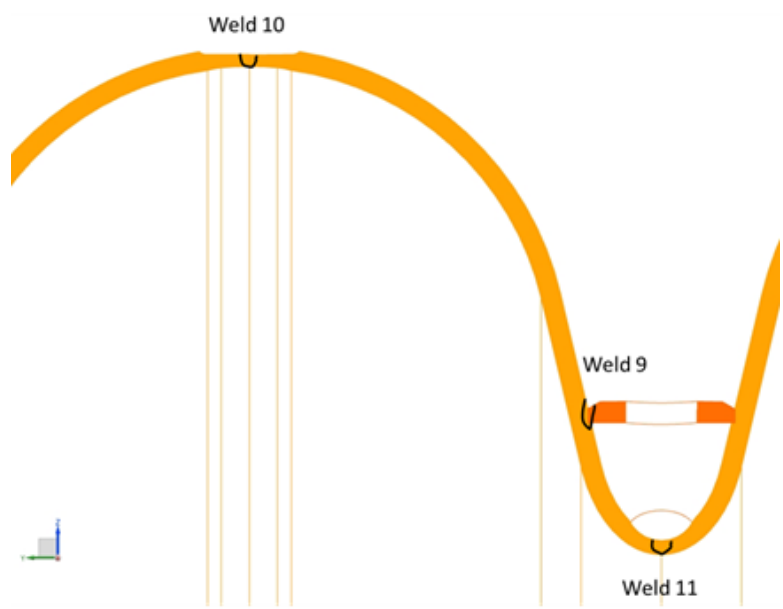

Figure 17: Assumed fusion zones - welds 9-11

Material	Elastic Modulus [GPa]	Yield Strength [MPa]		Ultimate Strength [MPa]		Integrated Thermal Contraction 293 K to 1.88 K [Δl/l]
		293 K	1.88 K	293 K	1.88 K	
Niobium	105	38	317	115	600	0.0014
55Ti-45Nb	62	476	476	545	545	0.0019
Titanium, Gr. 2	107	276	834	345	1117	0.0015

Table 7: Material Properties

	P_m [MPa]		P_l [MPa]	
Material	1.88 K	293 K	1.88 K	293 K
Nb	137	20	206	30
Ti-45Nb	125	125	187	187
Gr. 2 Ti	255	79	383	118

Table 8: Allowable primary membrane stress (P_m) and primary local membrane stress (P_l)

Material Properties The elastic modulus, yield strength, ultimate strength, and integrated thermal contraction from 293 K to 1.88 K are given in Table 5 for each material used in the construction of the cavity.

Allowable Stresses The Code-allowable stresses for unwelded materials for the various categories of stress (see "Stress Analysis Approach" of this report) are given in Tables 8 and 9.

The Code-allowable stresses for welded materials are calculated by multiplying the values of Tables 8 and 9 by the joint efficiency given in Table 6.

The allowed stresses for each Stress Category in Tables 8 and 9 are defined in the Code, Division 2, Paragraphs 5.2.2.4(e) and 5.5.6.1(d) and are reproduced here, where S is defined in Table 10:

$$P_m \leq S$$
$$P_l \leq 1.5\ S$$
$$(P_l + P_b) \leq 1.5\ S$$
$$(P_l + P_b + Q) \leq 3\ S$$

	$P_l + P_b$ [MPa]		$P_l + P_b + Q$ [MPa]	
Material	1.88 K	293 K	1.88 K	293 K
Nb	206	30	411	61
Ti-45Nb	187	187	375	374
Gr. 2 Ti	383	118	766	237

Table 9: Allowable primary local membrane stress plus primary bending stress ($P_l + P_m$) and primary local membrane stress plus primary bending stress plus secondary stress ($P_l + P_m + Q$)

	Allowable Stress (S) [MPa]		Established Values [MPa]	
Material	1.88 K	293 K	1.88 K	293 K
Nb	137	20	171	25
Ti-45Nb	125	125	156	156
Gr. 2 Ti	255	79	319	99

Table 10: Allowable Stress "S"

The allowable stresses for each stress category in Tables 8 and 9 are based on the value S, which is the allowable stress of the material at the design temperature. Table 10 shows the values of S for each material at 1.88K and 293K. Note that S includes the de-rating factor of 0.8 of the established allowable stress for a material for an experimental vessel. The de-rating follows the guidelines in FESHM Chapter 5031.

The established material properties used in SRF dressed cavities are stated at temperatures 293 K and 1.88 K. Recent measurements taken by Fermilab of the yield properties of niobium show that, at 77 K, the yield strength is at least 80% of the yield strength at 4 K.This matches what Walsh reported in another cold test in 1999. Walsh also reported that titanium's yield strength at 77 K is within 74% of the yield strength at 4 K.

Looking at FEA results of Load Cases 2 and 4, where the vessel is modeled at 4-bar, the calculated stresses of the niobium are far less than 40% of allowable at 4K. The calculated titanium stresses are less than 73% of allowable at 4K. So the vessel will remain safe at the higher design temperature for the design pressure of 4.0-bar.

A.4.5 Loadings

General The dressed cavity is shown in cross section in Figure 19. There are three volumes which may be pressurized or evacuated:

1. The LHe volume of the helium vessel
2. The volume outside the cavity typically evacuated for insulation
3. The volume through which the beam passes on the inside of the Nb cavity itself.

The pressures in these volumes are denoted as P1, P2, and P3, respectively. With regards to pressure, typical operation involves insulating vacuum, beam vacuum, and a pressurized LHe volume. Atypical operation may occur if the insulating or beam vacuums are spoiled, and the LHe space simultaneously evacuated. This reverses the normal operational stress state of the device, producing an external pressure on the Ti shell, and an internal pressure on the Nb cavity; however, this pressure is limited to a maximum differential of 1 bar.

In addition to the pressure loads, the cavity also sees dead weight forces due to gravity which are reacted at the tuner flanges, as well thermal contractions when cooled to the operating temperature of 1.88 K, and a strain-controlled extension by the tuner after cool down.

All of these loads are considered in this analysis. Specific load cases are defined in the next section.

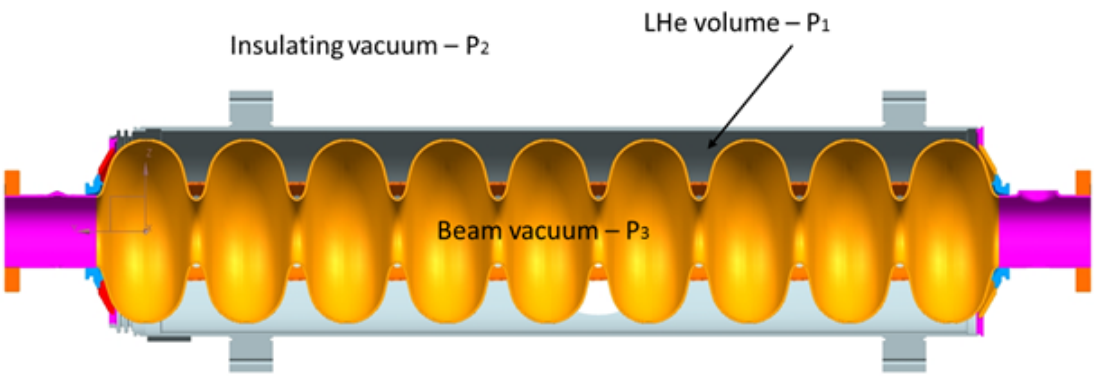

Figure 18: Volumes for Pressure/Vacuum

Load Cases

The cavity is subjected to five basic loads:
1. Gravity
2. LHe liquid head
3. Thermal contraction
4. Tuner extension
5. Pressure (internal and external)

Three of these loads - gravity, liquid head, and pressure - produce both primary and secondary stresses. The remaining loads - thermal contraction and tuner extension - are displacement - controlled loads which produce secondary stresses only. This results in five load cases. These load cases are shown in Table 11, along with the temperatures at which the resulting stresses were assessed, and the stress categories that were applied.

A.4.6 Stress Analysis Approach

The goal of the analysis is to qualify the vessel to the greatest extent possible in accordance with the rules of the Code, Section VIII, Div. 1. This Division of the Code provides rules covering many cases; however, there are features of this cavity and its loadings for which the Division has no rules. This does not mean that the vessel cannot be qualified by Div. 1, since Div. 1 explicitly acknowledges the fact that it does not prevent formulaic procedures ("rules") covering all design possibilities. From U-2(g)

"This Division of Section VIII does not contain rules to cover all details of design and construction. Where complete details are not given, it is intended that the Manufacturer, subject to the acceptance of the Inspector, shall provide details of design and construction which will be as safe as those provided by the rules of this Division."

Applying Division I Rules to the Cavity

Load Case	Loads	Condition Simulated	Temperature for Stress Assessment	Applicable Stress Categories
1	1. Gravity 2. P1= 0.205 MPa 3. P2=P3 = 0	Warm Pressurization	293 K	Pm, Pl , Pl + Q
2	1. Gravity 2. LHe Liquid head 3. P1=0.41 MPa 4. P2=P3 = 0	Cold operation, full, maximum pressure - no thermal contraction	1.88 K	Pm, Pl , Pl + Q
3	1. Cool down to 1.88 K 2. Tuner extension of 1.5 mm	Cool down and tuner extension, no primary loads	1.88 K	Q
4	1. Gravity 2. LHe liquid head 3. Cool down to 1.88 K 4. Tuner extension of 1.5 mm 5. P1=0.41 MPa 6. P2=P3 = 0	Cold operation, full LHe inventory, maximum pressure - primary and secondary loads	1.88 K	Q
5	1. Gravity 2. P1 = 0 3. P2 = P3 = 0.205 MPa	Insulating and beam vacuum upset, helium volume evacuated	293 K	Pm, Pl , Pl + Q

Table 11: Load Cases

Component	Internal/External Pressure Load	Thermal Contraction Load	Tuner Extension Load
Nb cavity	U-2(g)	U-2(g)	U-2(g)
Conical heads	U-2(g)	U-2(g)	U-2(g)
Ti shells	UG-27/UG-28	U-2(g)	U-2(g)
Ti bellows	Appendix 26	U-2(g)	U-2(g)

Table 12: Applicable Code, Div. 1 Rules for 1.3 GHz Cavity

Division 1 rules relate to both geometries and loads. For either, there are few rules applicable to the features of the cavity. The only components of the cavity which can be designed for internal and external pressure by the rules of Div. 1 are the Ti shells and the Ti bellows. In the Ti shell, there are two penetrations for connection of externals for which the required reinforcement can also be determined by Code rules.

The conical heads have half-apex angles exceeding 30 degrees, and no knuckles; Div. 1, Appendix 1, 1-5(g) states that their geometry falls under U-2(g).

The Nb cavity itself resembles an expansion joint, but does not conform to the geometries covered in Div. 1, Appendix 26. Therefore, U-2(g) is again applied.

UG-22(h) states that "temperature gradients and differential thermal contractions" are to be considered in vessel design, but provides no rules to cover the cavity. In this analysis, all thermal contraction effects are addressed under U-2(g).

The cavity is also subjected to a controlled displacement loading from the tuner. There are no rules in Div. 1 covering such a loading, so U-2(g) is applied.

The applicable Code rules for each component are summarized in Table 12.

Applying U-2(g)

U-2(g) is satisfied in this analysis by the application of the design-by-analysis rules of the Code, Section VIII, Div. 2, Part 5.

These rules provide protection against plastic collapse, local failure, buckling, fatigue, and ratcheting. The specific sections of Part 5 applied here are:

1. Plastic collapse - satisfied by an elastic stress analysis performed according to 5.2.2.
2. Ratcheting - satisfied by an elastic stress analysis performed according to 5.5.6.1
3. Local failure - satisfied by an elastic stress analysis performed according to 5.3.2
4. Buckling - satisfied by a linear buckling analysis performed according to 5.4.1.2(a).
5. Fatigue assessment - the need for a fatigue analysis is assessed according to 5.5.2.3

In general, an elastic stress analysis begins by establishing stress classification lines (SCLs) through critical sections in the structures according to the procedures of Part 5, Annex 5A, so they are chosen near the discontinuities and are through the thickness of the part. The stresses along these lines are then calculated (in this case, by an FEA), and "linearized" to produce statically equivalent membrane stress and bending stress components. The allowable stress for each component depends

on the category of the stress. This category (or classification) depends on the location of the SCL in the structure, and the origin of the load. Stresses near discontinuities have higher allowables to reflect their ability to redistribute small amounts of plasticity into surrounding elastic material. Stresses produced solely by strain-controlled loads (e.g., thermal contractions and tuner extension) are given higher allowables regardless of their location in the structure.

Allowable stresses are expressed in terms of multiples of S, which is the allowable general primary membrane stress. The values of S used in this analysis are given in Table 10.

A.4.7 Division 1 Calculations by Rule

Ti Cylindrical Shells

Thickness for Internal Pressure

The minimum thickness required for the Ti cylindrical shells under internal pressure can be calculated from UG-27(c)(1):

$$t = \frac{P \cdot R}{S \cdot E - 0.6 \cdot P} \tag{1}$$

Where:
t = required thickness
P = pressure = 0.205 MPa (warm), 0.41 MPa (cold)
R = inside radius of the shell = 115 mm
E = efficiency of seam weld (Type 3 TIG weld: one sided butt weld, no radiography) = 0.6
S = maximum allowable membrane stress = 79 MPa (warm), 255 MPa (cold)

Substituting, the minimum required thickness when warm and pressurized to 0.205 MPa is 0.49 mm. The minimum required thickness when cold and pressurized to 0.41 MPa is 0.31 mm. The actual minimum thickness of the shells is 2.5 mm (0.098 in). Therefore, the Ti cylindrical shells meet the minimum thickness requirements of UG-27 for internal pressure.

Thickness for External Pressure (Buckling)

The minimum thickness required for the Ti cylindrical shells under external pressure can be calculated from UG-28(c). This procedure uses charts found in the Code, Section II, Part D. These charts are based on the geometric and material characteristics of the vessel.

Using:
L = 965 mm
Do = 230 mm
t = 1.4 mm

Then:
L/D = 2.2
Do/t = 165

From the Code, Section II, Part D, Subpart 3, Figure G, the factor A is 0.0003.

The allowable pressure is then

$$P = \frac{2}{3} A E_m \frac{t}{D} = 0.11 MPa \tag{2}$$

Where E_m is the Young modulus of Titanium (107 GPa) and the other parameter have already been introduced.

Substituting gives P = 0.11 MPa. This is approximately equal to the 0.105 MPa maximum external pressure for which the vessel must be qualified.

The actual minimum thickness of the Ti shell is 2.5 mm. This occurs near the ends, and it is unlikely that the collapse is well predicted by this thickness, due to its short length, and proximity to the conical head, which will tend to stiffen the region. If we assume, however, that the entire shell is this thickness, and repeat the calculations above, the allowable external pressure is 0.23 MPa.

If we assume the collapse is better predicted by the predominant thickness of 5 mm, then the factor A = 0.0009, and the allowable external pressure is 0.7MPa.

In any case, the required minimum thickness of 1.4 mm is less than the actual minimum thickness anywhere on the Ti cylindrical shell. Therefore, the Ti shell satisfies the Code requirement for external pressure.

Penetrations

The Ti cylindrical shell contains three penetrations two of which have the same diameter. These are shown in Figure 19. The largest of these penetrations is 95.5 mm (3.76 in.) in diameter.

From UG-36(c)(3):

"Openings in vessels not subject to rapid fluctuations in pressure do not require reinforcement other that inherent in the construction under the following conditions: welded, brazed, and flued connections meeting applicable rules and with a finished opening not larger than 3.5 in diameter - in vessel shells or heads with a required minimum thickness of 3/8 inch or less."

The minimum required thickness of the shell is largest for the case of 0.205 MPa pressurization (warm). This thickness (calculated in 7.1.1) is 0.49 mm. This is less than 9 mm (3/8 in). The two smaller penetrations have a diameter of 16 mm (0.63 in.) which is smaller than 3.5 in. therefore no additional reinforcement is required for these penetrations. However the largest penetration has a diameter of 95.5 mm (3.76 in.) so for this penetration we need further calculations to see if the reinforcement is needed or not.

The following equations are to be used.

$$X = max \begin{cases} d \\ 0.5d + t + t_n \end{cases} \tag{3}$$

and

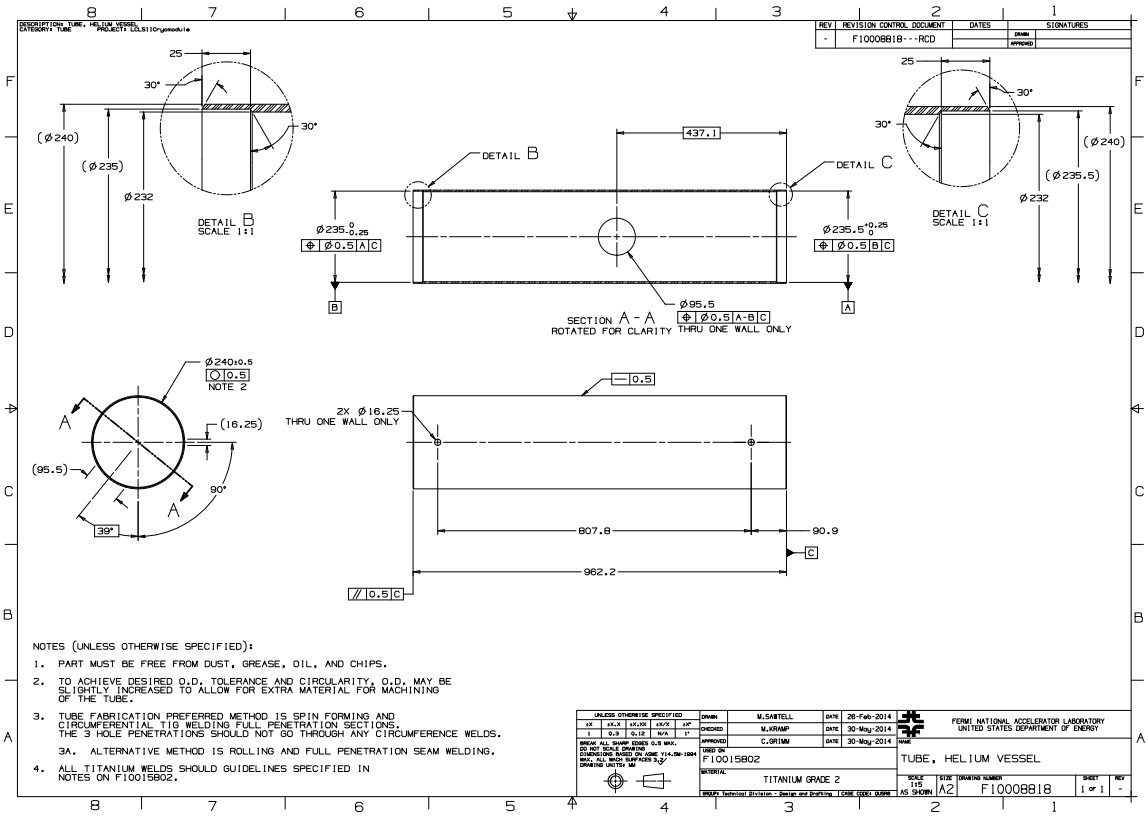

Figure 19: Penetrations in Ti shell

$$Y = min \begin{cases} 2.5t \\ 2.5t_n \end{cases} \tag{4}$$

where

d = diameter of the nozzle = 95.5 mm
t = thickness of the vessel = 5 mm
tn = thickness of the nozzle = 1.65 mm
tr = minimum required thickness of the vessel = 0.49 mm
trn = minimum required thickness of the nozzle = 0.25 mm

Requested Area:

$$A_r = d \cdot t_r = 48.2mm^2 \tag{5}$$

Vessel Available Area:

$$A_1 = (2 \cdot X - d) \cdot (t - t_r) = d \cdot (t - t_r) = 433mm^2 \tag{6}$$

Nozzle Available Area:

$$A_2 = 2 \cdot Y \cdot (t - t_{rn}) = 5 \cdot t \cdot (t - t_{rn}) = 35mm^2 \tag{7}$$

Since the Requested Area is smaller than the total Available Area the reinforcement is not needed for the two phase opening.

Ti Bellows

The design of metallic expansion joints (e.g., bellows) is addressed by Appendix 26 of the Code. The formulas permit calculation of internal and external pressure limits. In a bellows, the pressure may be limited not only by stress, but by squirm (internal pressure), and collapse (external pressure.) The analysis shows that the bellows with an internal MAWP of 2.0-bar (30- psi) at room temperature or an external MAWP of 1.0-bar (14.5-psia) follows the rules of Appendix 26. The allowed value S is for titanium at room temperature (see Table 10).

Table 13 defines the stresses that are examined in the bellows analysis. Table 14 summarizes how the calculated or actual stresses comply with the allowed stresses.

The details of the Appendix 26 calculations are presented in Appendix C.

Longitudinal Weld in Bellows Convolution

The allowable stress S = 79 MPa for the bellows convolution assumes a weld joint efficiency of 1.0. The bellows is hydro formed from a rolled tube with a longitudinal (seam) weld that is not radiographed. Let's evaluate the weld by de-rating the allowable stress S by a factor of 0.6, which is the factor for a Type 3 weld that is not radiographed. The de-rated allowable stress is

S1	Circumferential membrane stress in bellows tangent, due to pressure P	[psi]
S2e	Circumferential membrane stress due to pressure P for end convolutions	[psi]
S2i	Circumferential membrane stress due to pressure P for end convolutions	[psi]
S11	Circumferential membrane stress due to pressure P for the collar	[psi]
S3	Meridional membrane stress due to pressure P	[psi]
S4	Meridional bending stress due to pressure P	[psi]
P	Design pressure	[psi]
S	Allowable stress of bellows material	[psi]
Cwc	Weld joint efficiency of collar to bellows (no radiography, single butt weld)	-
Sc	Allowable stress of collar material	[psi]
Kf	Coefficient for formed bellows	-
Psc	Allowable internal pressure to avoid column instability	[psi]
Psi	Allowable internal pressure based on in-plane instability	[psi]
Pa	Allowable external pressure based on instability	[psi]

Table 13: Definition of Stresses, Coefficients in the Bellows Analysis following the Code, Division 1, Appendix 26

Calculated or Actual Value	Allowed Value	Requirement	Applicable Paragraph
S1 = 428 psi	S = 11500 psi	S1 < S	26-6.3.1
S11 = 441 psi	Cwc*Sc = 6900 psi	S11 < Cwc*Sc	26-6.3.2
S2e = 995 psi	S = 11500 psi	S2e < S	26-6.3.3(a)(1)
S2i = 5545 psi	S = 11500 psi	S2i < S	26-6.3.3(a)(2)
S3+S4 = 4275 psi	Kf*S = 34500 psi	(S3+S4) < (Kf*S)	26-6.3.3(d)
P = 30 psi	Psc = 64760000 psi	P ≤ Psc	26-6.4.1
P = 30 psi	Psi = 198 psi	P ≤ Psi	26-6.4.2
External pressure = 14.5 psia	Pa = 1077 psi	Ext. pressure < Pa	26-6.5

Table 14: Complying with Appendix 26 Rules for Internal Pressure of 2.0-bar (30-psi)

79MPa*0.6=47.4MPa. This is still greater than the calculated circumferential stresses of S1, S2e, and S2i in the convolutions.

Fatigue Analysis for Titanium Bellows

The equations in the Code for fatigue analysis of a bellows are not valid for titanium. The manufacturer of the titanium bellows for the helium vessel provided design calculations following the Standards of the Expansion Joint Manufacturers Association [8]. The allowable fatigue life is calculated with the equation

$$N_c = \left(\frac{c}{S_T - b} \right)^a \tag{8}$$

where a, b, and c are material and manufacturing constants. The manufacturer uses the same material and manufacturing constants as what EJMA uses for austenitic stainless steel. In addition, the manufacturer includes a safety factor of two in their calculation of the allowable number of cycles since the titanium bellows is a custom-made project. The manufacturer calculated an allowable number of cycles to be NC = 37560.

The slow tuner system has the capability of increasing the vessel length less than 2.0-mm after each cool down. The bellows extension will occur 200 times over the lifetime of the vessel. This is far less than the allowable number of cycles, so the bellows is designed well within the limits of fatigue failure.

Detailed Code calculations are shown in the section Fatigue Analysis of the Titanium Bellows in Appendix C.

A.4.8 Finite Element Model

A 3-d finite element half model was created in ANSYS. Elements were 10-node tetrahedra, and 20-node hexahedra. Material behavior was linear elastic.

The lever tuner is very rigid. Axial constraint of the helium vessel was therefore simulated by constraining the outer surface of each flange in the Z (axial) direction. This constraint places the line of action at a maximum distance from the shell, producing the maximum possible moment on the welds between the tuner flanges and the shell.

For the cool down loading, the distance between the Ti flanges was assumed to close by an amount equivalent to the shrinkage of a rigid stainless steel mass spanning the flanges.

The constraint against gravity is simulated by fixing the flange outer surface nodes at 180 degrees in the Y (vertical) direction.

The finite element model is shown in Figure 20. Figure 21 shows the mesh detail at various locations within the model.

The complete model was used to demonstrate satisfaction of the plastic collapse, ratcheting, and local failure criteria. Subsets of the model were also used to address the linear buckling of the Nb cavity and conical head.

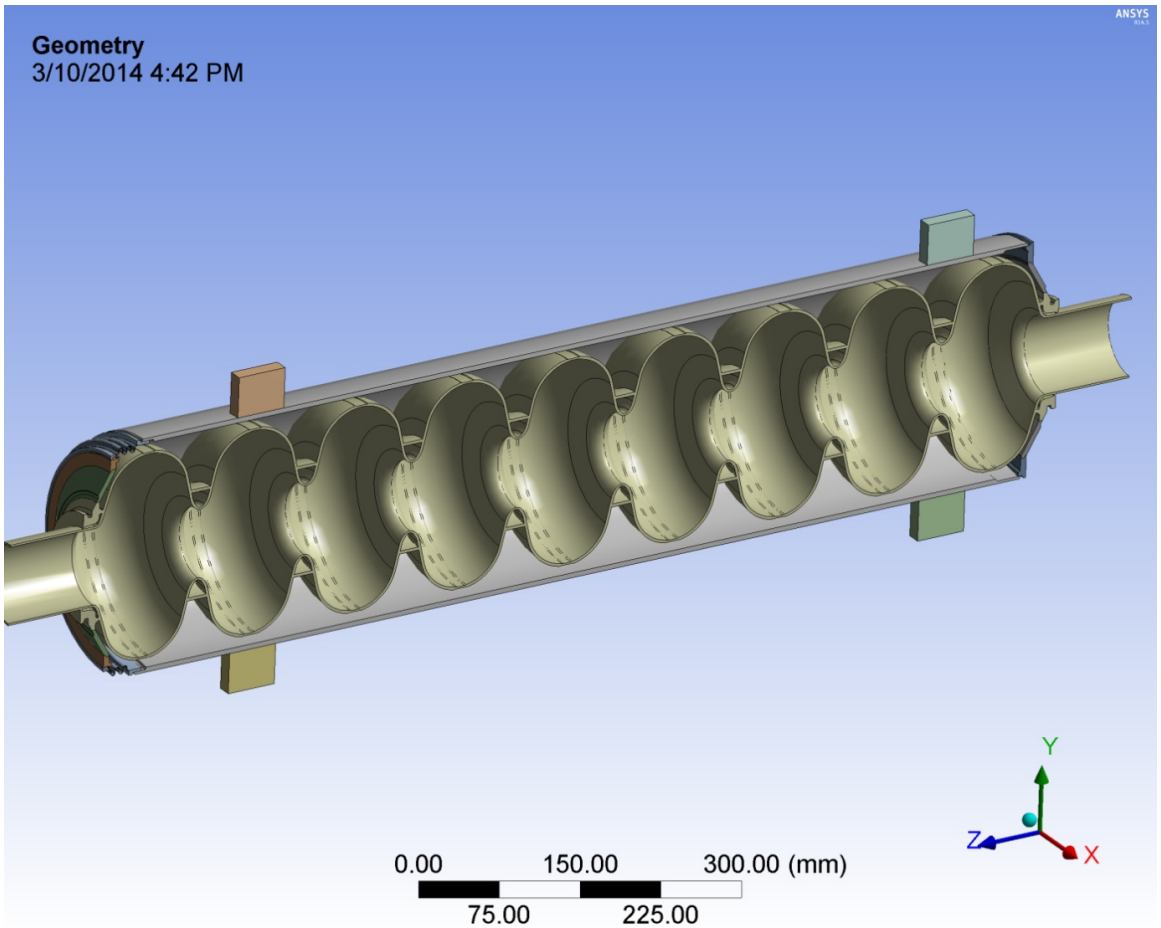

Figure 20: The Finite Element Model

A.4.9 Stress Analysis Results

General

The complete finite element model was run for the five load cases. Stress classification lines, shown in Figure 22, were established through the critical sections of the structure. The stresses along these lines were linearized with ANSYS, and separated into membrane and bending components. The linearized stresses (expressed in terms of Von Mises equivalent stress, as required by 5.2.2.1(b)) are categorized according to the Code, Div. 2, Part 5, 5.2.2.2 into primary and secondary stresses.

The primary and secondary stresses along each SCL for each of the five load cases are given from Tables 15, 16, 17, 18, and 19. Where more than one weld of a given number is present (as indicated in Figure 12 and in Figure 13) the weld with the highest stresses was assessed.

The stresses from Tables 15, 16, 17, 18, and 19 are used to demonstrate satisfaction of two of the criteria listed in the Stress Analysis Approach of this report: Protection against plastic collapse, and protection against ratcheting. Demonstrating protection against local failure employs the complete model, but requires the extraction of different quantities.

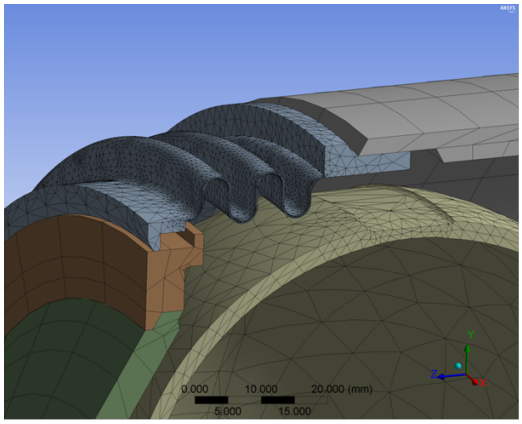

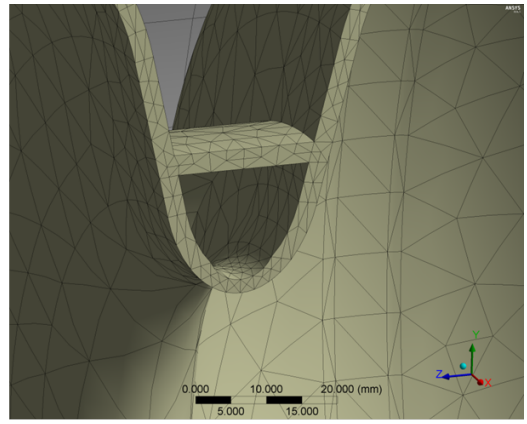

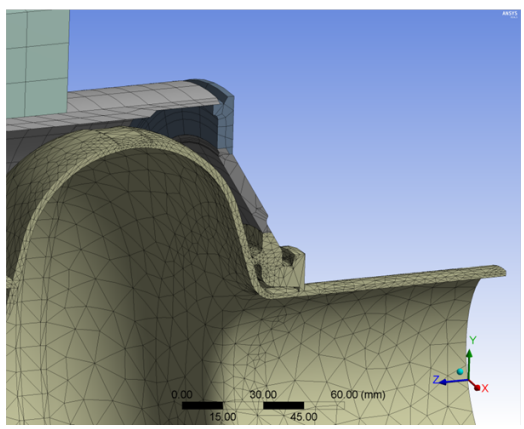

Figure 21: Mesh Details

Note: The required minimum thicknesses of the Ti shells for internal and external pressure are calculated by Div. 1 rules in the section Division 1 Calculations by Rule of this report. Therefore, no SCLs addressing the Ti shell thickness far from welds or other discontinuities are established here. See Appendix B for verification that the FEA produces the correct hoop stress in the Ti shell.

Collapse Pressure

The criterion for protection against plastic collapse is given in Div. 2, 5.2.2. The criterion is applied to load cases in which primary (load-controlled) stresses are produced. For this analysis, this is Load Case 1, Load Case 2, and Load Case 5.

The following stress limits must be met (per 5.2.2.4(e)):

Material	SCL	Weld No.	Weld Efficiency	Membrane Stress [MPa]	Classification	Allowable Stress [MPa]	Ratio
Nb weld	A	FP1	0.6	1.51	Pm	12	0.12
Nb weld	B	FP2	0.7	1.59	Pl	21	0.07
Nb weld	C	FP3	0.6	2.83	Pm	12	0.23
Nb weld to NbTi	D	MC4	0.6	3.19	Pm	12	0.26
Ti weld to NbTi	E	MC5	0.7	3.5	Pm	55	0.06
Ti weld	F	FP6	0.6	1.62	Pm	47	0.03
Ti weld	G	FP7	0.7	8.22	Pm	55	0.15
Nb weld	H	11	0.6	5.43	Pm	12	0.45
Nb weld	I	9	0.6	3.77	Pm	12	0.31
Nb weld	J	10	0.6	3.41	Pm	12	0.28
Ti	K	–	1	27.14	Pm	79	0.34
Ti weld	L	MC12	0.7	12.37	Pm	55	0.22
TI weld	M	8	0.6	3.67	Pm	47	0.08
Material	SCL	Weld No.	Weld Efficiency	Membrane + Bending [MPa]	Classification	Allowable Stress [MPa]	Ratio
Nb weld	A	FP1	0.6	3.76	Pm+Pb	18	0.21
Nb weld	B	FP2	0.7	2.17	Pl+Q	43	0.05
Nb weld	C	MC3	0.6	17.78	Q	36	0.49
Nb weld to NbTi	D	MC4	0.6	10.08	Pm+Pb	18	0.55
Ti weld to NbTi	E	MC5	0.7	20.18	Pm+Pb	83	0.24
Ti weld	F	FP6	0.6	1.14	Pm+Pb	71	0.02
Ti weld	G	FP7	0.7	10.19	Pm+Pb	83	0.12
Nb weld	H	11	0.6	5.6	Pm+Pb	18	0.31
Nb weld	I	9	0.6	4.5	Q	36	0.12
Nb weld	J	10	0.6	4.72	Pm+Pb	18	0.26
Ti	K	–	1	42.43	Pm+Pb	118	0.36
Ti weld	L	MC12	0.7	12.97	Pm+Pb	83	0.16
TI weld	M	8	0.6	5.49	Pm+Pb	71	0.08

Table 15: Load Case 1 - Stress Results

Material	SCL	Weld No.	Weld Efficiency	Membrane Stress [MPa]	Classification	Allowable Stress [MPa]	Ratio
Nb weld	A	FP1	0.6	3.31	Pm	82	0.04
Nb weld	B	FP2	0.7	3.59	Pl	144	0.02
Nb weld	C	FP3	0.6	5.22	Pm	82	0.06
Nb weld to NbTi	D	MC4	0.6	6.62	Pm	75	0.09
Ti weld to NbTi	E	MC5	0.7	7.39	Pm	87	0.08
Ti weld	F	FP6	0.6	3.17	Pm	153	0.02
Ti weld	G	FP7	0.7	16.43	Pm	179	0.09
Nb weld	H	11	0.6	10.53	Pm	82	0.13
Nb weld	I	9	0.6	7.31	Pm	82	0.09
Nb weld	J	10	0.6	6.8	Pm	82	0.08
Ti	K	–	1	54.07	Pm	255	0.21
Ti weld	L	MC12	0.7	25.67	Pm	179	0.14
TI weld	M	8	0.6	7.02	Pm	153	0.05
Material	SCL	Weld No.	Weld Efficiency	Membrane + Bending [MPa]	Classification	Allowable Stress [MPa]	Ratio
Nb weld	A	FP1	0.6	7.92	Pm+Pb	123	0.06
Nb weld	B	FP2	0.7	4.82	Pl+Q	288	0.02
Nb weld	C	MC3	0.6	33.42	Q	247	0.14
Nb weld to NbTi	D	MC4	0.6	20.37	Pm+Pb	112	0.18
Ti weld to NbTi	E	MC5	0.7	41.47	Pm+Pb	131	0.32
Ti weld	F	FP6	0.6	4.32	Pm+Pb	230	0.02
Ti weld	G	FP7	0.7	21	Pm+Pb	268	0.08
Nb weld	H	11	0.6	10.86	Pm+Pb	123	0.09
Nb weld	I	9	0.6	9.85	Q	247	0.04
Nb weld	J	10	0.6	9.22	Pm+Pb	123	0.07
Ti	K	–	1	83.03	Pm+Pb	383	0.22
Ti weld	L	MC12	0.7	26.91	Pm+Pb	268	0.1
TI weld	M	8	0.6	10.78	Pm+Pb	230	0.05

Table 16: Load Case 2 - Stress Results

Material	SCL	Weld No.	Weld Efficiency	Membrane Stress [MPa]	Classification	Allowable Stress [MPa]	Ratio
Nb weld	A	FP1	0.6	11.79	Pm	82	0.14
Nb weld	B	FP2	0.7	3.75	Pl	144	0.03
Nb weld	C	MC3	0.6	29.74	Pm	82	0.36
Nb weld to NbTi	D	MC4	0.6	37.06	Pm	75	0.5
Ti weld to NbTi	E	MC5	0.7	22.74	Pm	87	0.26
Ti weld	F	FP6	0.6	17.71	Pm	153	0.12
Ti weld	G	FP7	0.7	2.38	Pm	179	0.01
Nb weld	H	11	0.6	15.95	Pm	82	0.19
Nb weld	I	9	0.6	29.48	Pm	82	0.36
Nb weld	J	10	0.6	13.31	Pm	82	0.16
Ti	K	–	1	57.81	Pm	255	0.23
Ti weld	L	MC12	0.7	22.83	Pm	179	0.13
TI weld	M	8	0.6	19.14	Pm	153	0.12
Material	SCL	Weld No.	Weld Efficiency	Membrane + Bending [MPa]	Classification	Allowable Stress [MPa]	Ratio
Nb weld	A	FP1	0.6	14.34	Q	247	0.06
Nb weld	B	FP2	0.7	5.3	Q	288	0.02
Nb weld	C	MC3	0.6	51.11	Q	247	0.21
Nb weld to NbTi	D	MC4	0.6	45.91	Q	224	0.2
Ti weld to NbTi	E	MC5	0.7	59.69	Q	262	0.23
Ti weld	F	FP6	0.6	17.85	Q	460	0.04
Ti weld	G	FP7	0.7	23.91	Q	536	0.04
Nb weld	H	11	0.6	20.54	Q	247	0.08
Nb weld	I	9	0.6	42.69	Q	247	0.17
Nb weld	J	10	0.6	16.28	Q	247	0.07
Ti	K	–	1	509.66	Q	766	0.67
Ti weld	L	MC12	0.7	23.73	Q	536	0.04
TI weld	M	8	0.6	19.87	Q	460	0.04

Table 17: Load Case 3 - Stress Results

Material	SCL	Weld No.	Weld Efficiency	Membrane Stress [MPa]	Classification	Allowable Stress [MPa]	Ratio
Nb weld	A	FP1	0.6	11.05	Pm	82	0.13
Nb weld	B	MC2	0.7	1.79	Pl	144	0.01
Nb weld	C	MC3	0.6	28.6	Pm	82	0.35
Nb weld to NbTi	D	FP4	0.6	35.43	Pm	75	0.47
Ti weld to NbTi	E	FP5	0.7	20.99	Pm	87	0.24
Ti weld	F	FP6	0.6	17.61	Pm	153	0.11
Ti weld	G	FP7	0.7	14.35	Pm	179	0.08
Nb weld	H	11	0.6	5.71	Pm	82	0.07
Nb weld	I	9	0.6	30.06	Pm	82	0.37
Nb weld	J	10	0.6	14.76	Pm	82	0.18
Ti	K	–	1	6.65	Pm	255	0.03
Ti weld	L	MC12	0.7	2.89	Pm	179	0.02
TI weld	M	8	0.6	12.42	Pm	153	0.08
Material	SCL	Weld No.	Weld Efficiency	Membrane + Bending [MPa]	Classification	Allowable Stress [MPa]	Ratio
Nb weld	A	FP1	0.6	12.76	Q	247	0.05
Nb weld	B	FP2	0.7	2.64	Q	288	0.01
Nb weld	C	MC3	0.6	72.99	Q	247	0.3
Nb weld to NbTi	D	FP4	0.6	42.59	Q	224	0.19
Ti weld to NbTi	E	MC5	0.7	53.81	Q	262	0.21
Ti weld	F	FP6	0.6	17.91	Q	460	0.04
Ti weld	G	FP7	0.7	31.53	Q	536	0.06
Nb weld	H	11	0.6	13.38	Q	247	0.05
Nb weld	I	9	0.6	48.95	Q	247	0.2
Nb weld	J	10	0.6	14.95	Q	247	0.06
Ti	K	–	1	561.03	Q	766	0.73
Ti weld	L	MC12	0.7	3.17	Q	536	0.01
TI weld	M	8	0.6	12.93	Q	460	0.03

Table 18: Load Case 4 - Stress Results

Material	SCL	Weld No.	Weld Efficiency	Membrane Stress [MPa]	Classification	Allowable Stress [MPa]	Ratio
Nb weld	A	FP1	0.6	1.47	Pm	12	0.12
Nb weld	B	FP2	0.7	1.4	Pl	21	0.07
Nb weld	C	MC3	0.6	2.72	Pm	12	0.22
Nb weld to NbTi	D	MC4	0.6	2.11	Pm	12	0.17
Ti weld to NbTi	E	MC5	0.7	2.23	Pm	55	0.04
Ti weld	F	FP6	0.6	0.82	Pm	47	0.02
Ti weld	G	FP7	0.7	3.11	Pm	55	0.06
Nb weld	H	11	0.6	2.24	Pm	12	0.18
Nb weld	I	9	0.6	2.29	Pm	12	0.19
Nb weld	J	10	0.6	1.74	Pm	12	0.14
Ti	K	–	1	13.3	Pm	79	0.17
Ti weld	L	MC12	0.7	7.28	Pm	55	0.13
TI weld	M	8	0.6	1.63	Pm	47	0.03
Material	SCL	Weld No.	Weld Efficiency	Membrane + Bending [MPa]	Classification	Allowable Stress [MPa]	Ratio
Nb weld	A	FP1	0.6	2.84	Pm+Pb	18	0.16
Nb weld	B	FP2	0.7	1.84	Pl+Q	43	0.04
Nb weld	C	MC3	0.6	6.04	Q	36	0.17
Nb weld to NbTi	D	MC4	0.6	5.24	Pm+Pb	18	0.29
Ti weld to NbTi	E	MC5	0.7	11.44	Pm+Pb	83	0.14
Ti weld	F	FP6	0.6	1.09	Pm+Pb	71	0.02
Ti weld	G	FP7	0.7	4.98	Pm+Pb	83	0.06
Nb weld	H	11	0.6	2.38	Pm+Pb	18	0.13
Nb weld	I	9	0.6	4.15	Q	36	0.11
Nb weld	J	10	0.6	2.09	Pm+Pb	18	0.11
Ti	K	–	1	18.36	Pm+Pb	118	0.16
Ti weld	L	MC12	0.7	7.62	Pm+Pb	83	0.09
TI weld	M	8	0.6	2.62	Pm+Pb	71	0.04

Table 19: Load Case 5 - Stress Results

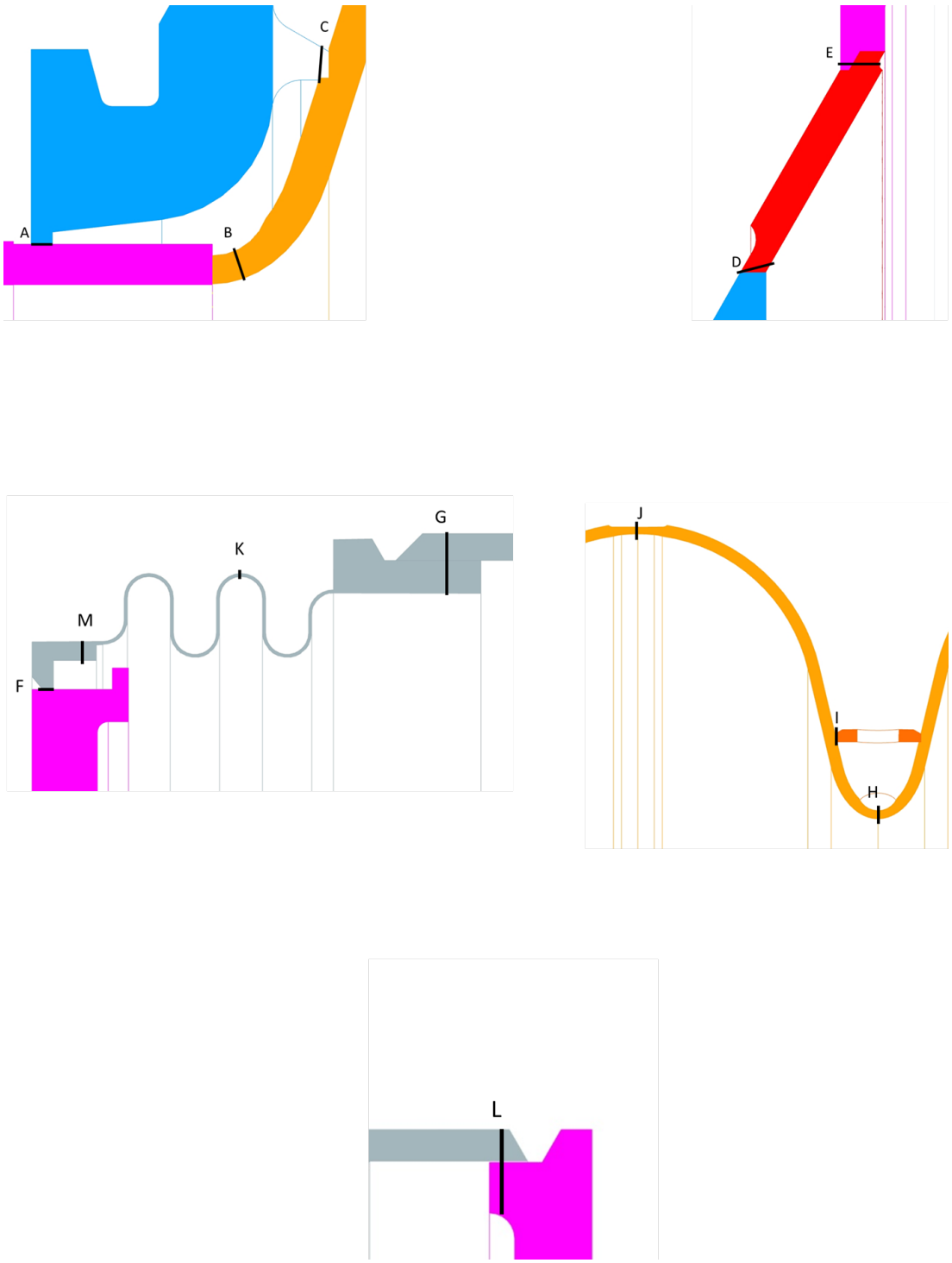

Figure 22: Stress Classification Lines

P_m=primary membrane stress $\leq$S
P_l=primary local membrane stress $\leq$1.5*S
P_l+P_b=primary local membrane +primary bending $\leq$1.5*S

where S = maximum allowable primary membrane stress.

In this work, the P_l classification is limited to SCL B (weld 2). All other membrane stresses extracted on the SCLs are classified as the more conservative P_m, which is then used in place of P_l in 3 above.

Examining Table 15, Table 16 and Table 19, it is found that the closest approach to the limiting stress for any load case occurs at SCL D (weld 4, the weld between the end disk flange and the transition ring) in Load Case 1, where the primary membrane stress plus the primary bending stress of 10.1 MPa psi compares to an allowable of 18 MPa.

Ratcheting

Protection against ratcheting, the progressive distortion of a component under repeated loadings, is provided by meeting the requirements of Div. 2, 5.5.6. Specifically, the following limit must be satisfied:

$\delta S_n, k \leq S_P S$

where:
$\delta S_n, k$=primary plus secondary equivalent stress range
$S_P S$=allowable limit on primary plus secondary stress range

The stress range $\delta S_n, k$ must take into account stress reversals; however, there are no stress reversals in normal operation of the cavity, so for this analysis $\delta S_n, k$ is equal to the primary plus secondary stresses given in Tables 15, 16, 17, 18, and 19.

Examination of the tables shows that the cavity satisfies the ratcheting criterion; the closest approach to the allowable primary plus secondary stress range limit occurs for Load Case 4 (gravity + liquid head + 0.4 MPa + blade tuner extension + cool down) in the Ti bellows. For this load case, the calculated primary plus secondary stress range reaches 73% of the allowable.

Local Failure

The criterion for protection against local failure is given in Div. 2, 5.3.2:

$$\sigma_1 + \sigma_2 + \sigma_3 \leq 4S \tag{9}$$

where σ_1, σ_2, σ_3 are the principal stresses at any point in the structure, and S is the maximum allowable primary membrane stress (see Table 10), multiplied by a joint efficiency factor if applicable.

This criterion is assumed to be satisfied if the sum of the principal stresses calculated at every element centroid in the model meets the stress limit for the material.

Table 20 lists the maximum allowable sum of principal stresses for each material at each load case. These values are four times the full values given for maximum primary membrane stress times a joint efficiency for a Type 3 butt weld of 0.6. For those locations which are not near a joint, or are near one of the Type 2 butt weld joints, this is conservative.

Load Case (Temperature)	Nb	TiNb	Ti
1 (293 K)	48	300	190
2 (1.88 K)	329	300	612
3 (1.88 K)	329	300	612
4 (1.88 K)	329	300	612
5 (293 K)	48	300	190

Table 20: Maximum Allowable Sum of Principal Stresses [MPa]

Load Case	Maximum Principal Stress Sum [MPa]	Allowable Stress [MPa]	Location	Ratio Sfe/Sa
1	44	48	Weld 3	0.92
2	115	329	Weld 3	0.35
3	287	329	Weld 3	0.87
4	308	329	Weld 3	0.94
5	11	48	Weld 3	0.23

Table 21: Local Failure Criterion for Niobium

The results for each material and each load case are given in Tables 21, 22, and 23. The closest approach to the allowable limit occurs in the iris support ring welds for Load Case 4 (cold, 0.41 MPa internal pressure, tuner extension), which reaches 0.94 of the allowable. For all other materials/load cases, the principal stress sum lies below the allowable.

Buckling

Ti Shells and Bellows

The buckling of the Ti shells and bellows is addressed by Div. 1 rules in an earlier section of this report.

The Nb Cavity

The Code, Div. 1, does not contain the necessary geometric and material information to perform a Div. 1 calculation of Nb cavity collapse. Therefore, the procedures of Div. 2, Part 5, 5.4

Load Case	Maximum Principal Stress Sum [MPa]	Allowable Stress [MPa]	Location	Ratio Sfe/Sa
1	23	300	Weld 5	0.08
2	44	300	Weld 5	0.15
3	53	300	Weld 4	0.18
4	53	300	Weld 4	0.18
5	7	300	Weld 5	0.02

Table 22: Local Failure Criterion for Ti-45Nb

Load Case	Maximum Principal Stress Sum [MPa]	Allowable Stress [MPa]	Location	Ratio Sfe/Sa
1	96	190	Bellows - SCL K	0.51
2	197	612	Bellows - SCL K	0.32
3	523	612	Bellows - SCL K	0.86
4	498	612	Bellows - SCL K	0.81
5	43	190	Bellows - SCL K	0.23

Table 23: Local Failure Criterion for TiGr2

"Protection Against Collapse from Buckling" are applied.

A linear elastic buckling analysis was performed with ANSYS. A design factor was applied to the predicted collapse pressure to give the maximum allowable external working pressure. This design factor, taken from 5.4.1.3(c) for spherical shells, is 16. Only the cavity was modeled. The ends are constrained in all degrees of freedom to simulate the effect of attachment to the conical heads and Ti shells of the helium vessel.

The predicted buckled shape is shown in Figure 23. The critical pressure is 96.7 MPa. Applying the design factor gives this component a maximum allowable external working pressure of 6 MPa, which is far greater than the required MAWP of 0.1 MPa external.

The ANSYS buckling pressure seems large; as a check, a calculation of the collapse of a sphere of similar dimensions to those of a cell was done using a formula from Ref. 4. This calculation, given in B.2 of this report, produces a similar result.

Conical Heads

The buckling pressure of the conical heads was calculated by the linear buckling approach used for the Nb cavity.

A model of the head only was made. It was constrained against axial motion where it connects to the Ti shell, but allowed to rotate freely, and translate radially.

The predicted buckling shape is shown in Figure 24. The critical buckling pressure is 358 MPa. Applying the design factor of 2.5 (from 5.4.1.3(b) for conical shells under external pressure) gives an MAWP for external pressure of 143 MPa, which is well above the actual maximum pressure of 0.1 MPa.

Fatigue Assessment

The need for a fatigue analysis can be determined by applying the fatigue assessment procedures of Div. 2, Part 5, 5.5.2.3, "Fatigue Analysis Screening, Method A."

In this procedure, a load history is established which determines the number of cycles of each

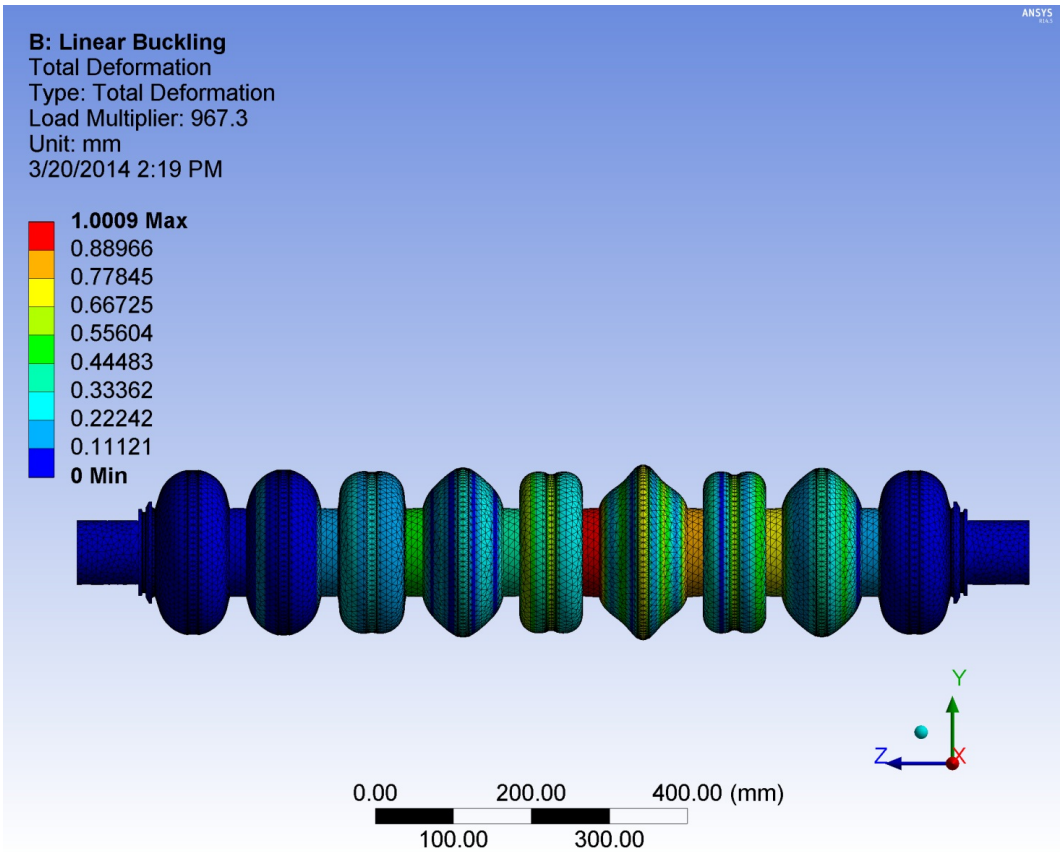

Figure 23: Lowest buckling mode of Nb cavity, Pcr = 96.7 MPa

loading experienced by the Dressed SRF Cavity. These numbers are compared against criteria which determine whether a detailed fatigue analysis is necessary.

The load history consists of multiple cool down, pressurization, and tuning cycles. Estimates for the number of cycles of each load a cavity might experience are given in Table 24.

The information of Table 24 is used with the criterion of Table 25 (a reproduction of Table 5.9 of Part 5 of the Code) to determine whether a fatigue analysis is necessary.

The tuning load has no direct analog to the cycle definitions of Table 25. Therefore, it will be assigned its own definition as a cyclic load $N_{\delta tuner}$ and treated additively.

For the Nb cavity, construction is integral, and there are no attachments or nozzles in the knuckle

Loading	Designation	Number of Cycles
Cooldown	$N_{\Delta TE}$	100
Pressurization	$N_{\Delta FP}$	200
Tuning	$N_{\Delta tuner}$	200

Table 24: Estimated Load History of Dressed SRF Cavity

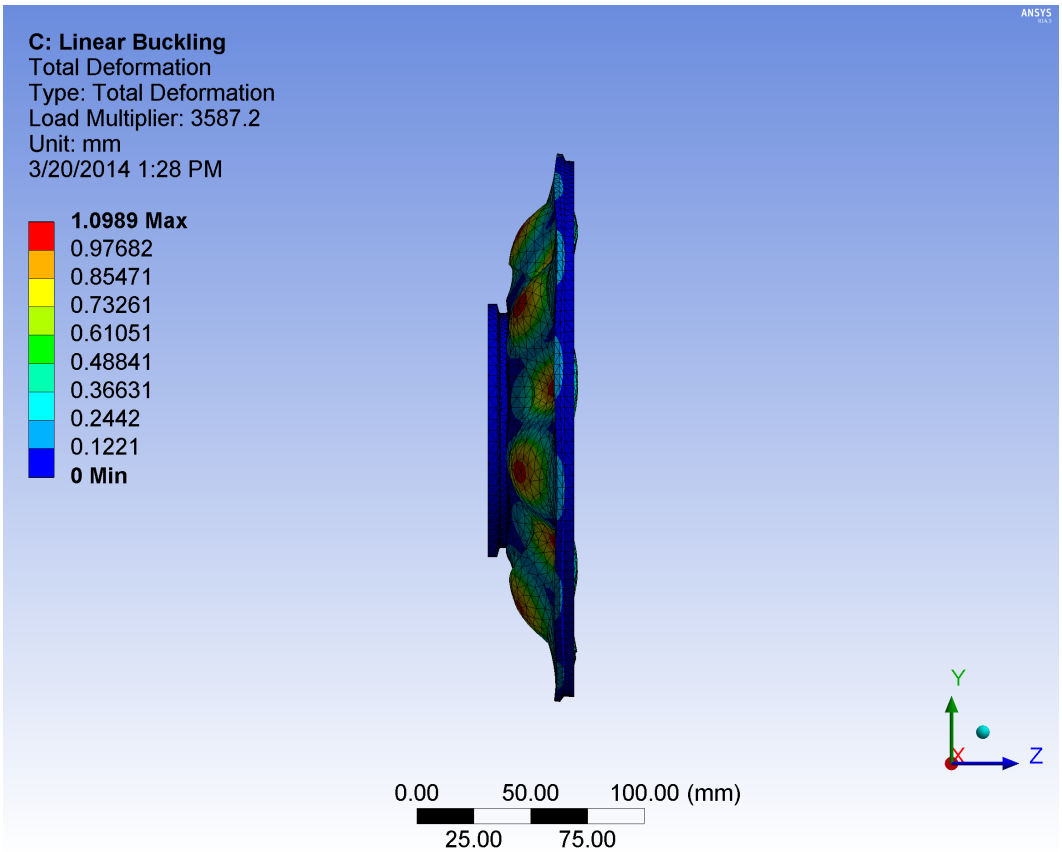

Figure 24: Buckling of the conical heads, P = 359 MPa

regions of the heads. Therefore, the applicable criterion is

$$N_{\delta TE} + N_{\delta FP} + N_{\delta tuner} \leq 1000 \tag{10}$$

$$100 + 200 + 200 = 500 \leq 1000 \tag{11}$$

The criterion is satisfied, and no fatigue assessment is necessary for the Nb cavity.

Beam Vacuum MAWP

The beam vacuum internal MAWP is 3.0-bar (45-psia). Referring to Figure 18 and the Load Case 5 of Table 11, the LHe volume (P1) is set at 0 bar, and the beam vacuum (P3) is set at 1 bar, resulting in a 0.1 MPa differential across the cavity wall. As shown in Figure 22, the stress classification lines (SCL) that show stresses in the cavity are B, C, H, I, and J. As seen in Table 19, the maximum ratio of the calculated stress to the allowable stress occurs in SCL C, which is the weld to the end disk flange. The ratio is 0.22.

At NML, where the string of dressed cavities within the cryomodule is tested, the niobium cavity would operate under vacuum as part of the beam vacuum. The beam pipe venting line has a

Description	
Attachments and nozzles in the knuckle region of formed heads	$N_{\Delta FP} + N_{\Delta PO} + N_{\Delta TE} + N_{\Delta T\alpha} \leq 350$
All other components that do not contain a flaw	$N_{\Delta FP} + N_{\Delta PO} + N_{\Delta TE} + N_{\Delta T\alpha} \leq 1000$
Attachments and nozzles in the knuckle region of formed head	$N_{\Delta FP} + N_{\Delta PO} + N_{\Delta TE} + N_{\Delta T\alpha} \leq 60$
All other components that do not contain a flaw	$N_{\Delta FP} + N_{\Delta PO} + N_{\Delta TE} + N_{\Delta T\alpha} \leq 400$
$N_{\Delta FP}$ = expected number of full-range pressure cycles, including startup and shutdown $N_{\Delta PO}$ = expected number of operating pressure cycles in which the range of pressure variation exceeds 20% of the design pressure for integral construction or 15% of the design pressure for non-integral construction $N_{\Delta TE}$ = effective number of changes in metal temperature difference between any two adjacent points $N_{\Delta T\alpha}$ = number of temperature cycles for components involving welds between materials having different coefficients of thermal expansion that cause the value of $(\alpha 1 - \alpha 2)\Delta T$ to exceed 0.00034	

Table 25: Reproduction of Table 5.9 of Part 5, "Fatigue Screening Criteria for Method A"

Source of Helium Pressure	Required relief capacity (SCFM air)	Available relief capacity (SCFM Air)
Loss of cavity vacuum	750	1311
Loss of insulating vacuum	683	1202

Table 26: Summary of Required and Available Relief Capacities at HTS

rupture disk with a set pressure as high as 25-psig (40-psia) (0.27 bar). In the failure mode where liquid helium leaks into the cavity, and then the cavity is warmed up, the helium would expand and pressurize the cavity. For this failure mode of helium expanding inside the cavity, the cavity can be pressurized to 3 bar, while the liquid helium volume (P1) is 0 bar. The ratio of calculated stress to the allowable stress would increase proportionally to the cavity pressure. At 45-psia (3 bar) the ratio increases to 0.66 so the stresses are well within the allowable. The niobium cavity within the helium vessel can safely see an internal pressure of 45 psia (3 bar).

A.5 System Venting Verification

The 1.3-GHz Dressed SRF Cavity may be performance tested in the Horizontal Test Stand (HTS). If the cavity becomes part of a cryomodule, then it may be used at New Muon Lab. The venting system of each location is documented by the AD/Cryo department, which operates the systems. The documents include a description of the venting system, available relief capacities, and pressure drop calculations. This pressure vessel note shows the required relief capacity and compares it to the available relief capacities.

A.5.1 Summary

The AD/Cryo document titled "Meson Detector Building, Horizontal Test System Main Relief Valve Analysis" http://www-cryo.fnal.gov/MDB/SitePages/Calculations.aspx, under the "HTS" folder) lists the most updated calculations on the relief system for the Horizontal Test System. The system is protected by two safety valves, which are shown on the flow schematic 5520.000-ME-440517. The available relief capacities are listed in Table 1 of the AD/Cryo document.

- SVH2: Set pt. = 15-psig, Leser relief valve, model 4414.7932, nominal size = 1.5" x 2.5"
- SVH1: Set pt. = 12-psig, BS&B burst disk, nominal size 3"

Table 26 shows the available and the required flow capacities for the HTS system.

The AD/Cryo document titled "New Muon Lab Cryomodule, Feed Cap, and End Cap Relief Valve System Analysis" http://www-cryo.fnal.gov/NML/SitePages/PipingSystemEngineeringNotes.aspx, under the folder "Approved") lists the most updated calculations on the NML relief system. There are two safety relief valves for venting helium from the cryomodule. The valves are shown on drawing 5520.000-ME-458097, the schematic of the cryomodule at NML with the relief valves. Both are rupture disks, as detailed below (see Tables 1, 2, and 3 in the AD/Cryo document):

Source of Helium Pressure	Required relief capacity (SCFM air)	Available relief capacity (SCFM Air)
Loss of cavity vacuum	6061	8053
Loss of insulating vacuum	3737	8053

Table 27: Summary of Required and Available Relief Capacities at NML

- SV-803-H: Set pt. = 43 psig (4-bar), Leser Model 4414.4722, nominal size = 6"x8", 8053-SCFM air (16,175-g/sec)
- SV-806-H: Set pt. = 15 psig (2-bar), Leser Model 4414.7942, nominal size = 2"x3", 951-SCFM air (217-g/sec)

Table 27 summarizes the possible sources of helium pressure and the calculated required flow rate for the cryomodule.

For the mass flow rates that are listed, the following equation is used for conversion to volumetric flow rate (SCFM-air): [9]

$$Q_a = \frac{13.1 \cdot WC_a}{60 \cdot C}\sqrt{\frac{ZTM_a}{MZ_aT_a}} \tag{12}$$

Where:

Qa = volumetric flow rate [SCFM air]
W = mass flow rate of helium [lbm/hr]
Ca = air gas constant = 356
Za = compressibility factor of air = 1
Ta = air temperature at standard conditions [°R]
Ma = air molecular weight = 4
C = helium gas constant = 378
M = helium molecular weight = 28 kg/kmol
Z = compressibility factor of helium

A.5.2 Detailed Calculation for System Venting

Temperature of relief flow (CGA S-1.3-2008 paragraph 6.1.3) [10]

The CGA specifies a temperature to calculate the flow capacities of pressure relief devices for both critical and supercritical fluids. The temperature to be used is determined by calculating the square root of fluid's specific volume and dividing it by the specific heat input at the flow rating pressure. The sizing temperature would be when this calculation is at a maximum. For the relief pressure of 4.4-bar (110% of the cold MAWP), the temperature is 6.8 K. This results in a compressibility factor of helium equal to 0.58.

At HTS: Loss of RF Cavity (Beam) Vacuum and Loss of Insulating Vacuum

Two independent scenarios are considered in calculating the helium boil-off: helium vaporization due to the loss of RF cavity (beam) vacuum and helium vaporization due to the loss of insulating vacuum. For both scenarios, at a helium pressure of 4.4-bar (110% MAWP), the heat absorbed per unit mass of efflux, equivalent to a latent heat but including the effect of significant vapor density is 23-J/g.

For helium boil-off during the loss of RF cavity vacuum due to an air leak, the total surface area of the RF cavity that is used in the calculations is 1302-in2 (0.84-m2). The heat flux of 4.0- W/cm2 is used [11] [12].

The helium boil-off during the loss of insulating vacuum is calculated based on the total surface area of the cold mass. At HTS, the cold mass is the total surface area of the helium vessel which is 1550-in2 (1.0 m2) (refer to drawing number 87285). The heat efflux for a superinsulated vacuum vessel with an uninsulated helium vessel is 2.0-W/cm2 [13].

The total mass flow rate is calculated using the equation:

$$\dot{m} = \frac{A \cdot Q}{\theta} \tag{13}$$

The equivalent volumetric flow rate is calculated based on the total mass flow rate. The detailed list of values for helium vaporization during the loss of cavity vacuum and loss of insulating vacuum at HTS are shown in Table 28.

At NML: Loss of RF Cavity (Beam) Vacuum and Loss of Insulating Vacuum

At NML, just as at HTS, the required flow rate during the helium vaporization for the loss of beam vacuum and loss of insulating is calculated at 4.4-bar (110% of the cold MAWP of 4-bar). For each scenario, the total surface area of the helium-to-vacuum boundary includes the surface areas of all eight dressed cavities plus the corrector dipole. For the loss of beam vacuum, the total helium-to-vacuum surface area of 6.8-m2 includes the surface area of eight cavities (0.84- m2 for each cavity) plus the surface area at the dipole corrector (0.067m2). For the loss of insulating vacuum, the total surface area of 8.9-m2 includes the area of the eight helium vessels (1.0-m2), the area of the dipole corrector (0.37-m2). Table 29 lists the values that leads to the required volumetric flow rate of helium for the NML relief system.

A.6 Welding Information

The weld characteristics were introduced earlier in this document in the sub-section titled "Welds" in the "Design Verification" section. As stated earlier, welds are produced by either the EBW process or the TIG process. All welds on the Dressed SRF Cavity are designed as full penetration butt welds. All welds are performed from one side, with the exception of the Ti-45Nb to Ti transition welds. Those welds are performed from two sides. No backing strips are used for any welds. Table 30 summarizes the welds, including the drawing, materials joined, weld type, and how the weld was qualified. Figure 25 shows the location of the welds on the vessel.

According to the Code, the welds must follow certain guidelines. Table 31 summaries the weld guideline, the paragraph in the Code which addresses the weld guideline, and how the weld does

		Cavity Vacuum Loss	Loss of Insulating Vacuum	Units
Q	Heat flux	4	2	[W/cm^2]
P_{relief}	110% of set pressure of cold MAWP	4.4 440	4.4 440	[bar] [kPa]
T	temperature when specific heat input is at a minimum for relief pressure	6.8 12.24	6.8 12.24	[K] [R]
θ	specific heat input for helium at T, P_{relief}	23	23	[J/g]
A	Surface area of helium-to-vacuum boundary	0.84	1	[m^2]
$\dot{m}$	mass flow rate of helium during vaporization	1461	870	[g/sec]
W	mass flow rate of helium during vaporization	11570	6887	[lbm/hr]
C	helium gas constant	378	378	
M	molecular weight of helium	4	4	[kg/kmol]
r	helium density at T, P_{relief}	53.39	53.39	[kg/m^3]
Z	compressibility factor for helium at flow condition	0.58	0.58	
Ca	air gas constant	356	356	
Za	air at Ta	1	1	
Ta	air at room temperature	520	520	[R]
Ma	air molecular weight	28.97	28.97	[kg/kmol]
Qa	volumetric flow rate of helium during vaporization	750	446	[SCFM air]

Table 28: Values used to Calculate the Requires Volumetric Flow Rate for Helium Vaporization at HTS

		Cavity Vacuum Loss	Loss of Insulating Vacuum	Units
Q	Heat flux	4	2	[W/cm^2]
P_{relief}	110% of set pressure of cold MAWP	4.4 440	4.4 440	[bar] [kPa]
T	temperature when specific heat input is at a minimum for relief pressure	6.8 12.24	6.8 12.24	[K] [R]
θ	specific heat input for helium at T, P_{relief}	23	23	[J/g]
A	Surface area of helium-to-vacuum boundary	6.8	8.9	[m^2]
$\dot{m}$	mass flow rate of helium during vaporization	11803.5	728.2	[g/sec]
W	mass flow rate of helium during vaporization	93484.6	57643.7	[lbm/hr]
C	helium gas constant	378	378	
M	molecular weight of helium	4	4	[kg/kmol]
r	helium density at T, P_{relief}	53.39	53.39	[kg/m^3]
Z	compressibility factor for helium at flow condition	0.58	0.58	
Ca	air gas constant	356	356	
Za	air at Ta	1	1	
Ta	air at room temperature	520	520	[R]
Ma	air molecular weight	28.97	28.97	[kg/kmol]
Qa	volumetric flow rate of helium during vaporization	6060.6	3737.1	[SCFM air]

Table 29: Values used to Calculate the Requires Volumetric Flow Rate for Helium Vaporization at NML

Weld	Weld Description	Drawing	Materials Joined	Weld Process	Weld Qualification
1	End Tube Spool Piece to End Cap Flange	MD-439178	Nb-Nb	EBW	Welded at vessel manufacturer
2	End Tube Spool Piece to RF Half Cell	MD-439178	Nb-Nb	EBW	Welded at vessel manufacturer
3	End Cap Flange to RF Half Cell	MD-439178	Nb-Nb	EBW	Welded at vessel manufacturer
4	End Cap Flange to End Cap Disk	MD-439178	Nb-Ti45Nb	EBW	Welded at vessel manufacturer
5	End Cap Disk to Transition Ring	MD-439180 MD-440003	Ti45Nb-Ti	EBW	Welded at vessel manufacturer
6	1.3GHz 9 Cell RF Cavity (Transition Ring) to Bellow Assembly	F10017493	Ti-Ti	TIG	Welded at FNAL, WPS, PQR, WPQ for Procedure No, TI-1 and TI-6
7 (FP End)	Bellow Assembly to LCLS II Helium Vessel Assembly	F10010493	Ti-Ti	TIG	Welded at FNAL, WPS, PQR, WPQ for Procedure No, TI-1 and TI-6
8	Bellow Convolutions to Weld Cuffs	F10010529	Ti-Ti	EBW	Welded at vessel manufacturer, WPS, PQR, WPQ
9	Support Ring to Half Cell	MC-439172	Nb-Nb	EBW	Welded at vessel manufacturer
10	Dumbbell to Dumbbell	MD-439173	Nb-Nb	EBW	Welded at vessel manufacturer
11	Half Cell to Half Cell	MC-439172	Nb-Nb	EBW	Welded at vessel manufacturer
12 (MC End)	Transition Ring to LCLS II Helium Vessel Assembly	F10017493	Ti-Ti	TIG	Welded at FNAL, WPS, PQR, WPQ for Procedure No, TI-1 and TI-6
13	Seam Welds of Helium Tubes	812995, 813005, X-Ray Report	Ti-Ti	TIG	Welded at vessel manufacturer, WPS, PQR, WPQ
14	2-phase pipe stub to helium vessel	812765, X-Ray Report	Ti-Ti	TIG	Welded at vessel manufacturer, WPS, PQR, WPQ. Final weld was radiographed (weld W1 in x-ray report).

Table 30: Weld summary for LCLS-II cavity

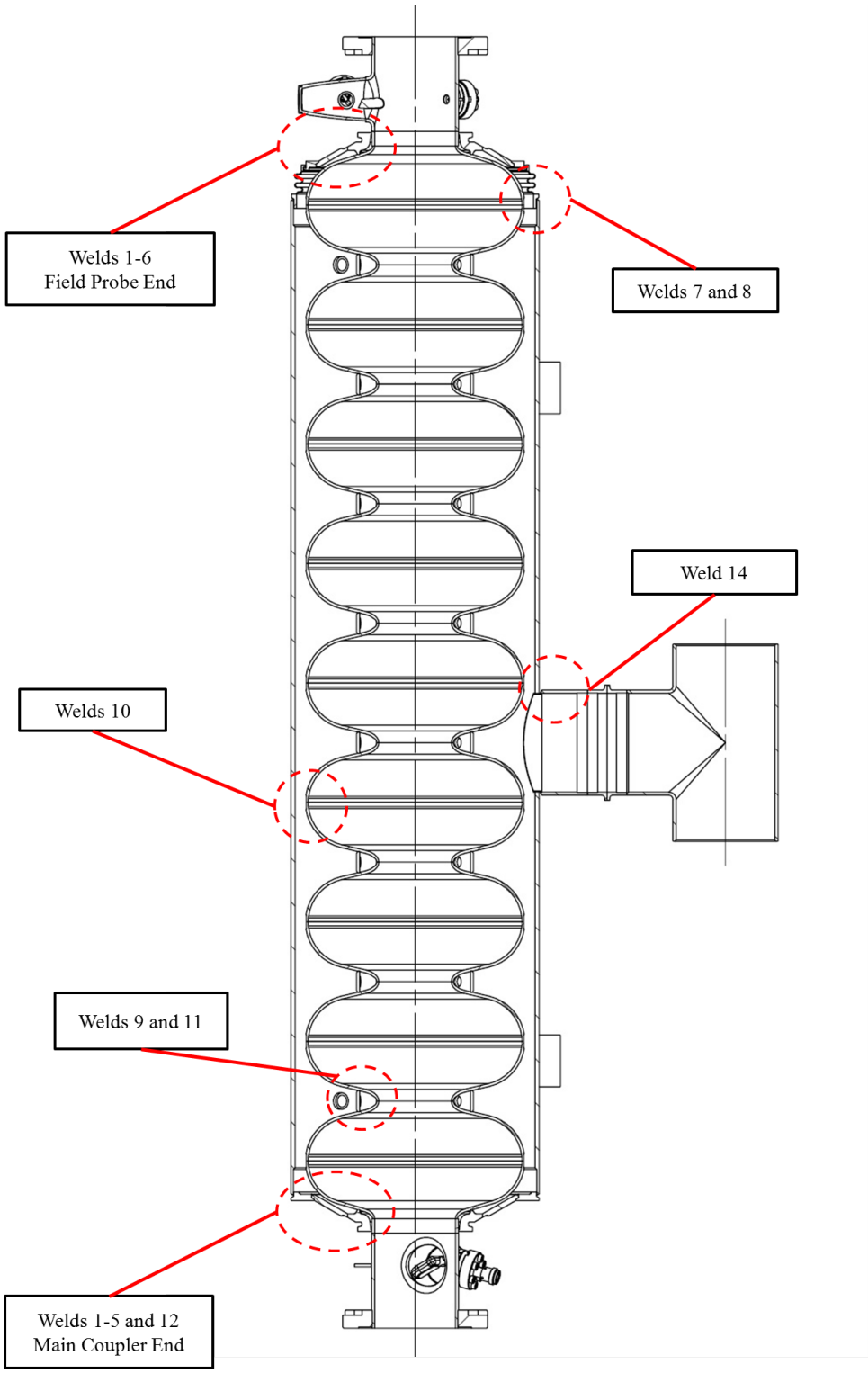

Figure 25: Weld Locations as numbered in Table 30

Weld Guideline	Code Paragraph	Exception to the Code	Explanation
Electron beam welds in any material must be ultrasonically examined along the entire length.	UW-11(e)	No ultrasonic examination was performed.	In the analysis, the joint efficiency is at least 0.6, as if the weld is not radiographed (see Table 3).
All Ti welds must be examined by the liquid penetrant method.	UNF-58(b)	No liquid penetrant testing was performed.	In the analysis, the joint efficiency is at least 0.6, as if the weld is not radiographed (see Table 3).
The welds of a bellows expansion joint must be examined by the liquid penetrant method.	26-11	No liquid penetrant testing was performed.	In the analysis of the seamweld, the joint efficiency is at least 0.6, as if the weld is not radiographed.

Table 31: Weld Exceptions to the Code

not follow the guideline. To accommodate for the exceptions, in the analysis of the design, the joint efficiency is at least 0.6, which is typical for a weld that is not radiographed (see Table 6).

Three welds are performed at Fermilab (welds 6-7 in Table 30). They are the final closure welds that bring the titanium helium vessel and the niobium RF cavity together to make the complete assembly. According to the Technical Appendix in the FESHM 5031 on Welding Information:

"Welding executed at Fermilab shall be done in a manner equivalent to a generic welding procedure specified and qualified under the rules of the A.S.M.E. Boiler and Pressure Vessel Code Section IX. The system designer of an in-house built vessel shall provide a statement from the welding supervisor or his designee certifying the welding was observed and accomplished in accordance to the specified generic welding procedure by a qualified welder and shall attach a copy of the welder's identification to the statement."

The Code Section IX requires three documents that specify and qualify a weld procedure and certify a welder. These documents are the Welding Procedure Specification (WPS), the Procedure Qualification Record (PQR), and the Welder/Welding Operator Performance Qualifications (WPQ). For the titanium closure welds that are completed at Fermilab, namely welds 6-7 in Table 30, the relevant documents are titled "TI-1" and "TI-6". The documents are available online at http://tdserver1.fnal.gov/tdweb/ms/Policies/Welding/.

All other welds were performed at vendors outside Fermilab. Any available documentation and inspection results are explained in the following paragraphs.

For the niobium cavity electronic beam (EB) welding that took place (welds 1-5, 9-11), no welding documents are available. In most cases the process is proprietary. How the welds and welders are qualified are not known other than what is specified in the engineering drawings. The quality

assurance for the niobium cavity is its RF performance. The RF performance is an indirect way of proving full penetration welds because if the weld is not full penetration, the RF performance is not acceptable.

For the bellows assembly, a single weld holds the bellows convolution to the weld cuff at each end (weld 12 in Table 30). The bellows assembly was fabricated at Ameriflex. A WPQ is available.

The titanium helium vessel assembly was manufactured at Incodema, who provided the WPS, PQR, and WPQ weld documents. All of the final welds (including welds 8, 12-14) were radiographed (x-rayed).

A detailed procedure, titled "1.3GHz Cavity Welding to Helium Vessel" lists all of the manufacturing steps that are taken for dressing a bare cavity after vertical testing in preparation for horizontal testing.

The welding documents, x-ray reports, and manufacturing procedure should be available in Teamcenter.

A.7 Fabrication Information

Fabrication documents for the titanium helium vessel assembly, the bellows assembly are available. These documents are not required by FESHM 5031 but are made available at a centralized location. These documents include material certifications, leak check results, and other quality assurance documents. The documents should be available in Teamcenter.

B Verification of ANSYS Results

B.1 Hoop Stress in Ti Cylinder

The hoop stress in the Ti cylinder, far from the ends or the flanges (which function like stiffening rings) can be calculated from

$$S = \frac{Pr}{t} \tag{14}$$

where:
S = hoop stress
P = pressure
r = mean radius of shell
t = thickness of shell

Substituting P = 0.205 MPa, r = 115 mm, t = 5 mm gives S = 4.7 MPa.

To check this number against the ANSYS results for 0.205 MPa, a path was created in the ANSYS model, and the hoop stress plotted along the path. Figure 26 shows the path; Figure 27 shows the comparison of the ANSYS results with those calculated from the expression above. Agreement is extremely good over the region away from the ends, averaging less than 1%.

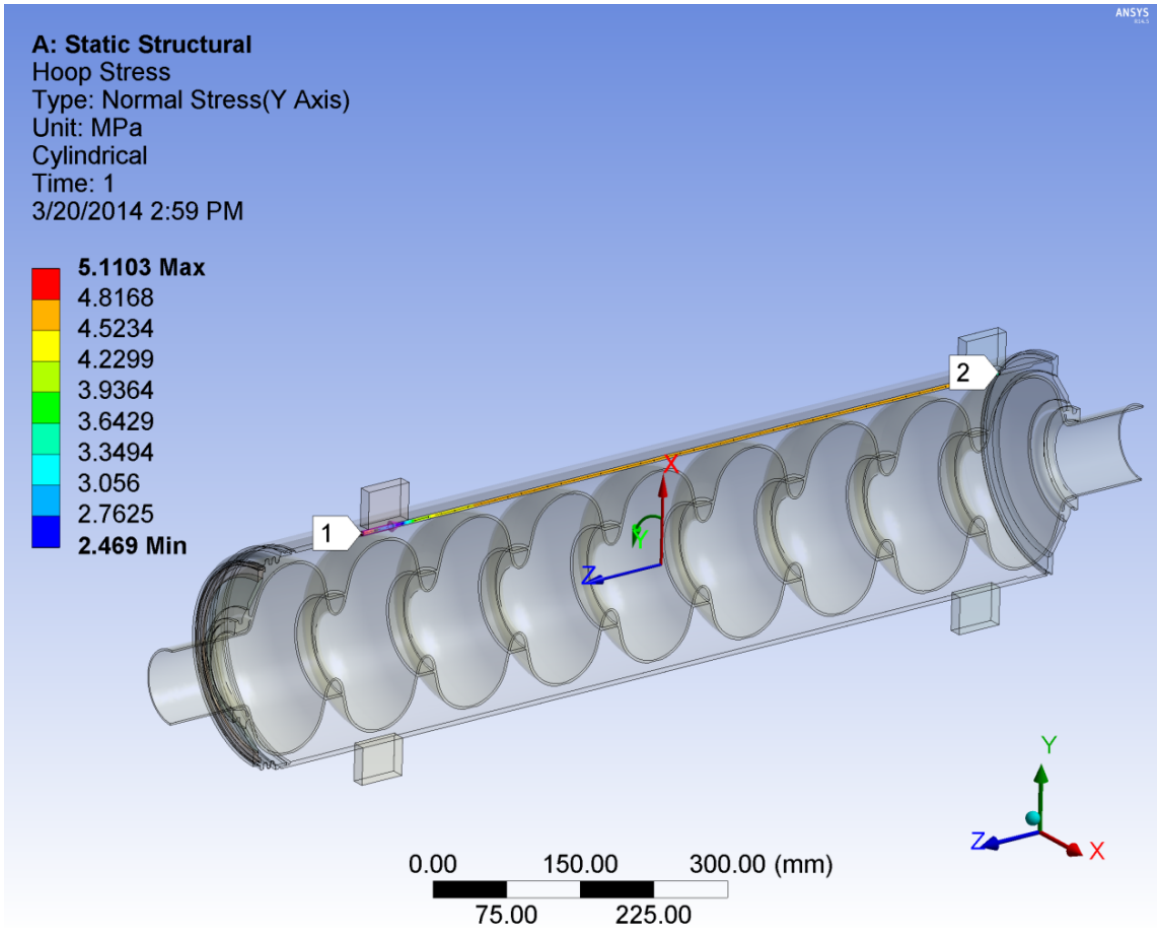

Figure 26: Path for hoop stress plot

B.2 Buckling of Spherical Shell - Approximation to Cell Buckling

The ANSYS model predicted Nb cavity buckling would occur at a pressure of 358 MPa. This numbers seems very large, so as a check a comparison was performed with the predicted collapse pressure for a thin sphere [14].

From Ref. 16, Table 35, Case 22, the critical buckling pressure of a thin sphere is:

$$q' = \frac{2Et^2}{r^2\sqrt{(3(1-v^2)}} \tag{15}$$

where:
q' = critical pressure, MPa
E = Young's modulus = 105000 MPa
r = radius of sphere = 105 mm
v = 0.38

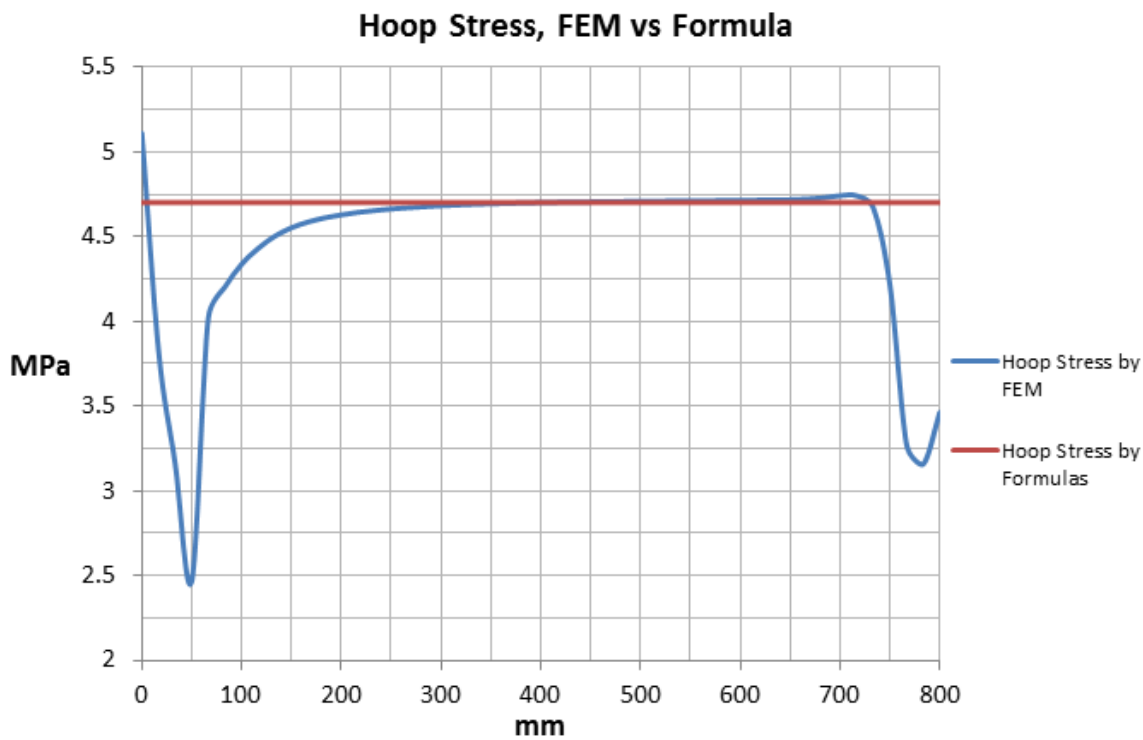

Figure 27: Hoop stress in Ti Cylinder along line 1-2 for Pressure of 0.205 MPa

Substituting gives q' = 93 MPa. This compares well with the ANSYS linear buckling prediction shown in Figure 23.

B.3 Bucking of Ti Cylinder

The maximum allowable external pressure of the Ti cylinder was determined in A.4.9 of this report using the chart techniques of Div. 1. This calculation can be checked by doing an ANSYS linear buckling calculation on the length of shell used in the Div. 1 calculations, and applying the design factors for linear buckling given in Div. 2, Part 5, 5.4.1. This calculation is also useful for verifying that the buckling pressure of the conical head (calculated as 359 MPa shown in Figure 24) is higher than that of the cylinder.

The FE model, which does not include the conical heads, is shown in Figure 29, in its buckled shape. The analysis predicts collapse at 7.3 MPa. The Code calculation of section 7.0 gives an maximum allowable external pressure for this part of 0.2 MPa. These numbers can be compared by noting that the factor B = σcr/2, where σcr is the hoop stress at which the cylinder buckles [15]. B is a factor dependent on materials and geometrical properties. Given the properties of the case we can infer from Figure NFT-2 (the material chart for Grade 2 TI) in the Code, Section II, Part D, Subpart 3 that the factor B is 10000 (psi) which is about 70 MPa. Substituting σcr = Pcr r/t, where Pcr is the critical buckling pressure, gives a theoretical buckling pressure for the cylinder of 6.1 MPa. This is reasonably close to the ANSYS value of 7.3 MPa.

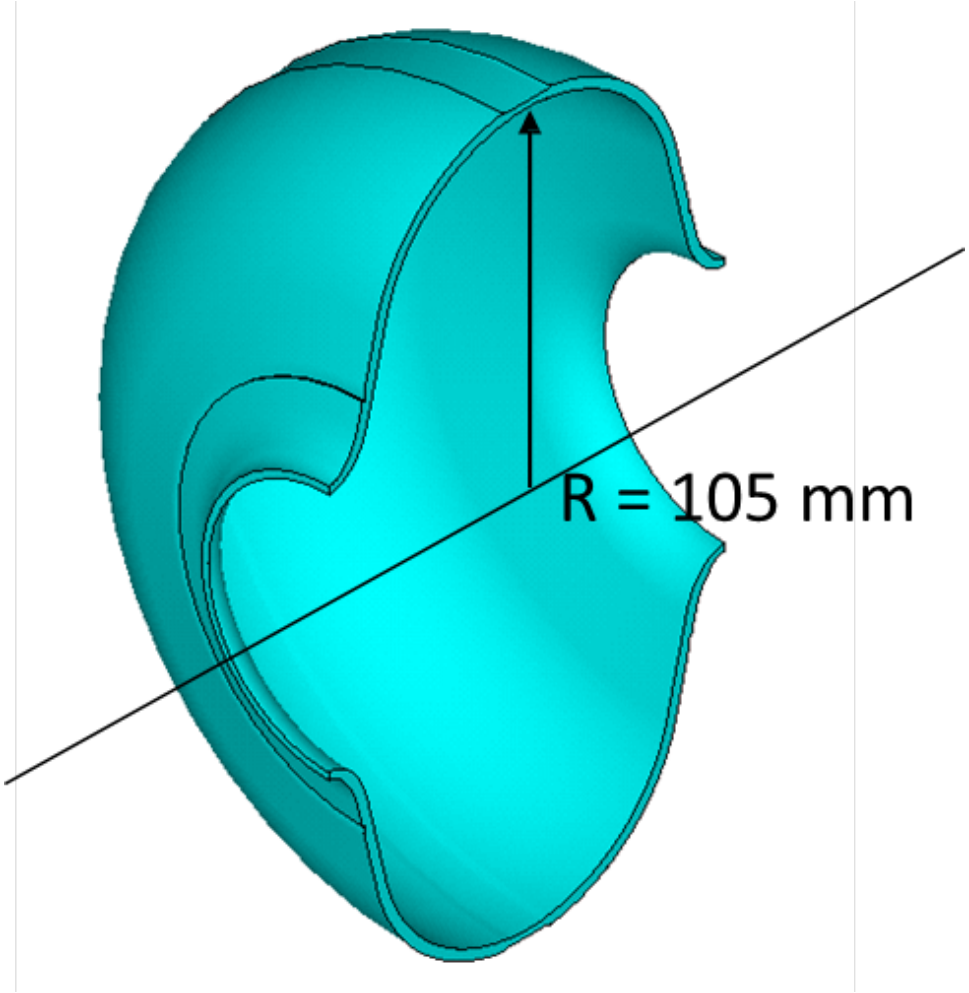

Figure 28: Single cell - radius for spherical shell buckling calculation

This alternative calculation of Ti shell buckling pressure also verifies that it lies well below the calculated buckling pressure of the conical head, even when that head is unconstrained by the Nb cavity.

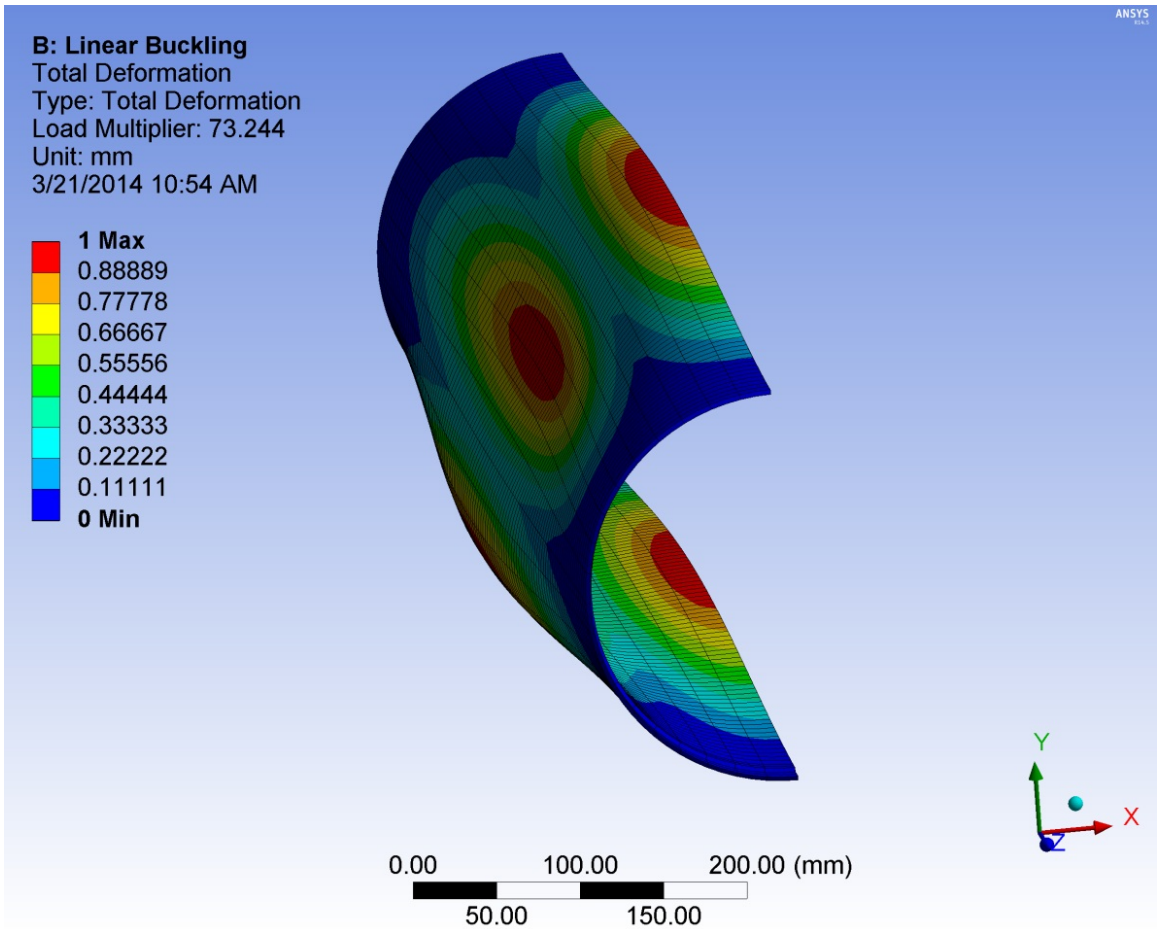

Figure 29: ANSYS linear buckling of the Ti cylindrical shell

C Fatigue Analysis of the Titanium Bellows

The following pages are the detailed calculations of the titanium bellows following the Code's Div. 1, Appendix 26 guidelines. Mathcad 14 was the software used.

Detailed calculation of the titanium bellows following the Code's Div.1, Appendix 26 guidelines.

Design pressure (psi)	$P := 30$
Bellows inside diameter (in)	$Db := 8.64$
Ply thickness (in)	$t := 0.012$
Number of Plies	$n := 1$
Bellows tangent length (in)	$Lt := 0.24$
Bellows Mean Diameter (in)	$Dmean := 8.9$
Modulus of Elasticity (psi)	$Eb := 15200000$
Convolution height (in)	$w := 0.25$
Collar length (in)	$Lc := 0.55$
Collar thickness (in)	$tc := 0.12$
Collar Modulus of Elasticity (psi)	$Ec := 15200000$
Convolution Pitch (in)	$q := 0.341$
Kf coefficient (formed)	$Kf := 3.0$
Allowable stress of bellows (psi)	$S := 11500$
Allowable stress of collar (psi)	$Sc := 11500$
Weld Joint Efficiency	$Cwc := 0.6$
Number of convolutions	$N := 2$
Bellows Axial Stiffness (N/micrometer)	$Kb_SI := 0.740$
(lbf/inch)	$Kb := Kb_SI \cdot \frac{2.2 \cdot 10^6 \cdot 2.54}{100} = 4.135 \times 10^4$
Allowable yield stress (psi)	$Sy := 40000$
Poisson's ratio of Ti G2	$\nu b := 0.37$
Bellows live length (in)	$L := 0.87$

Maximum axial extension (mm) $x_positive_SI := 1.8$

(in) $x_positive := \frac{x_positive_SI}{25.4} = 0.071$

Maximum axial compression (mm) $x_negative_SI := 0.33$

(in) $x_negative := \frac{x_negative_SI}{25.4} = 0.013$

$Dm := Db + w + n \cdot t = 8.902$

$k := \min\left[\left(\frac{Lt}{1.5 \cdot \sqrt{Db \cdot t}}\right), 1.0\right] = 0.497$

$tp := \left(t \cdot \sqrt{\frac{Db}{Dm}}\right) = 0.012$

$A := \left[\left(\frac{\pi - 2}{2}\right) \cdot q + 2 \cdot w\right] \cdot n \cdot tp = 8.212 \times 10^{-3}$

$Dc := Db + 2 \cdot n \cdot t + tc = 8.784$

$c1 := \frac{q}{2 \cdot w} = 0.682$

$cp := 0.59$

$c2 := \frac{q}{2.2 \cdot \sqrt{Dm \cdot tp}} = 0.478$

$Ixx := n \cdot tp \cdot \left[\frac{(2 \cdot w - q)^3}{48} + 0.4 \cdot q \cdot (w - 0.2 \cdot q)^2\right] = 5.429 \times 10^{-5}$ moment of inertia

$e_eq := \sqrt[3]{12 \cdot \left(1 - \nu b^2\right) \cdot \frac{Ixx}{q}} = 0.118$ equivalent thickness

$D_eq := Db + w + 2 \cdot e_eq = 9.126$ equivalent outside diameter for instability due to external

pressure

Total axial movement per convolution (mm) $\Delta q := \frac{(x_positive + x_negative)}{N} = 0.042$

$$S1 := \frac{(Db + n \cdot t)^2 \cdot Lt \cdot Eb \cdot k \cdot P}{2[n \cdot t \cdot (Db + n \cdot t) \cdot Lt \cdot Eb + tc \cdot Dc \cdot Lc \cdot Ec \cdot k]} = 427.83$$

$$S11 := \frac{Dc^2 \cdot Lt \cdot Ec \cdot k \cdot P}{2[n \cdot t \cdot (Db + n \cdot t) \cdot Lt \cdot Eb + tc \cdot Dc \cdot Lc \cdot Ec \cdot k]} = 440.984$$

$$S2e := \frac{P \cdot [q \cdot Dm + Lt \cdot (Db + n \cdot t)]}{2 \cdot (A + n \cdot tp \cdot Lt + tc \cdot Lc)} = 995.218$$

$$S2i := \frac{P \cdot q \cdot Dm}{2 \cdot A} = 5.545 \times 10^3$$

$$S3 := \frac{P \cdot w}{2 \cdot n \cdot tp} = 317.203$$

$$S4 := \left(\frac{w}{tp}\right)^2 \cdot \frac{P \cdot cp}{2 \cdot n} = 3.958 \times 10^3$$

$$Psc := 0.34 \cdot \frac{\pi \cdot Kb}{N \cdot q} = 6.476 \times 10^4$$

$$\delta := \frac{S4}{3 \cdot S2i} = 0.238$$

$$\alpha := 1 + 2 \cdot \delta^2 + \sqrt{1 - 2 \cdot \delta^2 + 4 \cdot \delta^4} = 2.062$$

$$Sy_eff := 2.3 \cdot Sy = 9.2 \times 10^4$$

$$Psi := (\pi - 2) \cdot \frac{A \cdot Sy_eff}{Dm \cdot q \cdot \sqrt{\alpha}} = 197.879$$

$Cf := 1.85$

$Cd := 1.95$

$$S5 := \frac{1}{2}\cdot\frac{Eb\cdot tp^2}{w^3\cdot Cf}\cdot\Delta q = 1.541\times 10^3$$

$$S6 := \frac{5}{3}\cdot\frac{Eb\cdot tp}{w^2\cdot Cd}\cdot\Delta q = 1.03\times 10^5$$

$$St := 0.7\cdot(S3 + S4) + (S5 + S6) = 1.076\times 10^5$$

Calculating the buckling pressure for the bellows as an equivalent cylinder

$$\frac{D_eq}{e_eq} = 77.25$$

$$\frac{L}{D_eq} = 0.095$$

$A_factor := 0.039$

$$Pa := \frac{2}{3}\cdot A\cdot Eb\cdot\frac{e_eq}{D_eq} = 1.077\times 10^3$$

circumferential membrane stress in bellows tangent (psi)	$S1 = 427.83$
circumferential membrane stress in collar (psi)	$S11 = 440.984$
circumferential membrane stress in bellows (psi) (for end convolution)	$S2e = 995.218$
meridional membrane stress in bellows (psi)	$S2i = 5.545\times 10^3$
meridional bending stress in bellows (psi)	$S3 = 317.203$
allowable internal pressure to avoid column instability (psi)	$S4 = 3.958\times 10^3$

allowable internal pressure b ased on in-plane instability (psi) $Psc = 6.476 \times 10^4$

allowable external pressure based on instability (psi) $Psi = 197.879$

meridional membrane stress (psi) $S5 = 1.541 \times 10^3$

meridional bending stress (psi) $S6 = 1.03 \times 10^5$

total stress range due to cyclic displacement (psi) $St = 1.076 \times 10^5$

ACCEPTANCE CRITERIA

$S1 = 427.83$

$S2e = 995.218$

$S2i = 5.545 \times 10^3$

$S = 1.15 \times 10^4$

$S11 = 440.984$

$Cwc \cdot S = 6.9 \times 10^3$

$S3 + S4 = 4.275 \times 10^3$

$Kf \cdot S = 3.45 \times 10^4$

$P = 30$

$Psc = 6.476 \times 10^4$

$Psi = 197.879$

$Pa = 1.077 \times 10^3$

$a := 3.4$

$b := 54000$

$c := 1.86 \cdot 10^6$

$Stpsi := 122465$

$$Nc := \frac{1}{2} \cdot \left(\frac{c}{Stpsi - b} \right)^a = 3.756 \times 10^4$$

D Pressure Test Results

The Pressure test permit is shown in the following pages, and a typical setup of a dressed cavity pressure test is shown in Figure .

Figure 30: Typical setup of dressed SRF cavity for pressure test.

Fermilab

Pressure Testing Permit

Type of Test: [ ] Hydrostatic [X] Pneumatic

Test Pressure 34.5 psig **Maximum Allowable Working Pressure** 29.7 psid

Items to be Tested

TB9AES031 Cavity Helium Vessel

Notes

Note1: Cavity beam-line is backfilled to atmospheric pressure with boiled off argon gas, outside of the helium vessel is air at atmospheric pressure.

Note 2: The Conflat flange on the 2-phase pipe of the helium vessel will be used to backfill the helium vessel with boiled off nitrogen gas during the test. Both of the VCR fittings at the bottom of the helium vessel will be blanked off during the test.

Note 3: The bellows brace arms (see attached images) are installed on the cavity and protect the cavity from excessive expansion. It is important to make sure that the titanium bellows at the end of the helium vessel is supported during the pressure test.

Note 4: The pressure test will include an RF frequency measurement before, during, and after pressurization

Note 5: Frequency change during pressure test should not exceed 10 kHz/psig with a maximum of 345 kHz at 34.5 psig for a pressurized cavity and 30 kHz total frequency shift for an unpressurized cavity. Test has to be promptly aborted in case of higher frequency change.

Note 6: MAWP = 29.7 psid, test pressure = 34.5 psig = 1.16*MAWP rounded to 0.5 psi (Pneumatic test per ASME code, Div. 1. requires at least 1.1*MAWP. The vessel will be tested to 1.16*MAWP.)

Location of Test MP9 **Date and Time** 5/29/15 12:30

Hazards Involved - See hazard analysis.

Safety Precautions Taken

System designed, fabricated, and inspected equivalent to ASME Boiler & Pressure Vessels code. Test will be conducted by trained personnel as described below. Access to test area will be limited only to those involved in the test during pressurization.

Special Conditions or Requirements

Follow the steps listed below.

1. Rope off area around pressure test.
2. Place sign on main entrance to announce a test is in progress and to use an alternate door.
3. Lock main entrance door.
4. Ensure cavity beam-line is backfilled to atmospheric pressure with air or nitrogen gas, outside of the helium vessel is air at atmospheric pressure
5. Ensure the Conflat flange on the 2-phase pipe of the helium vessel will be used to backfill the helium vessel with boiled off nitrogen gas during the test and that both of the VCR fittings at the bottom of the helium vessel will be blanked off during the test.
6. Ensure the bellows brace arms (see attached images) are installed on the cavity and protect the cavity from excessive expansion. It is important to make sure that the titanium bellows at the end of the helium vessel is supported during the pressure test.
7. Check to see all bolts are present and tight in the bellows brace arms (see attached images).
8. Take RF measurement. Record starting frequency. Make sure frequency is in the range of 1297.85 - 1298.05 MHz.
9. Pressurize to 9.0 psig.
10. Snoop line fittings.
11. Take RF measurement. Record frequency change. Make sure frequency change is less than 90 kHz.

12. Depressurize to 0 psig.
13. Take RF measurement. Record frequency change. Make sure frequency change is less than 20 kHz.
14. Pressurize to 17.0 psig.
15. Snoop line fittings.
16. Take RF measurement. Record frequency change. Make sure frequency change is less than 170 kHz.
17. Depressurize to 0 psig.
18. Take RF measurement. Record frequency change. Make sure frequency change is less than 28 kHz.
19. Pressurize to 20.5 psig.
20. Take RF measurement. Record frequency change. Make sure frequency change is less than 205 kHz.
21. Depressurize to 0 psig.
22. Take RF measurement. Record frequency change. Make sure frequency change is less than 33 kHz.
23. Pressurize to 24 psig.
24. Take RF measurement. Record frequency change. Make sure frequency change is less than 240 kHz.
25. Depressurize to 0 psig.
26. Take RF measurement. Record frequency change. Make sure frequency change is less than 38 kHz.
27. Pressurize to 27.0 psig.
28. Take RF measurement. Record frequency change. Make sure frequency change is less than 270 kHz.
29. Depressurize to 0 psig.
30. Take RF measurement. Record frequency change. Make sure frequency change is less than 43 kHz.
31. Pressurize to 31.0 psig.
32. Take RF measurement. Record frequency change. Make sure frequency change is less than 310 kHz.
33. Depressurize to 0 psig.
34. Take RF measurement. Record frequency change. Make sure frequency change is less than 45 kHz.
35. Pressurize to 34.5 psig.
36. Hold pressure for 5 minutes. Take RF measurement. Record frequency change. Make sure frequency change is less than 345 kHz.
37. Depressurize to 0 psig.
38. Take RF measurement. Record frequency change. Make sure frequency change is less than 45 kHz.
39. Pressurize to 30.0 psig.
40. Close valve between regulator and vessel.
41. Hold pressure for 10 minutes to make sure pressure is not dropping. Take RF measurement. Record frequency change. Make sure frequency change is less than 300 kHz.
42. Depressurize to 25 psig.
43. Take RF measurement. Record frequency change. Make sure frequency change is less than 250 kHz.
44. Depressurize to 17 psig.
45. Take RF measurement. Record frequency change. Make sure frequency change is less than 170 kHz.
46. Depressurize to 9 psig.
47. Take RF measurement. Record frequency change. Make sure frequency change is less than 90 kHz.
48. Depressurize to 0 psig.
49. Take RF measurement. Record frequency change. Make sure frequency change is less than 45 kHz.

Qualified Person and Test Coordinator Jerba Kg
Dept/Date TD/SRF Department

Division/Section Safety Officer for R. Ruthe
Dept/Date TD/ESH

Results
Held at 34.5 for 5 minutes and 30 for 10 minutes

Witness for R Ruthe **Dept/Date** TD/ESH 5/29/15
Rich Ruthe or designee

Table 1 – Pressure Test Steps

F= 1297.978 MHz

RF representative: Mohamed Hassan

Pressure (psig) (psig equals differential pressure for this test)	Dwell time (minutes)	Activity at pressure	Frequency Change [kHz]	Maximum Frequency Change [kHz]
0	As needed	RF check	0	0
9.0	As needed	Snoop line fitting, RF check	43	90
0	As needed	RF check	2	20
17.0	As needed	Snoop line fitting, RF check	80	170
0	As needed	RF check	3	28
20.5	As needed	RF check	99	205
0	As needed	RF check	5	33
24.0	As needed	RF check	111	240
0	As needed	RF check	7	38
27.0	As needed	RF check	125	270
0	As needed	RF check	7	43
31.0	As needed	RF check	144	310
0	As needed	RF check	9	45
34.5	5	Peak test pressure, RF check	162	345
0	As needed	RF check	13	45
30.0	10*	Test pressure hold point*, RF check	145	300
25.0	As needed	RF check	126	250
17.0	As needed	Visual inspection, RF check	88	170
9.0	As needed	RF check	53	90
0	As needed	RF check	14	45

*The pressure hold point of 30 psig is the MAWP rounded to 0.5 psi. Dwell time is set long enough to assure that pressure is not dropping.

Test Setup

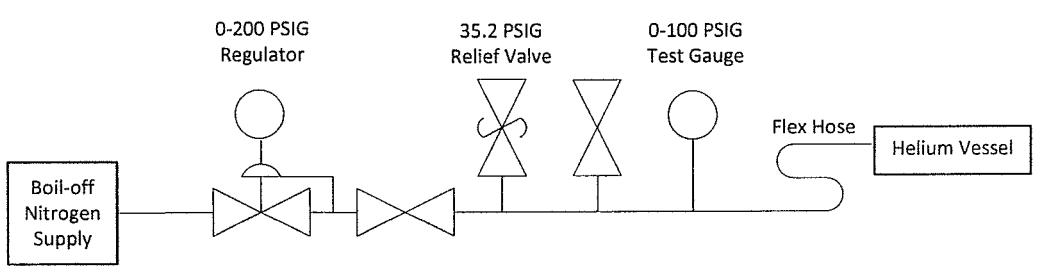

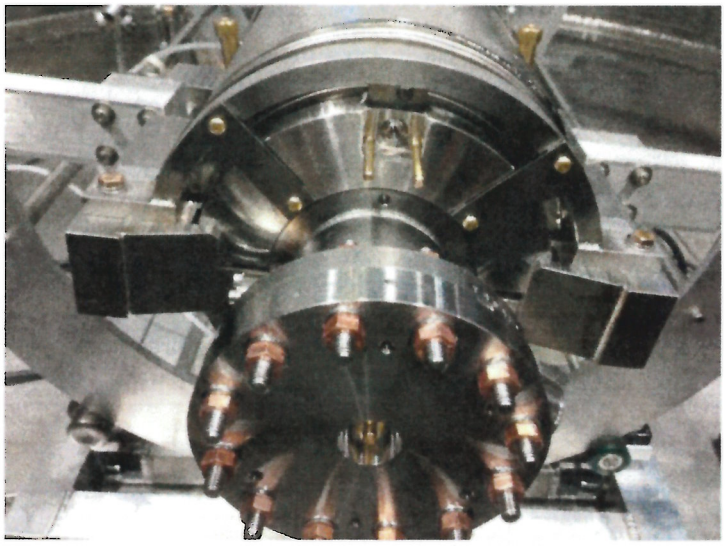

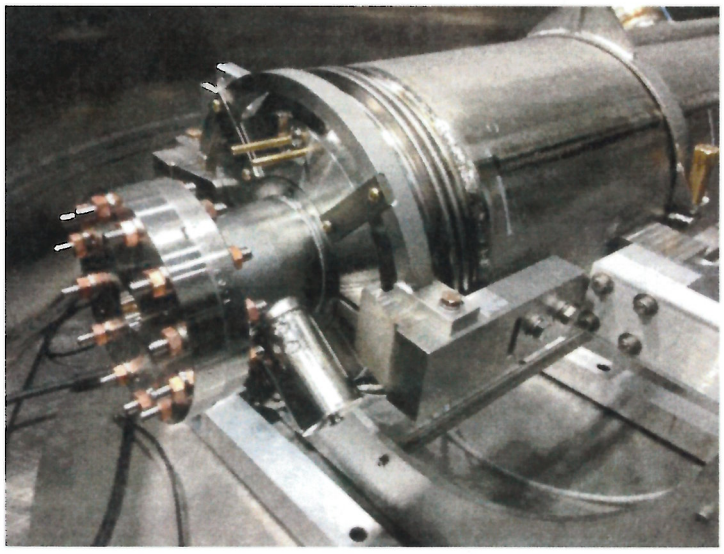

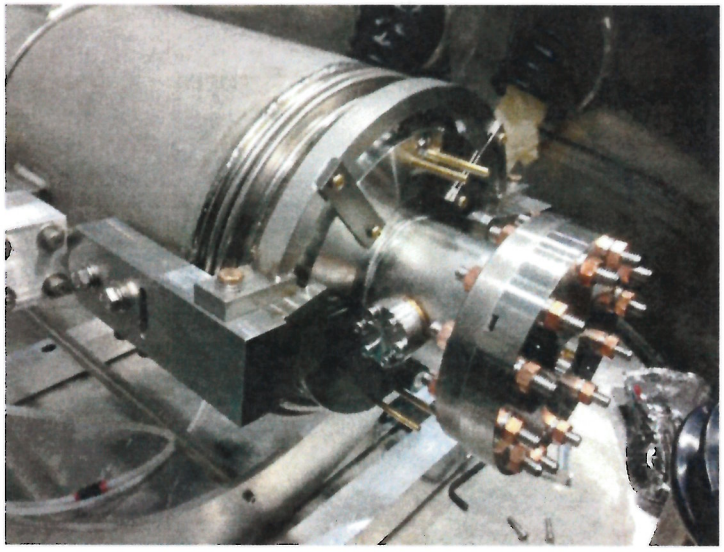

E HTS Adapting Hardware

For use in HTS, an adapter will be needed due to the increaesed size of the two phase pipe in the LCLS-II design. A drawing of the adapter is shown in Figure 31.

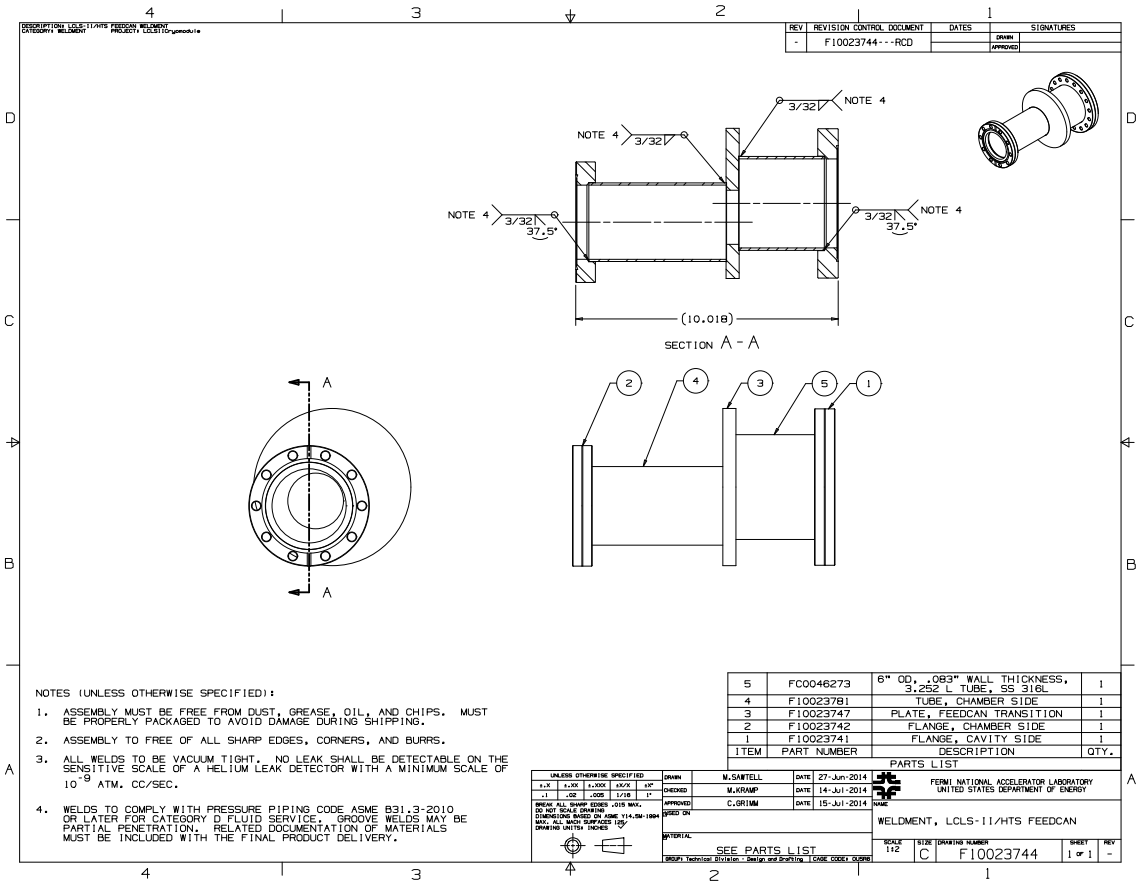

Figure 31: HTS LCLS-II Helium Vessel adapter weldment

F Stainless Steel to Titanium Transitions

Donato Passarelli x3972
Joshua Kaluzny x2302

The connection to the two-phase helium line and the cooldown helium supply lines for the dressed cavities within the LCLS-II cryomodule have a transition joint from Titanium grade 2 to Stainless Steel 316L. The bi-metallic tube is obtained by machining a solid piece of two plates explosion welded together with a very thin layer (0.010" thick) of tantalum between the two metals. The case 2493 of ASME BPVC is used to qualify the butt joint transitions for cryogenic applications, which can then be welded using conventional processes to adjacent similar metals.

Similar transition joints have been developed and used at Jefferson Lab in SNS. The original Jefferson lab design did not have a tantalum layer and had a length of base metal extending 0.38" from the joint. This short length allowed the joint to get too hot during welding. The solution that was tested and implemented included adding a layer or tantalum to increase the allowed temperature and lengthening the base metal to reduce the temperature during welding. Additional welding restrictions such as heat sinking and waiting times were put in place to keep the joint at reduced temperatures. The new lengths for the Jefferson lab transition were 0.5" for the titanium and 1.0" for the stainless steel [16]. The lengths for the Fermilab transition are 1.0" on each side of the joint. The Fermilab transition also has an increased surface area at the joint to provide extra strength.

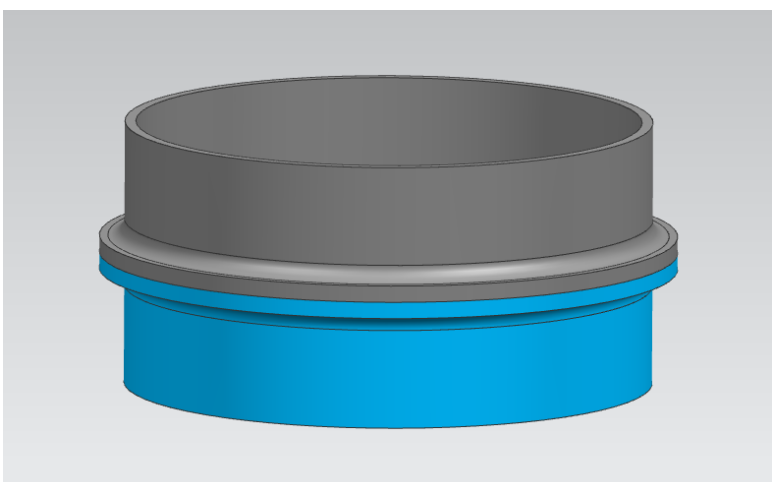

Figure 32: Transition joint for the two-phase helium line.

F.1 Samples

A sample of the material used to machine the transitions was EDM cut into 24 samples. Some of these samples were sent to St. Louis Testing Laboratories to be tested at ambient temperature and liquid helium temperature. These tests are described in F.2 and F.3.

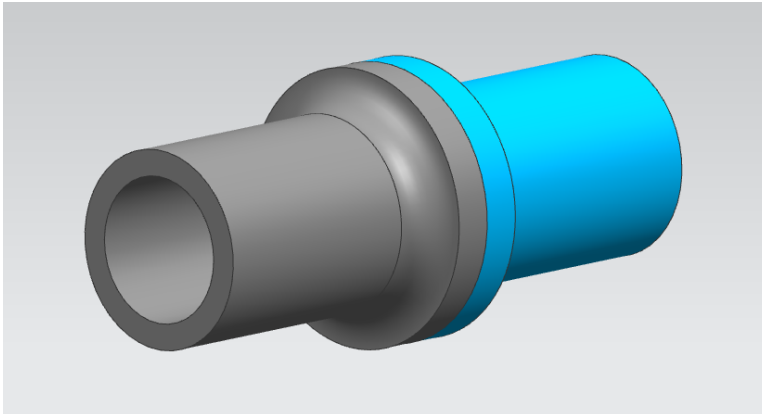

Figure 33: Transition joint for the cooldown line.

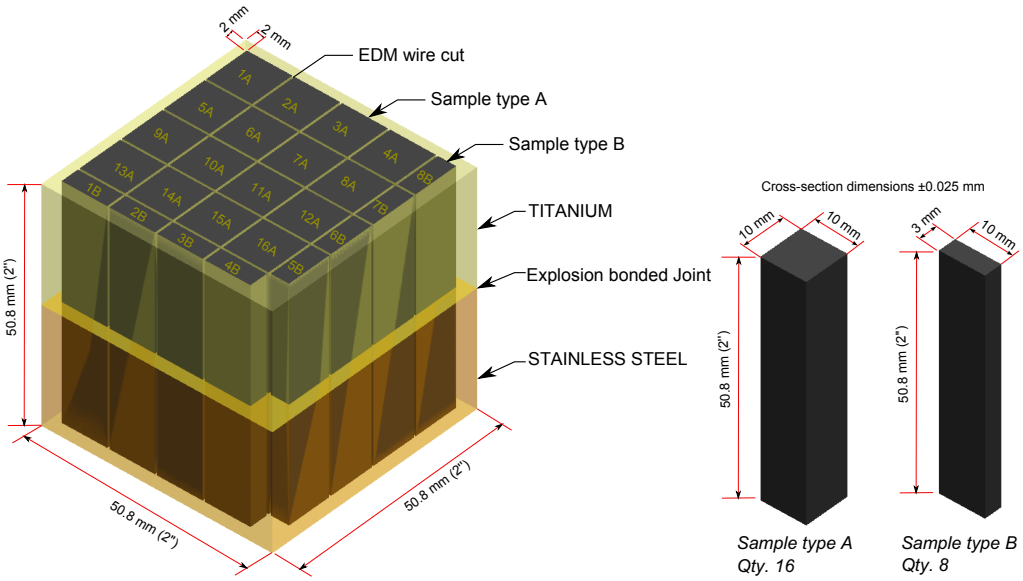

Figure 34: Size and method of machining samples

F.2 Tensile Test

The ultimate strength of the joint was measured at 290 K and 4 K pulling six specimens with the methodology described in ASTM A370-14, see Table 32. The samples tested at 290 K had a ductile break at the Titanium side "far" from the joint, see Figures 36(a), 36(b). This means the joint at room temperature has an ultimate stress higher than the values listed in Table 32. At 4 K, the three samples had a fragile break at the joint interface (see Figures 36(c), 36(d)), with an ultimate stress value slightly above the reference data for the Titanium grade 2 at 2 K. Comparing the results of the test to the ultimate strength of base materials listed in Table 33, it can be affirmed

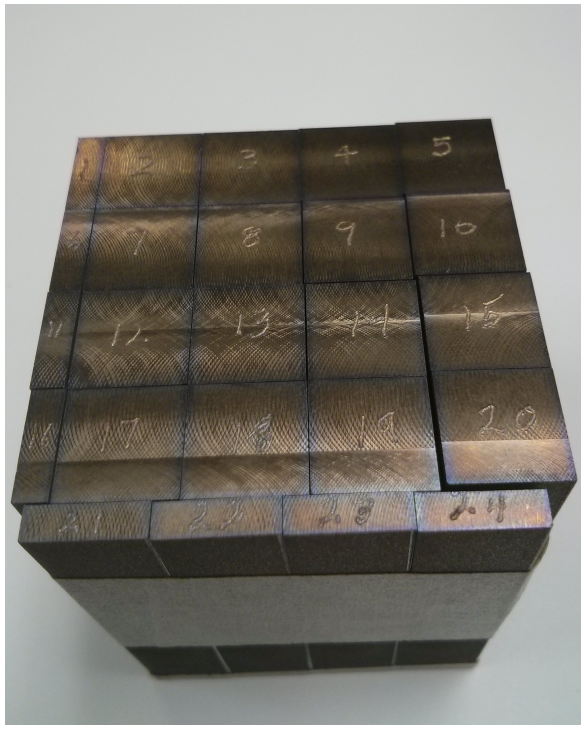

Figure 35: Machined samples

the joint behaves as or even better than the reference Ultimate Stress used for Titanium grade 2 at 4 K and 290 K. Thus, the allowable stresses of the joint (S_{Ti-SS}) can be taken equal to those of Titanium (see Table 10) and are listed in Table 34.

Tensile Test - Ultimate strength	
Test temperature 290 K	
Sample #4	789 MPa
Sample #5	788 MPa
Sample #7	774 MPa
Average	784 MPa
Test temperature 4 K	
Sample #12	1138 MPa
Sample #13	1259 MPa
Sample #18	1328 MPa
Average	1242 MPa

Table 32: Tensile test of Ti-SS316L explosion bonded joint at 290 K and 4 K.

Ultimate strength of base materials	
Room Temperature	
SS316L	560 MPa
Ti gr.2	345 MPa
Tantalum	276 MPa
Cryogenic Temperature	
SS316L (4K annealed)	860 MPa
SS316L (4K 20% cold worked)	1734 MPa
Ti gr.2 (2 K)	1117 MPa
Tantalum (70 K)	1034 MPa

Table 33: Typical values of the base materials within the explosion weld at room and cryogenic temperatures. [17] [18] [19]

Allowable stress of Ti-SS joint	
S_{Ti-SS}^{290K}	79 MPa
S_{Ti-SS}^{2K}	255 MPa

Table 34: Allowable stress of the transition Titanium-Stainless steel joint.

F.3 Charpy Impact Test

Even tough our system of vessels and pipes is statically loaded and it is designed to *carry loads*, six samples ("A" V-notch type) were tested to measure the ability of the joint to *absorb energy*. Table 35 lists the results at 290 K and 4 K. The energy absorbed by the samples at room temperature is about five times larger than at 4 K, a similar ratio (around three) was measured impact loading Titanium grade 2 samples at 290 K and 4 K, as reported in [20]. That is due to the transition from ductile to brittle fracture, already noticed in the tensile test. If the joints were subject to impact loads, additional tests may need to be performed to fully characterize the Ti-SS transition joint. Again, the joints are not subject to impact loads during operation.

F.4 Transition Test

A sample transition was welded into an assembly that has been put through a variety of tests:

1. X-ray joint
2. Orbital and TIG welding Ti and SS
3. X-ray joint
4. Room temperature to Liquid nitrogen cold shock (12 times)
5. Leak check

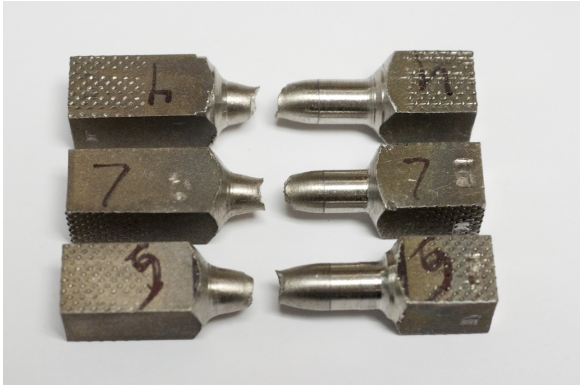

(a) Samples tested at 290 K with the break on the Ti side.

(b) Typical cross section of ductile break (Titanium).

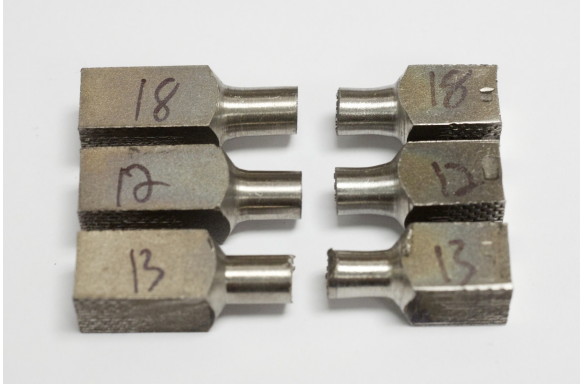

(c) Samples tested at 4 K with the break around the joint interface.

(d) Typical cross section of brittle break at joint interface.

Figure 36: Pictures of the samples tensile tested at 290 K and 4 K.

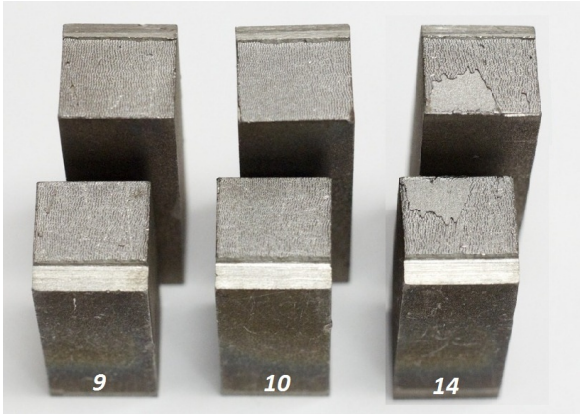

(a) Samples tested at 290 K.

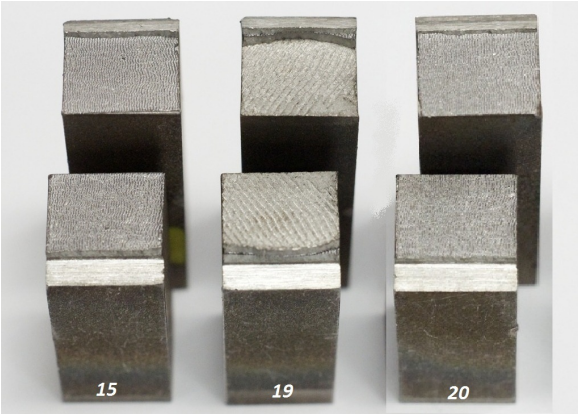

(b) Samples tested at 4 K.

Figure 37: Pictures of the Charpy samples.

Charpy test	
Test temperature 290 K	
Sample #1	12.9 J
Sample #2	8.1 J
Sample #3	10.2 J
Average	10.4 J
Test temperature 4 K	
Sample #4	2.7 J
Sample #5	2.7 J
Sample #6	2.0 J
Average	1.8 J

Table 35: Charpy test of Ti-SS316L explosion bonded joint at the operational temperatures.

6. X-ray joint

There was no sign of leaks or degradation of the joint during the tests.

F.5 Finite Element Analysis

Finite element analyses were performed in order to quantify the von-Mises equivalent stress for the two transition joints at the two operating condition:

- Room temperature (290 K) and maximum pressure of 0.2 MPa
- Cryogenic temperature (2 K) and maximum pressure of 0.4 MPa

Figures 39, 40, 41 and 42 show the map of von-Mises equivalent stress of the two transition joints at the operating condition described above. In all cases, the maximum equivalent stress is below the allowable stress at the operating temperature reported in table 34.

Figure 38: Stainless Steel Titanium transisiton test tube.

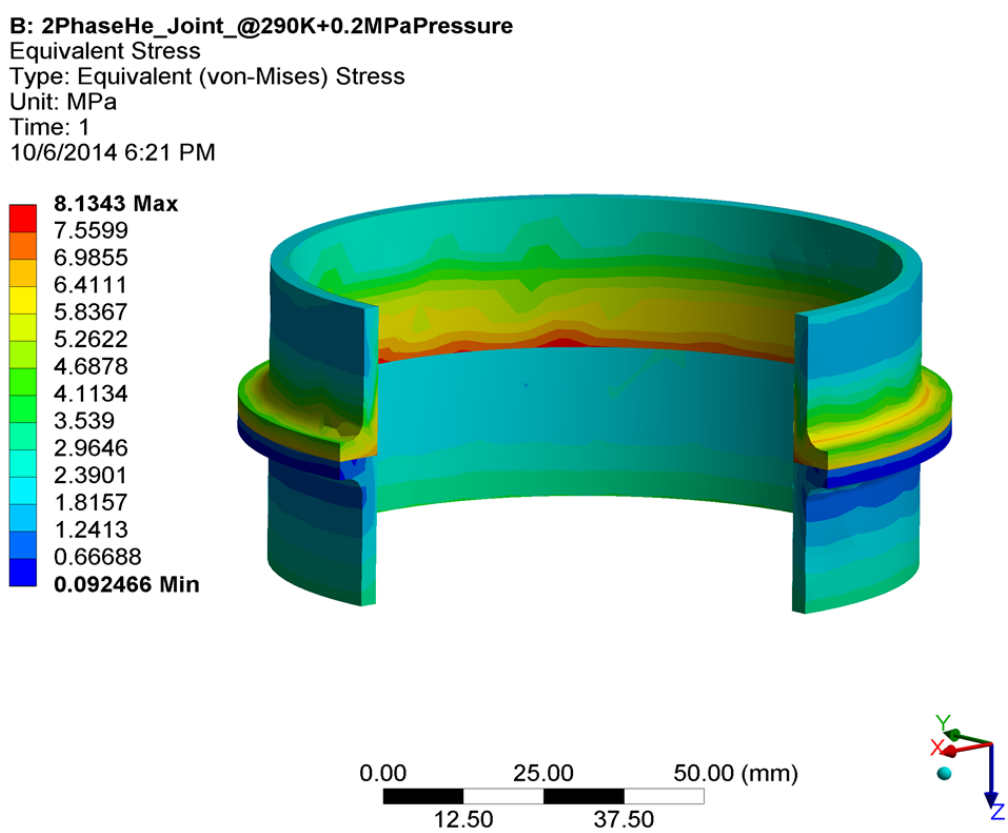

Figure 39: Equivalent stress map of the transition joint for the two-phase pipe line at the temperature of 290 K and maximum pressure of 0.2 MPa. The equivalent stress is below the allowable stress, $S_{Ti-SS}^{290K} = 79\,\mathrm{MPa}$, with a safety factor of 9.7.

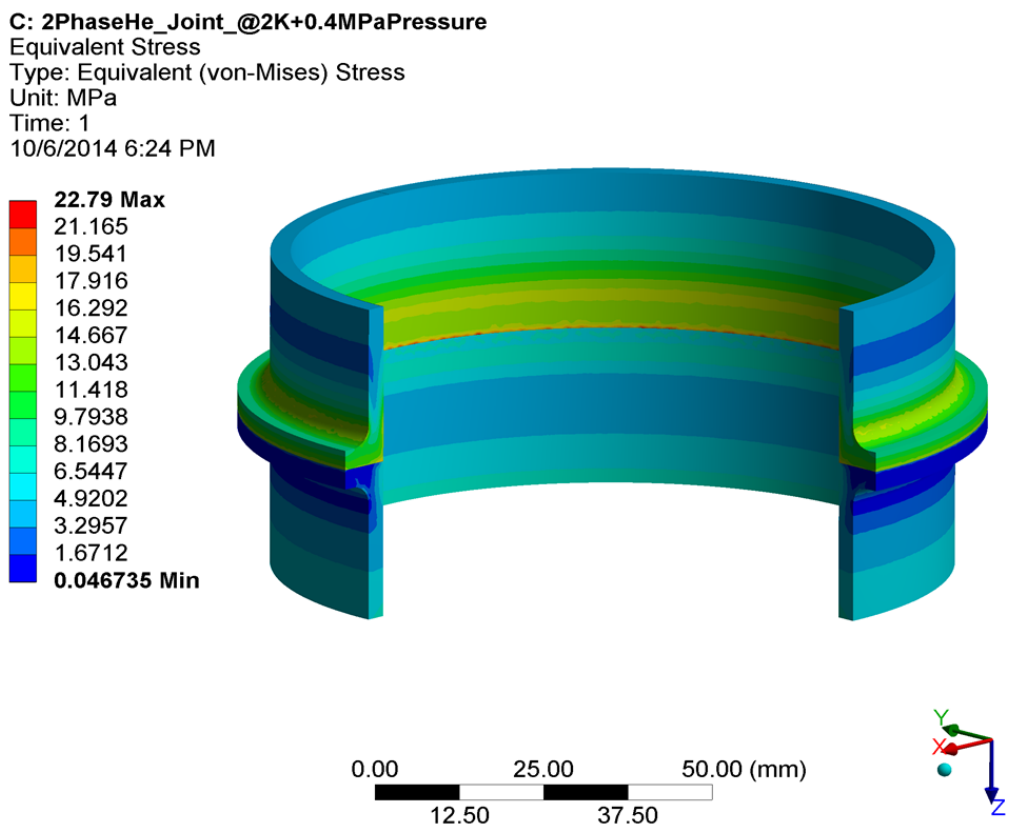

Figure 40: Equivalent stress of the transition joint for the two-phase pipe line at the temperature of 2 K and maximum pressure of 0.4 MPa. The equivalent stress is below the allowable stress, $S^{2K}_{Ti-SS} = 255\,\mathrm{MPa}$, with a safety factor of 11.2.

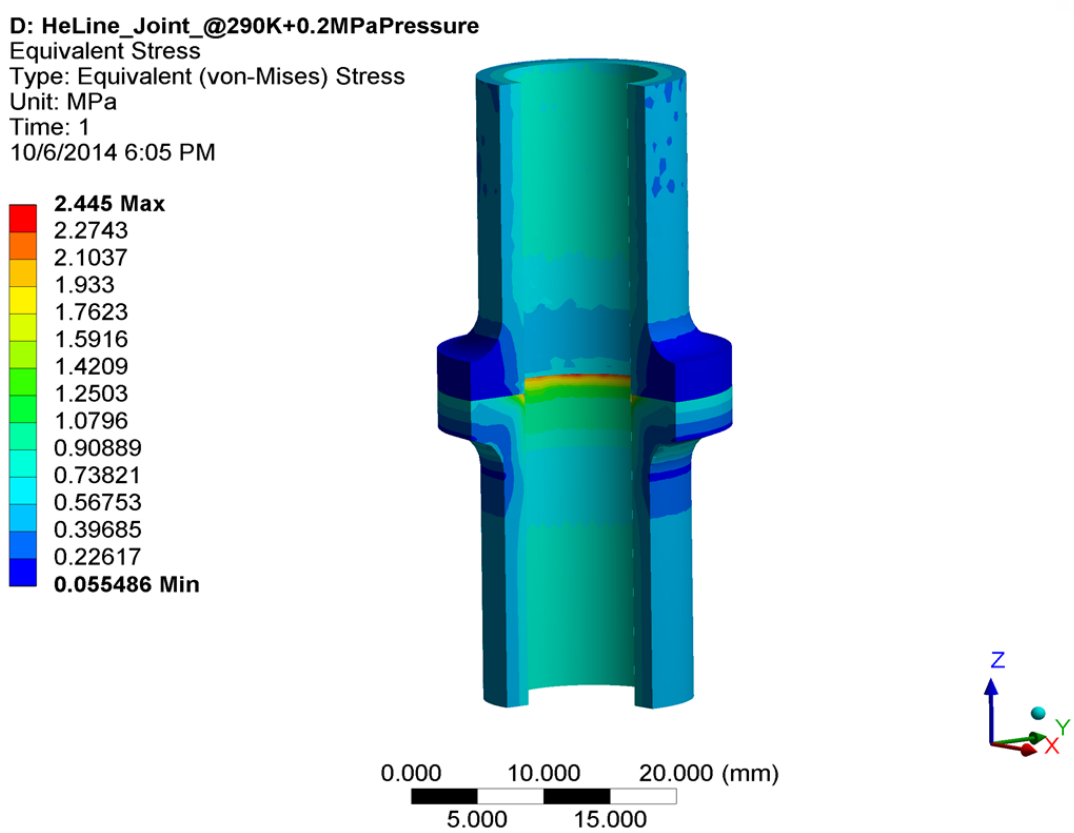

Figure 41: Equivalent stress map of the transition joint for the helium supply line at the temperature of 290 K and maximum pressure of 0.2 MPa. The equivalent stress is below the allowable stress, $S_{Ti-SS}^{290K} = 79\,\mathrm{MPa}$, with a safety factor of 32.3.

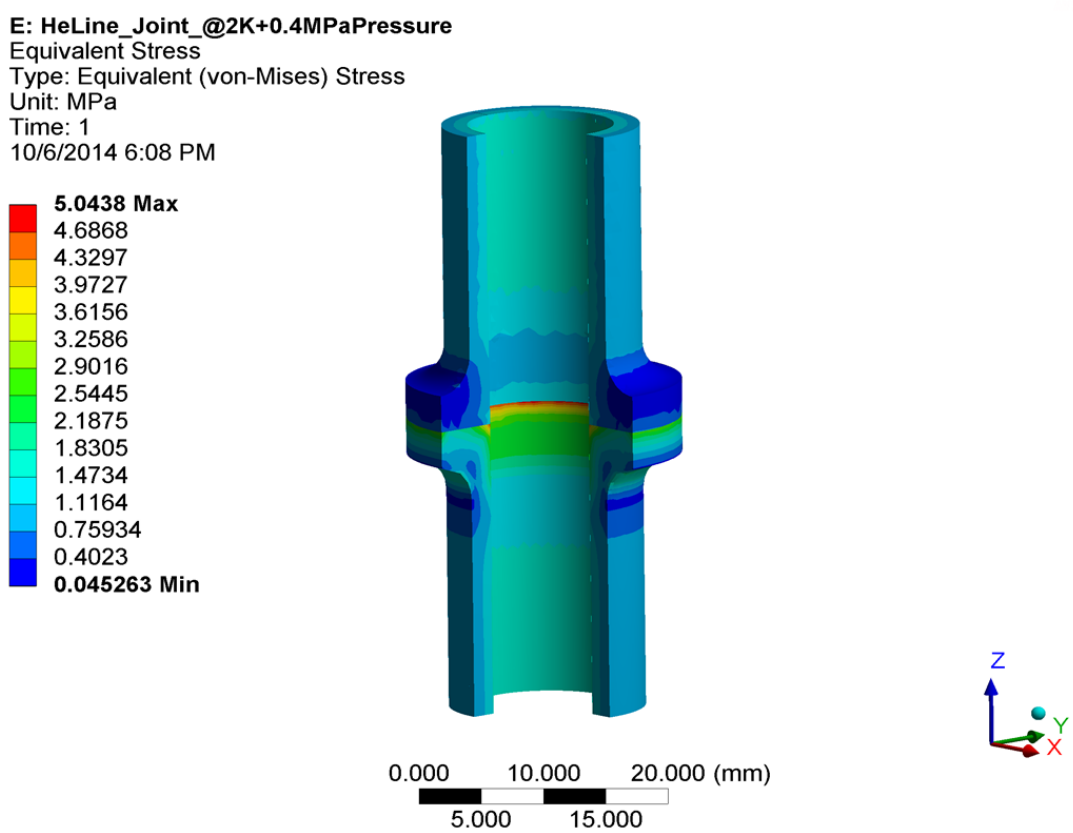

Figure 42: Equivalent stress of the transition joint for the two-phase pipe line at the temperature of 2 K and maximum pressure of 0.4 MPa. The equivalent stress is below the allowable stress, $S^{2K}_{Ti-SS} = 255\,\mathrm{MPa}$, with a safety factor of 50.6.

G Bellows Brace and Analysis

Evgueni Borissov x8904
Ivan Gonin x6769
Valeri Poloubotko x8310

The titanium bellows in the helium vessel design allow for movement in the vessel in order to tune the cavity. When a tuner is not installed, the bellows brace should be installed across the bellows to prevent excessive movement during pressure test, transport, test preparation, and vessel MAWP.

G.1 Brace Analysis

An analysis was performed on the model shown in Figure 43. The part is machined in two pieces and welded together. The material properties used for the analysis are shown in Figure 44, and the mesh is shown in Figure 45.

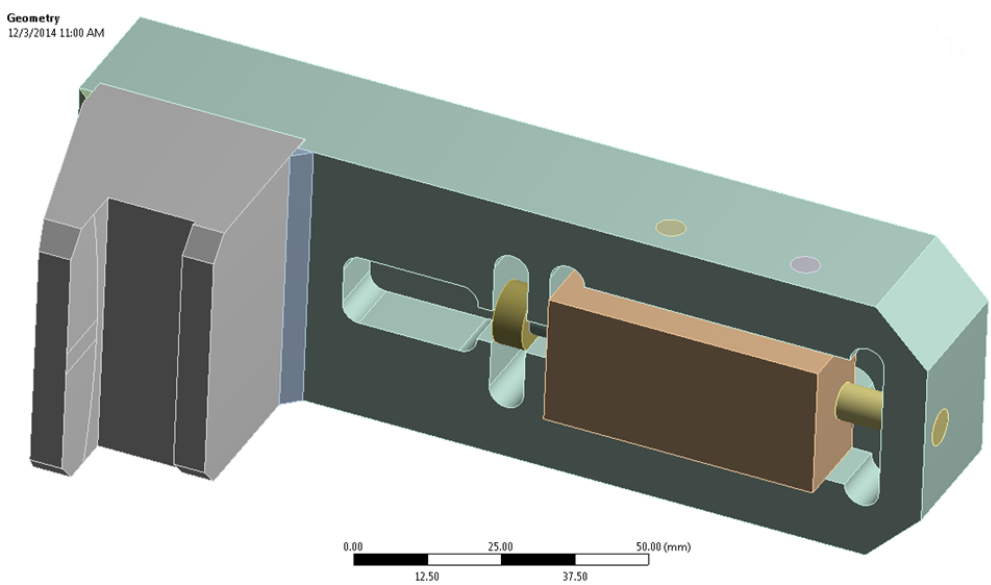

Figure 43: Half seciton of brace that is analyzed.

The forces on the brace represent a pressure in the helium vessel of 2.3 bar for the pressure test, 4 bar for the cold MAWP, and full vacuum for leak checking purposes. The location of the forces in the analysis are shown in Figure 46. The total load on the braces is 3670 N with vacuum in the helium vessel, 15047 N with 4 bar in the helium vessel, and 8441 N with 2.3 bar in the helium vessel.

Figures 47, 48, and 49 show the deformation of the bracket with the loads described. The deformation is small and acceptable to the cavity. The stresses on the bracket are shown in Figures 50, 51, 52, 53, and 54. A cross-section of the critical stress areas are shown in Figures 52 and 54 and are due to a sharp edge that will not occur in the actual machined part. The real stresses do not exceed 210 MPa, and this yields a safety factor of 1.14.

Property	Value	Unit
Density	7750	kg m^-3
Isotropic Secant Coefficient of Thermal Expansion		
Isotropic Elasticity		
Derive from	Young's Modulus and...	
Young's Modulus	1.93E+05	MPa
Poisson's Ratio	0.31	
Bulk Modulus	1.693E+11	Pa
Shear Modulus	7.3664E+10	Pa
Tensile Yield Strength	207	MPa
Compressive Yield Strength	207	MPa
Tensile Ultimate Strength	586	MPa

Figure 44: Material properties used to model bracket part.

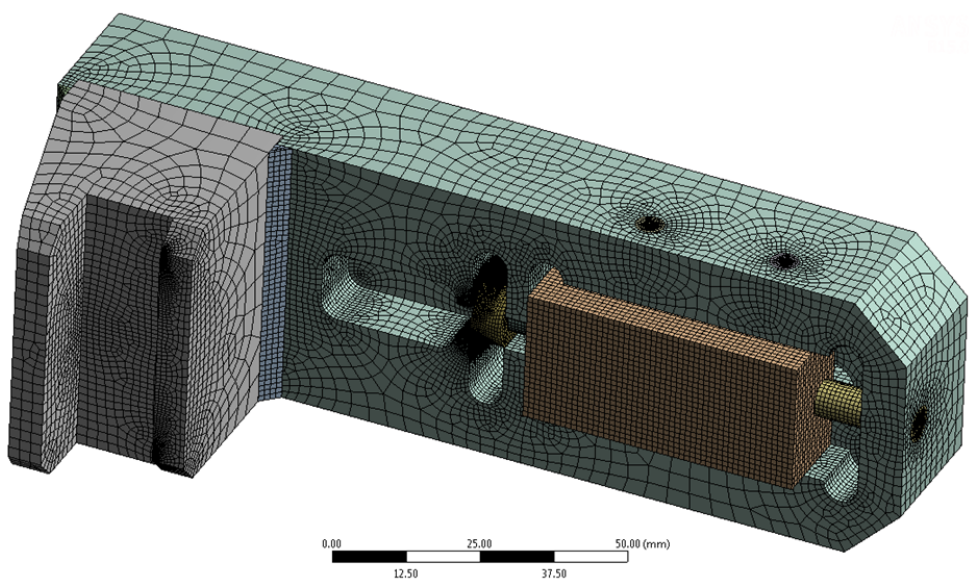

Figure 45: Mesh of analyzed brace.

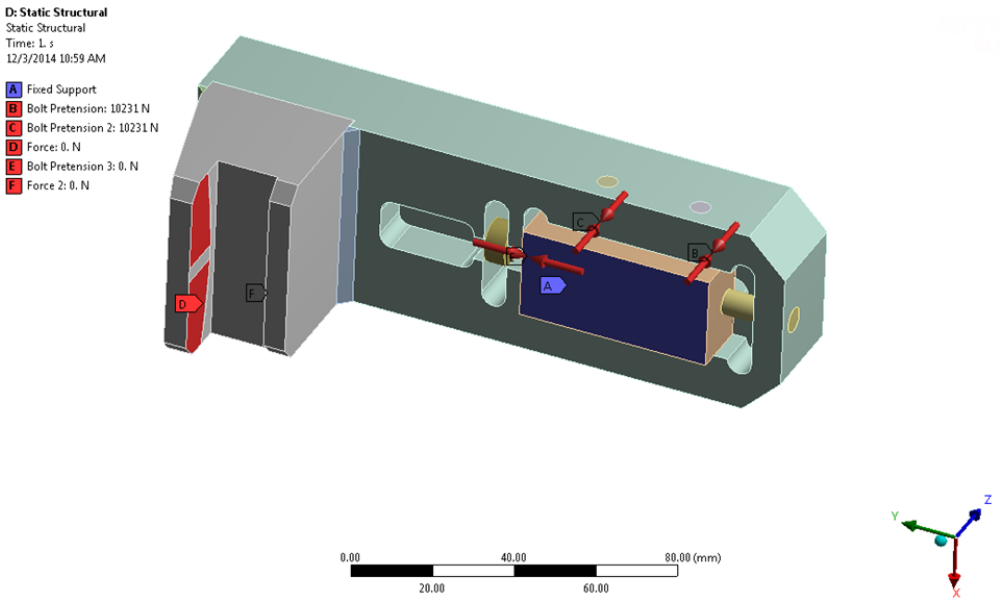

Figure 46: Force locations on bracket during simulation. Magnitude of forces change throughout simulation.

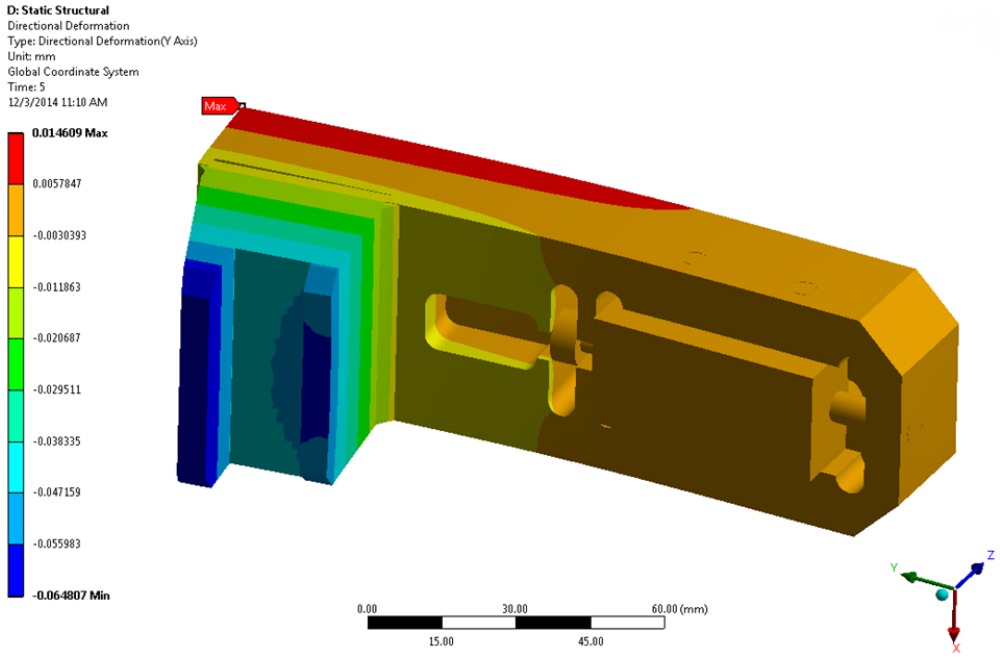

Figure 47: Deformation of the bracket with vacuum in the helium vessel.

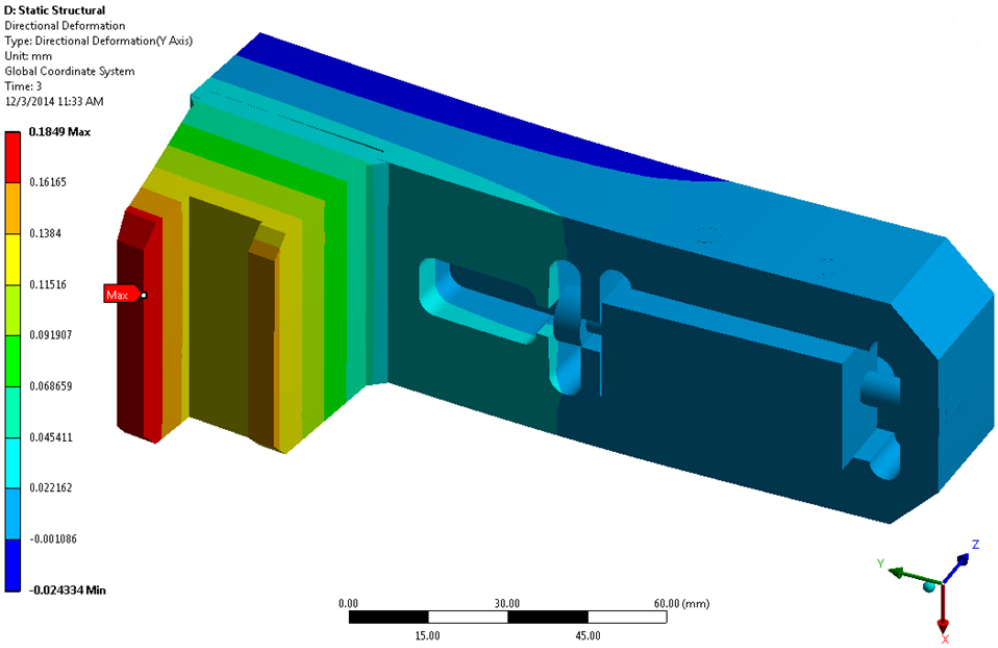

Figure 48: Deformation of the bracket with 2.3 bar in the helium vessel.

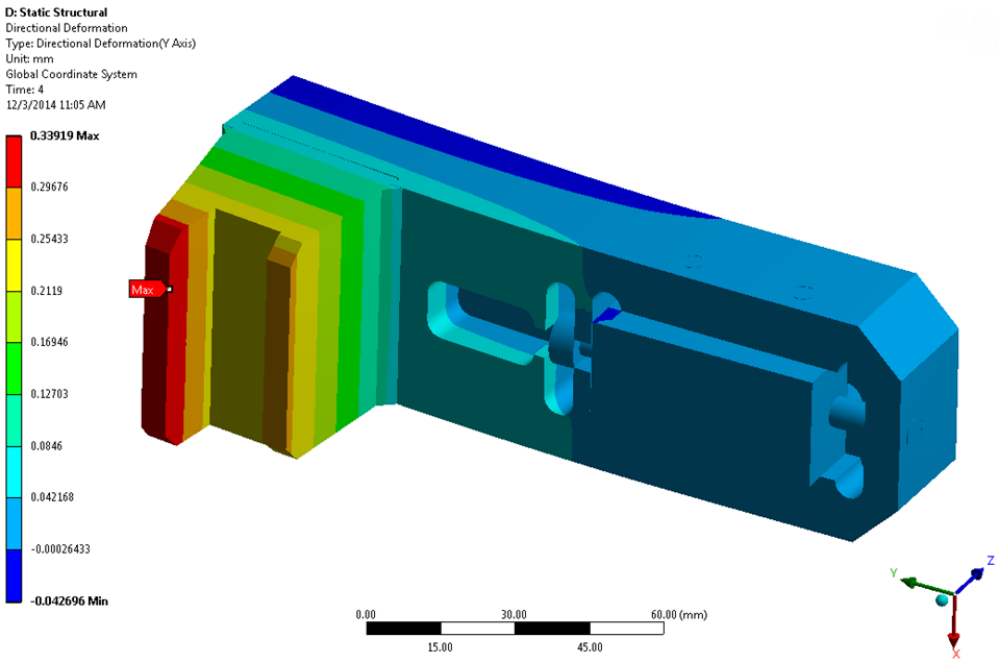

Figure 49: Deformation of the bracket with 4 bar in the helium vessel.

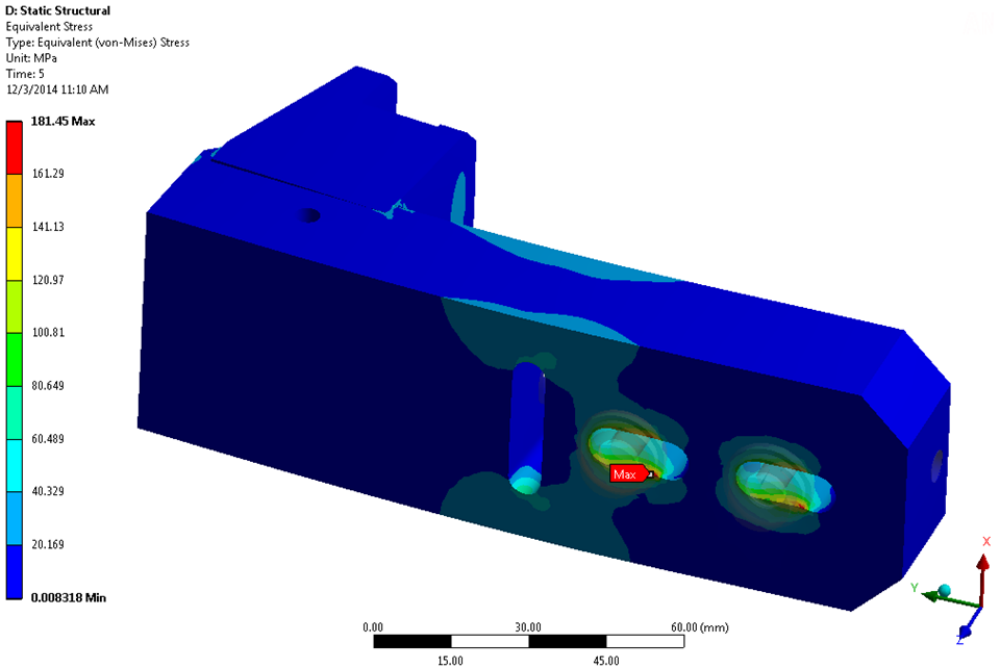

Figure 50: Stress of the bracket with vacuum in the helium vessel.

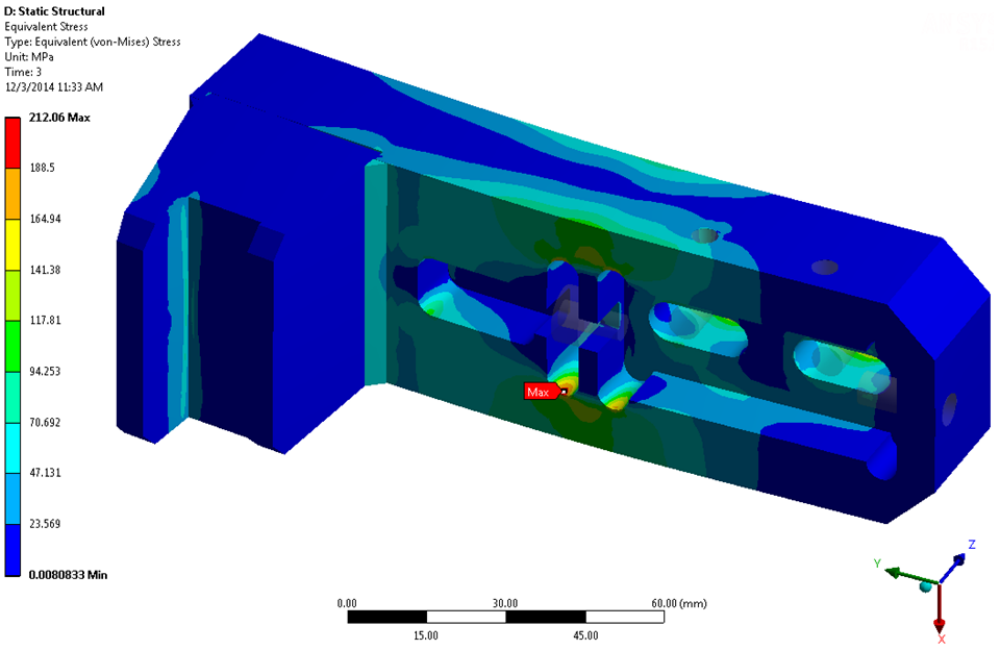

Figure 51: Stress of the bracket with 2.3 bar in the helium vessel.

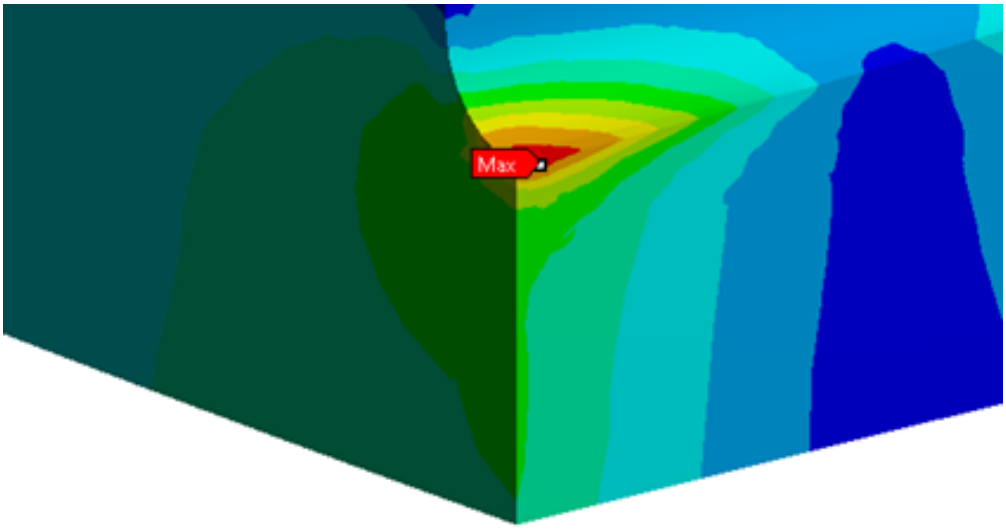

Figure 52: Close up stress of the bracket with 2.3 bar in the helium vessel.

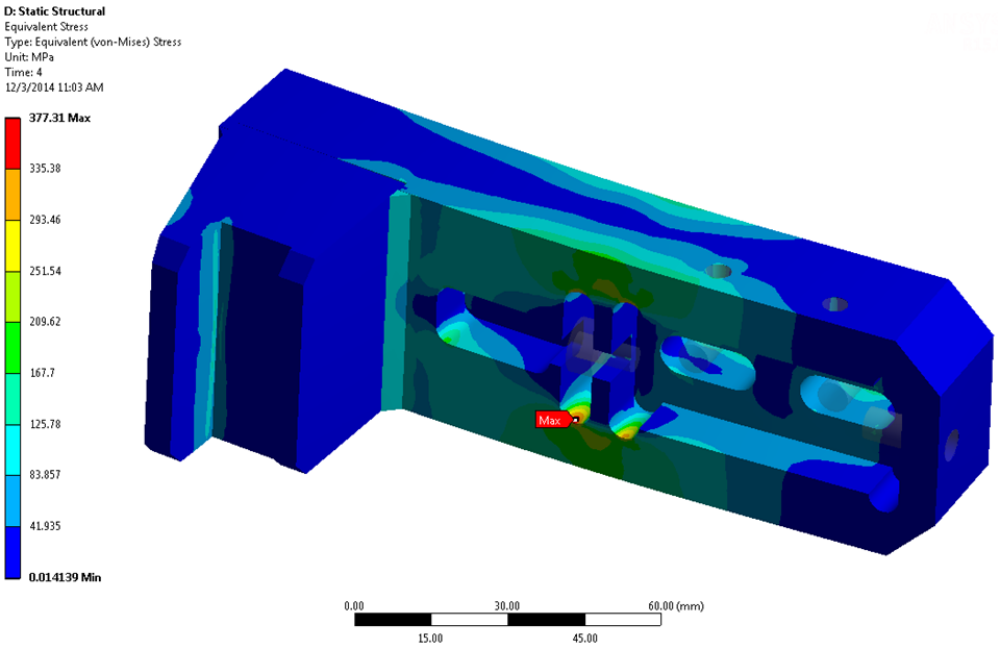

Figure 53: Stress of the bracket with 4 bar in the helium vessel.

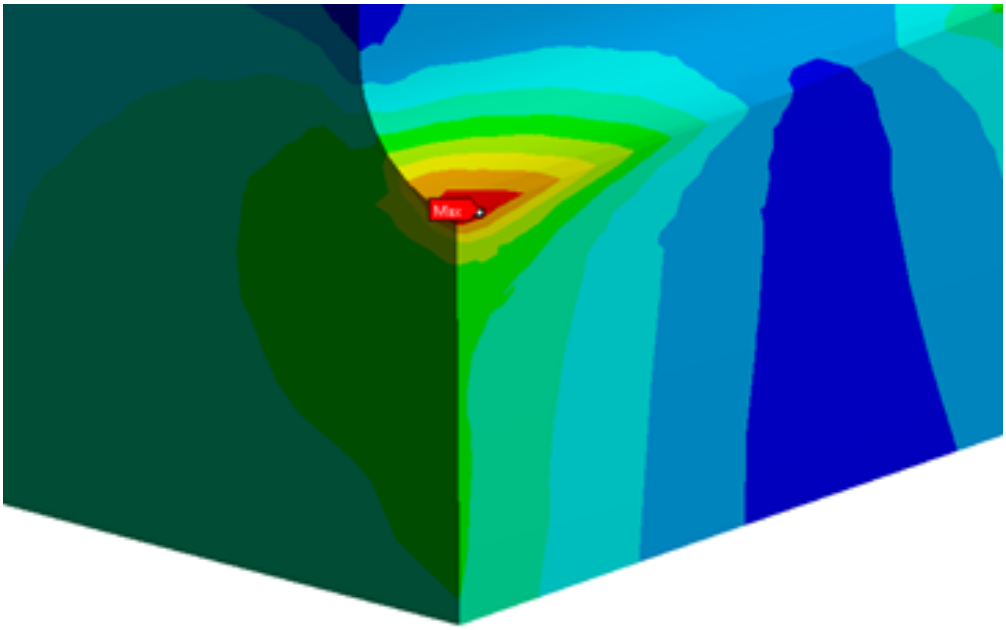

Figure 54: Close up stress of the bracket with 4 bar in the helium vessel.

G.2 Full Analysis

COMSOL simulations of the LCLS-II dressed cavity were performed with a brace system designed by E. Borissov. The analysis was done regarding a helium vessel pressure of 2.3 bar at room temperature and a helium vessel pressure of 4 bar at 2K. The goal is to prevent non-elastic deformation of the cavity. The assembly consists of four different materials: Cavity - Niobium, Helium Vessel - Titanium, Conical Flanges - Niobium-Titanium, and Braces - 316L SS. Material properties used for room temperature and 2K are shown in Table 36.

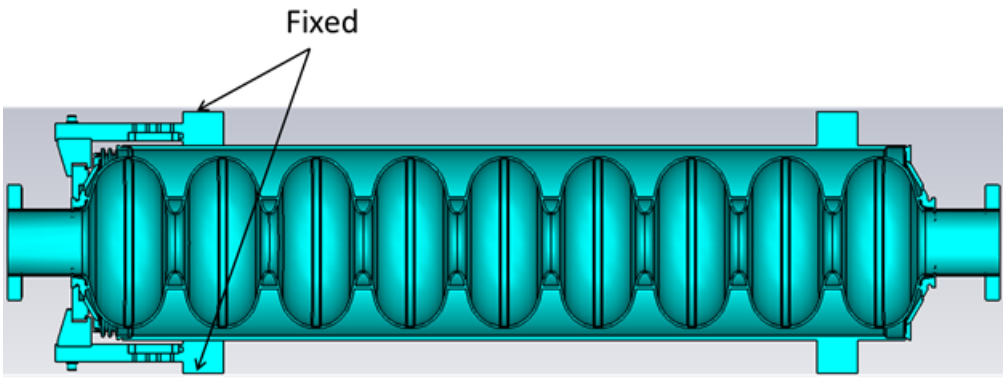

Figure 55: CAD model of the assembly. Positions of fixed boundary conditions applied are shown. The advantages of symmetry are used in the simulation.

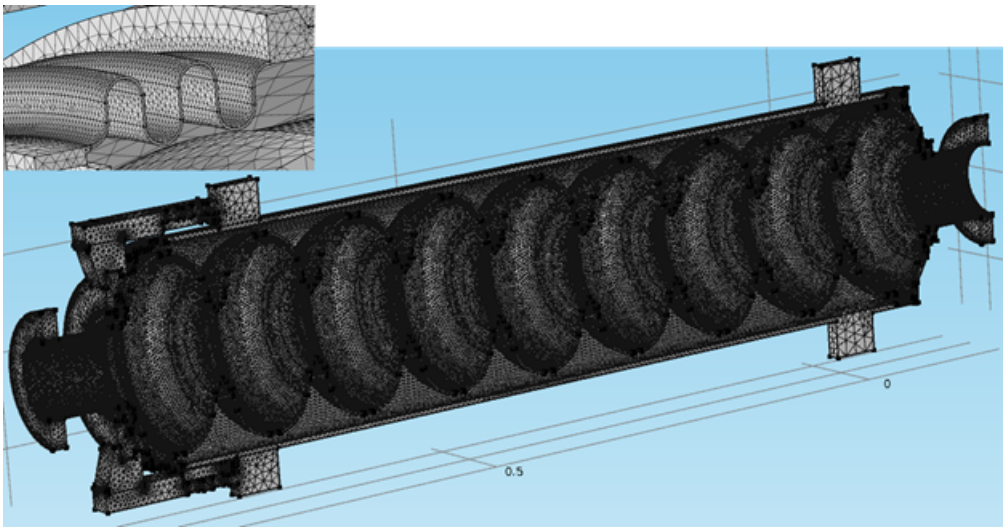

Figure 56: FE mesh used in COMSOL analysis. To increase accuracy, the mesh is more dense in critical areas such as the bellows shown here.

Figure 56 shows the FE mesh used in the COMSOL analysis. 1.5 million second order ten-node tetrahedral elements were used.

Figures 58 and 59 present the deformation and stress maps for the 2.3 bar analysis. The left flange moves 78 microns and the right moves 42 microns in the opposite direction. The total cavity

	Young's modulus 293K/2K	Poisson ratio 293K/2K
Niobium	105/118	0.38
Titanium	106/117	0.37
Niobium-Titanium	62/68	0.33
SS 316	195/208	0.33

Table 36: Material properties used in the analysis of the cavity, vessel, and brace. [21]

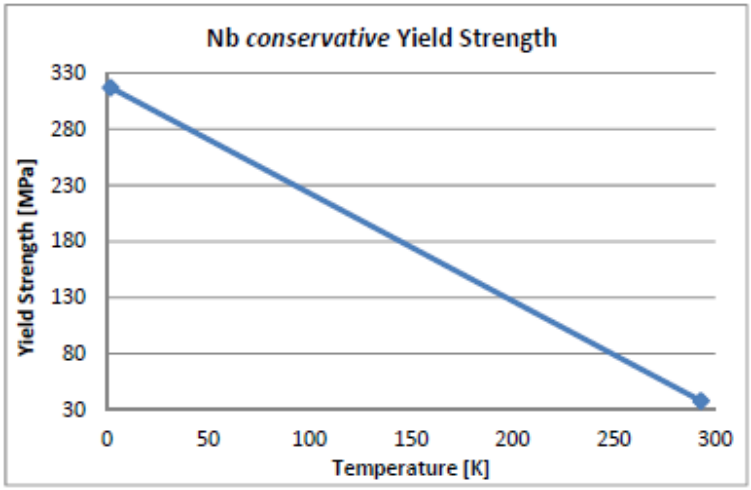

T [K]	[MPa]
1.88	317
293	38

Figure 57: Conservative yield strength of Niobium.

elongation is about 120 microns, which is much lower than allowed 0.5 mm at room temperature. Maximum stresses around 70 MPa are in the bellows. In the brace area, stresses are below 30 MPa. All these values are acceptable.

Figures 60 and 61 present the deformation and stress maps for the 4 bar condition. The left flange has a displacement of 130 microns and right flange moves 66 microns in the opposite direction. The total cavity elongation is around 196 microns, which is much lower than allowed 2.0 mm at 2K. Maximum stresses around 110 MPa are in the bellows. In the brace area, stresses are below 50 MPa. All these values are acceptable.

Figures 62 and 63 present the deformation and stress maps. The left flange has a displacement of 1.42 mm and right flange has a displacement of 40 microns in the opposite direction. Total cavity elongation is about 1.46 mm, which exceeds the allowed 0.5 mm of elongation at room temperature. Maximum stresses are around 310 MPa are in the bellows. In the cavity, maximum stresses are around 65 MPa in the cavity wall close to the stiffening ring. All simulations have been done for a 2.8 mm cavity wall thickness. In reality, the thickness will be less than 2.8 mm and one can expect larger stresses. Cavity stresses exceed conservative yield, 38 MPa, at room temperature.

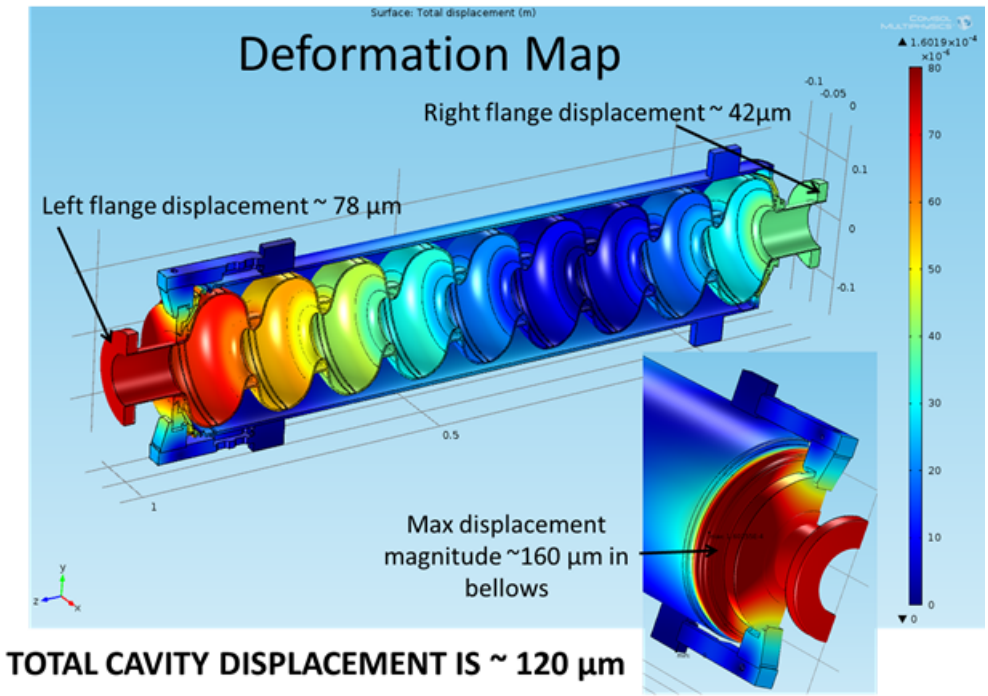

Figure 58: Deformation of the cavity and helium vessel with 2.3 bar pressure in the helium vessel.

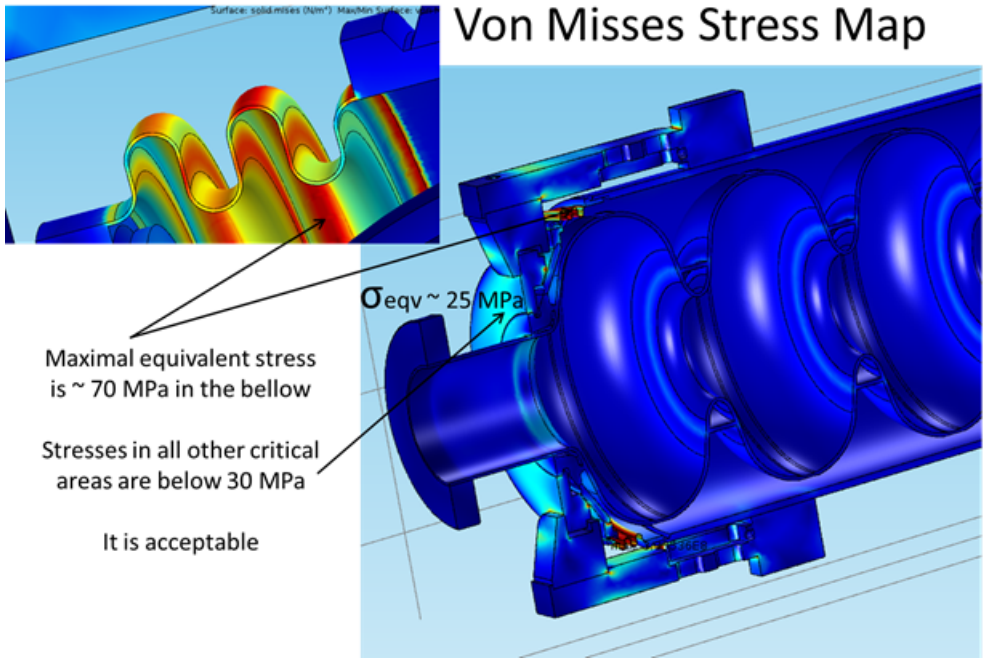

Figure 59: Stresses in the cavity and helium vessel with 2.3 bar pressure in the helium vessel.

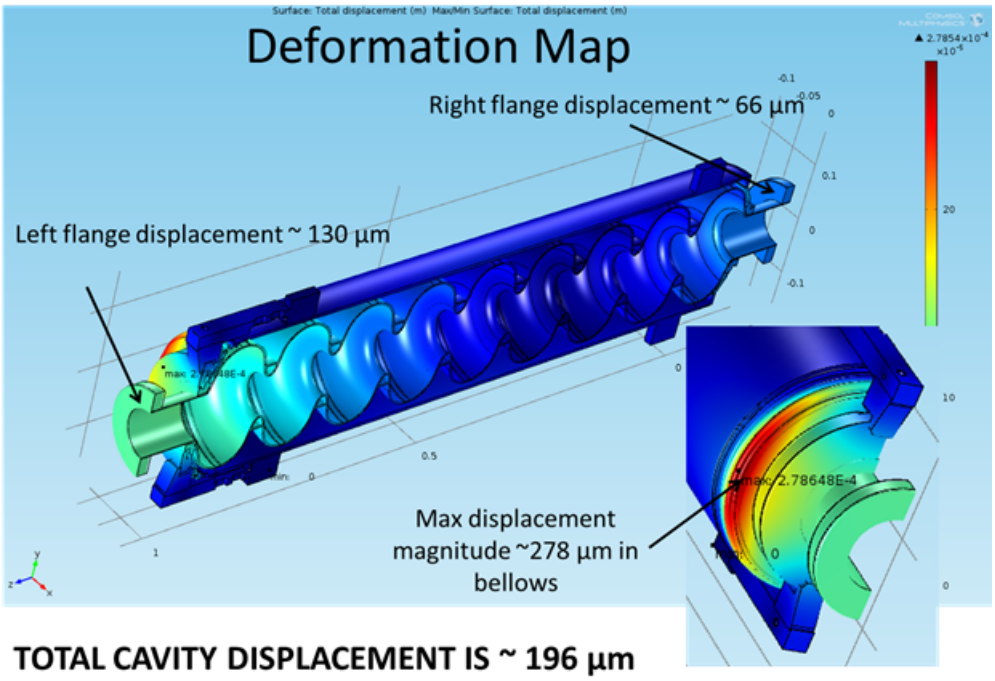

Figure 60: Deformation of the cavity and helium vessel with 4 bar pressure in the helium vessel.

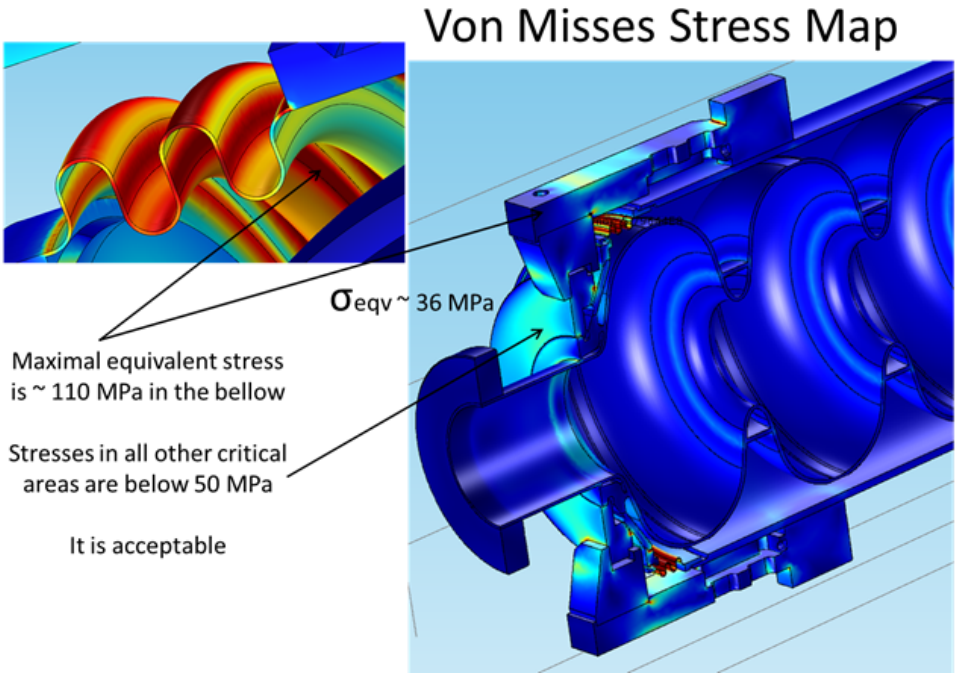

Figure 61: Stresses in the cavity and helium vessel with 4 bar pressure in the helium vessel.

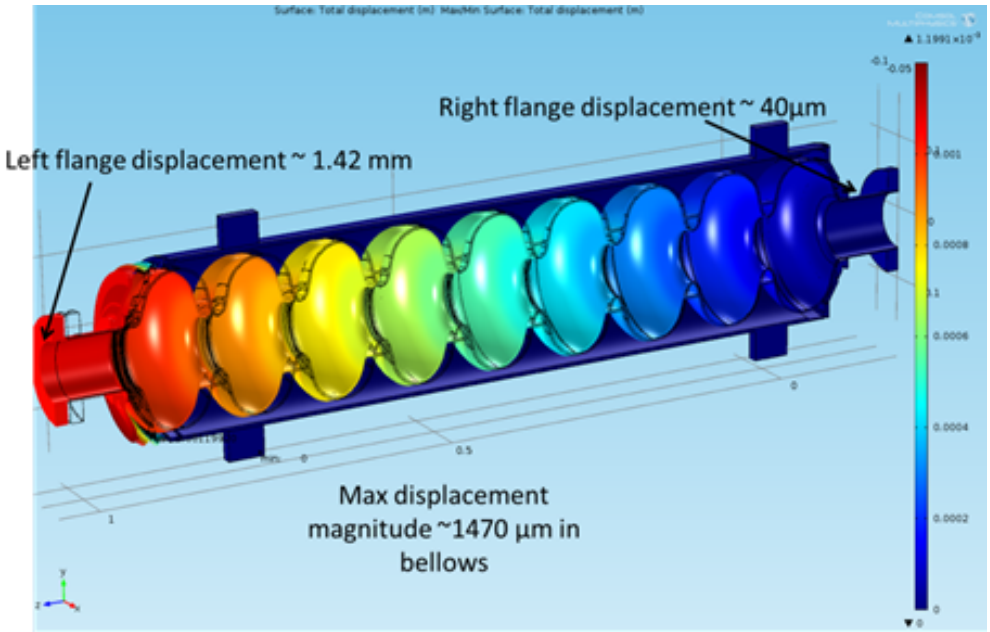

TOTAL CAVITY DISPLACEMENT IS ~ 1.46 mm

Figure 62: Deformation of the cavity and helium vessel with 2.3 bar pressure in the helium vessel and no brace.

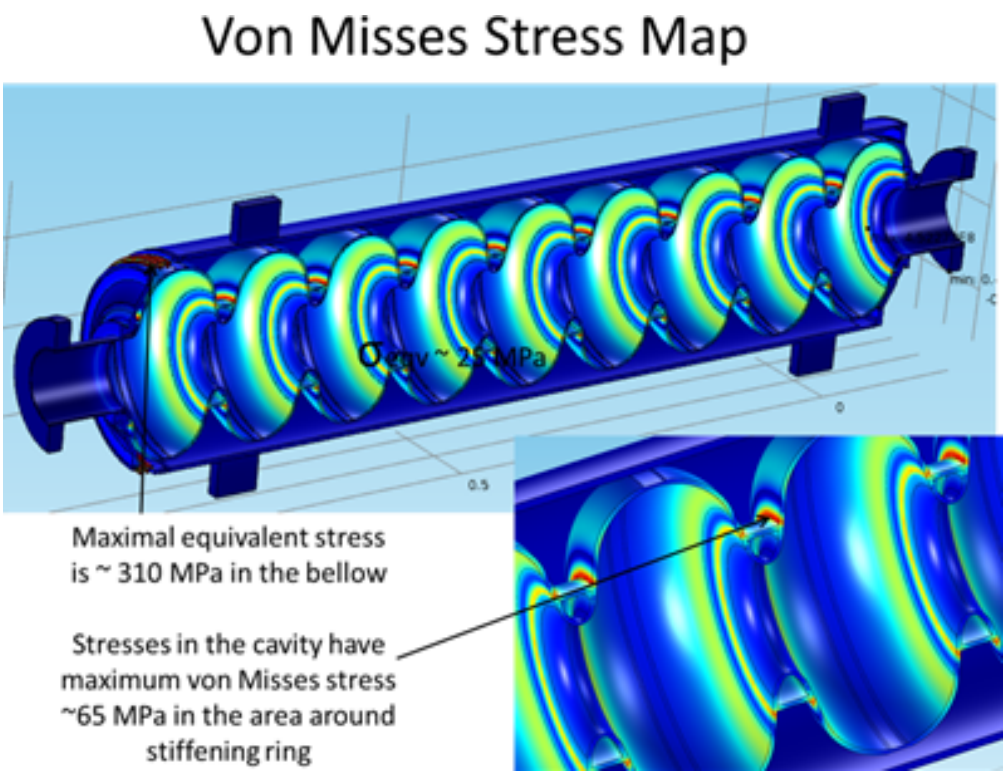

Figure 63: Stresses in the cavity and helium vessel with 2.3 bar pressure in the helium vessel and no brace.

References

[1] FESHM Chapter 5031.6: TD-09-005 Guidelines for the Design, Fabrication, Testing and Installation of SRF Nb Cavities. http://esh-docdb.fnal.gov/cgi-bin/ShowDocument?docid=1097.

[2] ASME Boiler and Pressure Vessel Code, 2013.

[3] Y. Pischalnikov, et al, "Resonance Control in SCRF Cavities," September, 2008.

[4] Y. Pischalnikov, email 30 Sep 2014.

[5] Pressure Vessel Engineering Ltd. "Use of Type (3) welds in ASME Pressure Vessel Design" December 2014, http://www.pveng.com/ASME/ASMEComment/Type3Welds/Type3Welds.php

[6] "Pressure Vessel Engineering Note for the 3.9-GHz Helium Vessel, Cavity # 5," IND- 102, July 2008.

[7] Peterson, T., "3.9-GHz Helium Vessel, Low Temperature Maximum Allowable working Pressure," March, 2009

[8] Standards of the Expansion Joint Manufacturers Association, Inc, 9th Edition.

[9] Kropschot, R.H., et al, "Technology of Liquid Helium," National Bureau of Standards, Monograph 111, October 1968.

[10] Compressed Gas Association, Inc., "Pressure Relief Device Standards, Part 3 - Stationary Storage Containers for Compressed Gases," CGA S-1.3-2008, 8th Edition.

[11] G. Cavallari, et al, "Pressure Protection Against Vacuum Failures on the Cryostats for LEP SC Cavities", European Organization for Nuclear Research, 27 Sep, 1989. CERN internal note AT-CR/90-09 presented at 4th Workshop on RF Superconductivity, Tsukuba, Japan (1998).

[12] W. Lehmann, et al, "Safety Aspects for LHe Cryostats and LHe Transport Containers," Proceedings of the 7th International Cryogenic Engineering Conference, London, 1978.

[13] TTF Design Report, Section 5.5.1.

[14] Roark, R.J. and Young, W.C., Formulas for Stress and Strain, 5th Edition, McGraw-Hill, 1975.

[15] Rao, K.R., et al, Companion Guide to the ASME Boiler and Pressure Vessel Code, Vol.1.

[16] Test Report for SNS He vessel Ti/SS joint, email from Ed Daly to Tom Peterson on 25 July 2014, tests from 2002.

[17] Cabot Supermetals, Product Information: Mechanical Properties of Tantalum and Alloys, http://www.cabot-corp.com/wcm/download/en-us/ta/Mechanical%20Properties%20of%20Tantalum%20and%20Alloys.pdf

[18] R.M. McClintock, H.P. Gibbons, Mechanical Properties of Structural Materials at Low Temperatures, NBS Monograph 13, 1960.

[19] R.P. Walsh, L.T. Summers, and J.R. Miller; "The 4 K Tensile and Fracture Toughness Properties of a Modified 316LN Conduit Alloy" National High Magnetic Field Laboratory, 1997.

[20] K. Mukugi, Low Temperature Mechanical Properties of Titanium and Weld Joints (Ti/Ti, Ti/Nb) for Helium Vessels, The 10th Workshop on RF Superconductivity, 2001, Tsukuba, Japan

[21] M.Merio, TD ER-10163, October 2011.